NASA Technical Memorandum 1999–206892, Volume 4

SeaWiFS Postlaunch Technical Report Series

Stanford B. Hooker, Editor
NASA Goddard Space Flight Center
Greenbelt, Maryland

Elaine R. Firestone, Senior Technical Editor
SAIC General Sciences Corporation
Beltsville, Maryland

Volume 4, The 1997 Prelaunch Radiometric Calibration of SeaWiFS

B. Carol Johnson and Edward E. Early
National Institute of Standards and Technology
Gaithersburg, Maryland

Robert E. Eplee, Jr. and Robert A. Barnes
SAIC General Sciences Corporation
Beltsville, Maryland

Robert T. Caffrey
NASA Goddard Space Flight Center
Greenbelt, Maryland

Abstract

The Sea-viewing Wide Field-of-view Sensor (SeaWiFS) was originally calibrated by the instrument's manufacturer, Santa Barbara Research Center (SBRC), in November 1993. In preparation for an August 1997 launch, the SeaWiFS Project and the National Institute of Standards and Technology (NIST) undertook a second calibration of SeaWiFS in January and April 1997 at the facility of the spacecraft integrator, Orbital Sciences Corporation (OSC). This calibration occurred in two phases, the first after the final thermal vacuum test, and the second after the final vibration test of the spacecraft. For the calibration, SeaWiFS observed an integrating sphere from the National Aeronautics and Space Administration (NASA) Goddard Space Flight Center (GSFC) at four radiance levels. The spectral radiance of the sphere at these radiance levels was also measured by the SeaWiFS Transfer Radiometer (SXR). In addition, during the calibration, SeaWiFS and the SXR observed the sphere at 16 radiance levels to determine the linearity of the SeaWiFS response. As part of the calibration analysis, the GSFC sphere was also characterized using a GSFC spectroradiometer. The 1997 calibration agrees with the initial 1993 calibration to within ±4%. The new calibration coefficients, computed before and after the vibration test, agree to within 0.5%. The response of the SeaWiFS channels in each band is linear to better than 1%. In order to compare to previous and current methods, the SeaWiFS radiometric responses are presented in two ways: using the nominal center wavelengths for the eight bands; and using band-averaged spectral radiances. The band-averaged values are used in the flight calibration table. An uncertainty analysis for the calibration coefficients is also presented.

1. INTRODUCTION

The Sea-viewing Wide Field-of-view Sensor (SeaWiFS) is an optical sensor, launched on 1 August 1997, which measures the radiance of Earth from orbit. Measurements occur at eight spectral regions from about 410–870 nm; at each band, the bandwidths are between 20 nm and 40 nm (Barnes et al. 1994a). The purpose of the SeaWiFS Project is to obtain valid ocean color data, which is then used to determine biological parameters. The required relative standard uncertainty in the water-leaving spectral radiance from the SeaWiFS measurements is 5% (Hooker et al. 1992).

SeaWiFS was originally calibrated by the instrument manufacturer, Raytheon Santa Barbara Research Center† (SBRC), in November 1993 at the SBRC facility in California. Since that time, the instrument was integrated onto the OrbView-2 spacecraft (formerly called SeaStar) by Orbital Sciences Corporation (OSC) and underwent several rounds of environmental testing. In preparation for an August 1997 launch of OrbView-2, the SeaWiFS Project, the National Institute of Standards and Technology (NIST), and OSC undertook a second calibration of SeaWiFS in January and April 1997 at OSC's Germantown, Maryland facility. In addition, limited electronic data were taken in June 1997 at Vandenberg Air Force Base (VAFB), California to ensure that the instrument had survived shipment from OSC to VAFB for launch.

There were several reasons for recalibrating SeaWiFS prior to launch. First, more than four years had elapsed from the initial calibration of the instrument, raising concerns about long-term changes in the optical, electrical, and mechanical components of the instrument. Second, the effects of spacecraft environmental testing on the instrument needed to be quantified. Third, the initial radiometric calibration of the instrument did not include a determination of the radiometric uncertainties in the calibration, and that analysis is presented here. For these reasons, SeaWiFS was recalibrated in January 1997 after the final thermal vacuum test of OrbView-2. The calibration was repeated in April 1997 after the final vibration test of the spacecraft to quantify possible changes in the response of the instrument.

For the calibration at OSC, SeaWiFS observed the spectral radiance of a 1.07 m diameter (40 in) integrating sphere [from the National Aeronautics and Space Administration (NASA) Goddard Space Flight Center (GSFC)] at four radiance levels. Measurements were obtained with SeaWiFS at all 4 electronic gains and for the 32 channels in the 8 bands. The standard gain setting for ocean observations is gain 1, denoted $g = 1$. The standard operating mode for ocean observations is to average the output of the four channels in each band. Alternatively, four sequential measurements with the same channel are averaged (Table 1 in Woodward et al. 1993). In Woodward et al. (1993), these modes are denoted as the 4:1 and 1:1 time delay and integration (TDI) setting, respectively‡. The central results

† Formerly known as Hughes Santa Barbara Remote Sensing, a subsidiary of Hughes Aircraft.

‡ In some earlier references, the notation 1:1, 2:2, 3:3, and 4:4 is used, thereby denoting which of the four channels was involved.

from this work correspond to $g = 1$ and the 1:1 TDI setting, but the other results are also reported. On orbit, SeaWiFS uses $g = 1$ and the 4:1 TDI setting.

A six channel filter radiometer, the SeaWiFS Transfer Radiometer (SXR),† was used as a transfer standard for the GSFC sphere in 1995 and 1997. The SXR is described in Johnson et al. (1998). Measurements of the sphere output were made with the SXR as part of the sphere's calibration at NIST (Early and Johnson 1997). It was expected that the SeaWiFS calibration would occur in 1995 and that SXR measurements would verify the stability of the sphere's output between the NIST calibration of the sphere, and the calibration of SeaWiFS using the sphere at OSC. There were various delays, however, and the 1997 SXR measurements indicated that the spectral radiance of the sphere source decreased by approximately 6% at 411 nm, and by lesser amounts at longer wavelengths. Consequently, the sphere radiance had to be determined using the 1995 and 1997 SXR measurements. The six SXR wavelengths range from 410–775 nm. For wavelengths outside of this region, measurements were made using a model 746 spectroradiometer (Optronic Laboratories, Inc.) with an integrating sphere irradiance collector (746/ISIC) to determine the source spectral shape‡. This system from GSFC is described in Johnson et al. (1996).

The measurements described here were made using the SeaWiFS/OrbView-2 system on 10 separate days between 21 January 1997 and 16 June 1997. The events occurred in three major steps:

1) Measurements after the OrbView-2 final thermal vacuum test;
2) Measurements after the OrbView-2 final vibration test; and
3) Measurements after the shipment of OrbView-2 to VAFB.

These instrument tests are summarized in Tables 1–3. The measurement of the sphere source with the 746/ISIC was a separate experiment, done at OSC, when SeaWiFS was involved in other tests.

This document begins with a summary of the initial calibration of SeaWiFS by SBRC. This is followed by a discussion of the equipment and procedures used in the calibration of SeaWiFS at OSC in Germantown, Maryland. Then, the calibration of the GSFC sphere is presented using the SXR along with the conversion of the flux measured by the SXR to the radiance observed by SeaWiFS. The calculation of the SeaWiFS calibration coefficients from the sphere radiances, including their uncertainties, is then derived. Finally, the 1993 and 1997 calibrations of SeaWiFS are compared.

† There is an ambiguity in the nomenclature for SeaWiFS and the SXR. SeaWiFS is an eight band instrument, each band having its own interference filter and electronic output. The SXR is a six channel instrument, each channel having its own interference filter and electronic output. In this document, an SXR channel is functionally equivalent to a SeaWiFS band.

‡ Identification of commercial equipment to adequately specify the experimental problem does not imply recommendation or endorsement by NASA or NIST, nor does it imply that the equipment identified is necessarily the best available for the purpose.

2. 1993 SeaWiFS CALIBRATION

The initial characterization and calibration of SeaWiFS was performed by the instrument's manufacturer, SBRC, in 1993. Those tests are described in the SeaWiFS Calibration and Acceptance Data Package (an SBRC internal document) and in the *SeaWiFS Technical Report Series* (Barnes et al. 1994a, Barnes et al. 1994b, and Barnes and Eplee 1997). The original tests at SBRC that relate to the radiometric calibration at OSC are summarized below. A comparison of the results of the 1993 SBRC calibration of SeaWiFS and the 1997 calibration of SeaWiFS is discussed in Sects. 8 and 9.

2.1 Channel Configuration

Barnes and Holmes (1993) and Barnes et al. (1994b) described the SeaWiFS instrument in depth. SeaWiFS is an eight-band filter radiometer which measures the upwelling Earth radiance in the visible and near-infrared spectral regions. The specified wavelengths for these bands are 412 nm, 443 nm, 490 nm, 510 nm, 555 nm, 670 nm, 765 nm, and 865 nm (Barnes et al. 1994b). These values, also known as the *nominal center wavelengths*, are denoted λ_{D} and are part of the instrument specifications to the manufacturer. The actual center wavelengths differ from the nominal values by up to 2 or 3 nm (Barnes and Yeh 1996). Each SeaWiFS band has four independent channels. A channel consists of a silicon photodiode, transimpedance amplifier, intermediate electronics, and an analog-to-digital (A/D) converter. The photodiodes for each band are etched from a single piece of silicon and are located behind a single interference filter. This gives each channel in that band a nearly identical spectral response.

Three channels in each band have almost equal overall gains, and the other channel has a different gain. The overall gains are adjusted so the three *high gain* (ocean) channels are optimized for the low radiance levels associated with measurements of the Earth's oceans. The A/D converter (but not the photodiode, transimpedance amplifier, or the intermediate amplifiers) saturates when observing bright sources, such as clouds or bright calibration sources. Saturation occurs at 1,023 digital counts. When SeaWiFS is operated in the standard 4:1 TDI setting, the output of the four channels in each band are averaged (Sect. 1). Consequently, a knee in the digital output of the band, as a function of radiance, occurs when the ocean channels reach saturation; the band has high gain (sensitivity to radiance) below the knee and lower sensitivity above (Barnes et al. 1994b). This change in sensitivity of

Table 1. Calibration measurements following the final thermal vacuum test of OrbView-2.

Date	*Measurements*
3 January 1997	Initial characterization of the GSFC sphere output prior to moving the sphere from NIST in Gaithersburg, Maryland to OSC in Germantown, Maryland. The changes in the sphere radiance were first noted.
21 January 1997	Verification of the sphere output at OSC using the SXR.
22 January 1997	Preliminary measurements of the sphere with SeaWiFS. Data were obtained at the standard SeaWiFS gain and TDI settings for the sphere output with a lamp configuration of 16, 8, 1, and 0.
23 January 1997	Repeat measurements of the sphere with SeaWiFS and the SXR. Data were obtained for the sphere output with 16, 8, 4, 1, and 0 lamps in operation three times, once in the morning and twice in the afternoon.
24 January 1997	SeaWiFS prelaunch calibration, part 1. Measurements were made for all gain and TDI settings for the sphere output with 16, 8, 4, 1, and 0 lamps operating. Gain ratios for each detector were made using the electronic calibration pulse.
6 March 1997	Characterization of the spectral radiance of the sphere output with 16 lamps operating using the SXR and the GSFC 746/ISIC. FEL lamp F182 was used.
7 March 1997	Characterization of the spectral radiance of the sphere output with 16 lamps operating using the SXR and the GSFC 746/ISIC. FEL lamp F391 was used.

Table 2. Calibration measurements following the final vibration test.

Date	*Measurements*
11 April 1997	SeaWiFS prelaunch calibration, part 2. Measurements were made for all gain and TDI settings for the sphere output with 16, 8, 4, 1, and 0 lamps operating. Measurements were also made at all 16 possible radiance levels from the sphere (the standard gain and TDI settings) to measure the linearity of the SeaWiFS responses.
23 April 1997	Postvibration calibration pulse test. Gain ratios were obtained for each detector.

Table 3. Calibration measurements following the shipment of OrbView-2 to VAFB.

Date	*Measurements*
16 June 1997	Post-shipment calibration pulse test. Gain ratios were measured for each detector.

the band is referred to as *bilinear gain*. It is possible to change the TDI mode to provide the average of four readings from one channel in a band (denoted 1:1 TDI in this document); other possible combinations of the individual channels in each band can also be implemented (Woodward et al. 1993). In the 1:1 TDI setting, the low sensitivity channel in each band does not saturate during the laboratory measurements, while the high sensitivity channels have constant digital output above the saturation radiance. For extremely bright sources, the low sensitivity channel would also saturate. SeaWiFS was designed so measurements of clouds and land surfaces would not saturate the low sensitivity channels; however, in some cases, sun glint from the ocean could result in saturation of these channels.

The electronic gains for the high sensitivity channels in each band can be changed, while the gains for the low sensitivity (or cloud) channels are fixed. The standard gain for ocean measurements is $g = 1$, and $g = 2$ is used for unusually dark oceans, such as when the solar zenith angle is exceptionally large. The gain settings of $g = 3$ and $g = 4$ are used for measurements of the moon and the SeaWiFS solar diffuser, which are used as calibration targets. For each choice, the gain is the same for all of the high sensitivity ocean channels for all bands.

The SeaWiFS calibration at OSC included measurements at $g = 1$ for each band using the 4:1 and 1:1 integration modes (an average of the four channels in each band and an average of the four readings of each channel separately). This required five measurements for each band. In addition, measurements were made for $g = 2$, $g = 3$, and $g = 4$, and for spectral radiances above and below the knees in the bilinear gains.

2.2 Initial Calibration

SBRC performed the radiometric calibration of SeaWiFS in November 1993. For that calibration, the 1:1

Table 4. SeaWiFS calibration coefficients from the SBRC calibration for $g = 1$ and the 1:1 TDI setting. Results are given using two methods: band-centered (columns 3 and 4) and band-averaged (columns 5 and 6). The wavelength is expressed in nanometers and the calibration coefficients are in units of $\mathrm{mW\,cm^{-2}\,sr^{-1}\,\mu m^{-1}\,count^{-1}}$.

Band Number	*Channel Number*	λ_D [A]	*Calibration Coefficients* [B]	λ_B [C]	*Calibration Coefficients* [D]
1	1	412	0.060039	415.5	0.062084
	2		0.010903		0.011275
	3		0.010994		0.011369
	4		0.010878		0.011248
2	1	443	0.010546	444.7	0.010676
	2		0.010533		0.010664
	3		0.010582		0.010713
	4		0.067570		0.068407
3	1	490	0.068075	493.0	0.069132
	2		0.008228		0.008356
	3		0.008163		0.008290
	4		0.008163		0.008290
4	1	510	0.007150	511.0	0.007145
	2		0.007150		0.007145
	3		0.007133		0.007128
	4		0.066333		0.066289
5	1	555	0.065167	558.2	0.065375
	2		0.005736		0.005754
	3		0.005757		0.005775
	4		0.005785		0.005804
6	1	670	0.003241	668.8	0.003220
	2		0.003228		0.003207
	3		0.003292		0.003270
	4		0.054820		0.054449
7	1	765	0.042978	767.5	0.042974
	2		0.002298		0.002297
	3		0.002306		0.002305
	4		0.002298		0.002297
8	1	865	0.001633	865.0	0.001626
	2		0.001646		0.001638
	3		0.001628		0.001621
	4		0.034280		0.034113

[A] Table 5 in Barnes et al. (1994b).
[B] Table 21 in Barnes and Eplee (1997).
[C] Table 23 in Barnes and Eplee (1997).
[D] Table 25 in Barnes and Eplee (1997).

TDI setting was used and SeaWiFS observed the SBRC integrating sphere, model SIS-100, at six radiance levels. These radiance levels, selected by operating subsets of the lamps in the SIS-100, resulted in a determination of the calibration coefficient for each channel at a single radiance value. Seven of the SeaWiFS bands were calibrated at $g = 1$, while $g = 4$ was used for band 8 to avoid saturation of the channels. Ancillary data on the gain ratios for each channel were used to convert the calibration coefficient to those at the other instrument gains.

In October 1993, the spectral radiances of the SIS-100 were measured by SBRC at the six lamp levels by comparing them with NIST-traceable standard irradiance lamps†. The goal was to achieve a relative standard uncertainty of 5% for the radiometric calibration of SeaWiFS. The 1993 calibration coefficients at the values of λ_D are given in Table 4. These results are derived from the original method used to analyze the calibration data; it is best suited to instruments with narrow spectral bandwidths. Once the actual relative spectral responsivities, $R(\lambda)$, for SeaWiFS were determined, it was realized a more thorough approach

† For a diagram of the sphere calibration facility at SBRC, see Appendix B in Mueller (1993).

was necessary (Barnes and Yeh 1996). Table 4 also reports the 1993 SBRC results using this approach for the SeaWiFS calibration. In reference to determining the radiance of the calibration source, the two methods are termed "band-centered" and "band-averaged" (Sect. 6.1).

The band-averaged method of determining the measurement wavelength for each band uses the actual $R(\lambda)$ functions for SeaWiFS. The value for the band-averaged center wavelength, $\lambda_{\rm B}$, is dependent on the relative spectral shape of the radiance of the SBRC sphere source:

$$\lambda_{\rm B} = \frac{\int \lambda L_{\rm SBRC}(\lambda)\, R(\lambda)\, d\lambda}{\int L_{\rm SBRC}(\lambda)\, R(\lambda)\, d\lambda}. \qquad (1)$$

The spectral radiance $L_{\rm SBRC}(\lambda)$ in (1) corresponded to the brightest of the six radiance levels from the SIS-100, as determined in 1993. The band-averaged radiances were calculated using the $L_{\rm SBRC}(\lambda)$ and the $R(\lambda)$ values and the equation for band-averaged radiance [Barnes 1996b or (5) below]. Table 4 gives these wavelengths and the corresponding band-averaged calibration coefficients from the 1993 measurements. The inclusion of both methods in this document is for historical reasons and for comparison purposes (Sect. 6.1).

2.3 Gain Ratios

The gain ratios for the SeaWiFS channels, that is, the output of the individual channels at $g = 2$, $g = 3$, or $g = 4$, normalized by the gain at $g = 1$, were measured by the manufacturer in November 1993. A square-wave (voltage) calibration pulse was injected into the post-photodiode electronics during a portion of the SeaWiFS scan when the detectors were not illuminated. The output of the photodiode's transimpedance amplifier and the voltage pulse are summed and fed into the amplifier that controls the different gain settings (Woodward et al. 1993). The ratios of the channel output, relative to that at $g = 1$, are the gain ratios. The gain ratios in the SeaWiFS performance specifications (Barnes et al. 1994a) are given for each of the eight bands for the standard 4:1 TDI setting. Because the instrument has bilinear gains, the gain ratios must be determined for each channel. The gain ratios, as determined in November 1993, are listed in Table 5. This test was repeated during the prelaunch calibration of SeaWiFS, and it will be repeated routinely on orbit.

2.4 Linearity

The linearity of SeaWiFS was tested at SBRC in February 1993 and again in November 1993 (Barnes et al. 1994a). In the February test, SeaWiFS observed 8 radiance levels, with 25 individual measurements at each level. This linearity test was performed for each band at radiance levels where the instrument output was not saturated. During the February 1993 test, the values from band 1 were not saturated for all eight radiance levels. The measurements from band 2 were not saturated for seven of the radiance levels (saturation occurred for the brightest level). The values from band 3 were unsaturated for six of the radiance levels (saturation occurred for the two brightest levels). This sequence continued to band 8, where the values were unsaturated for only one radiance level (the lowest). Except for one radiance level where the output of the SBRC sphere was an outlier, the calibration coefficients deduced for SeaWiFS for each band at a particular radiance level agreed with the average calibration coefficient for that band to better than 1%. With the radiance level that was suspect included, the agreement was from 1.4–1.9%.

Table 5. SeaWiFS gain ratios, relative to $g = 1$, from the SBRC calibration [from Table 6 in Barnes et al. (1994b)].

Band No.	*Channel No.*	*Gain Setting*			
		$g = 1$	$g = 2$	$g = 3$	$g = 4$
1	1	1.000	1.000	1.000	1.000
	2	1.000	1.988	1.320	1.681
	3	1.000	1.988	1.320	1.681
	4	1.000	1.988	1.320	1.681
2	1	1.000	1.989	1.319	1.682
	2	1.000	1.989	1.319	1.682
	3	1.000	1.989	1.319	1.682
	4	1.000	1.000	1.000	1.000
3	1	1.000	1.000	1.000	1.000
	2	1.000	1.989	0.896	1.681
	3	1.000	1.989	0.896	1.681
	4	1.000	1.989	0.896	1.681
4	1	1.000	1.989	0.789	1.682
	2	1.000	1.989	0.789	1.682
	3	1.000	1.989	0.789	1.682
	4	1.000	1.000	1.000	1.000
5	1	1.000	1.000	1.000	1.000
	2	1.000	1.989	0.642	1.595
	3	1.000	1.989	0.642	1.595
	4	1.000	1.989	0.642	1.595
6	1	1.000	1.989	0.364	0.665
	2	1.000	1.989	0.364	0.665
	3	1.000	1.989	0.364	0.665
	4	1.000	1.000	1.000	1.000
7	1	1.000	1.000	1.000	1.000
	2	1.000	1.987	0.311	0.575
	3	1.000	1.987	0.311	0.575
	4	1.000	1.987	0.311	0.575
8	1	1.000	1.991	0.261	0.499
	2	1.000	1.991	0.261	0.499
	3	1.000	1.991	0.261	0.499
	4	1.000	1.000	1.000	1.000

In November 1993, SeaWiFS observed three radiance levels with all eight bands. These reference radiances are those expected at the top of the atmosphere, and are also called typical radiances in the SeaWiFS specifications (Barnes et al. 1994a). The radiance levels for the November 1993 test were the typical radiance for each band, two-thirds of the typical radiance, and one-third of the typical radiance. For band 1 and bands 3–8, the agreement between the calibration coefficients at each radiance level and the average value for each band was better than 1%. For band 2, the agreement was from 1.2–1.3%. Again, there was an outlier in the SIS-100 sphere output for one of the band 2 measurements (Barnes et al. 1994a).

3. TEST EQUIPMENT

The equipment used during the 1997 calibration of the SeaWiFS instrument is described below, and references that include detailed descriptions of the equipment are cited. The equipment includes the SXR, the GSFC integrating sphere, and the 746/ISIC spectroradiometer. The experimental configuration at OSC and the method of data acquisition for SeaWiFS on the OrbView-2 system are also described.

3.1 SXR

The SXR is a six-channel radiometer calibrated for spectral radiance over the wavelength range from 410–775 nm (Johnson et al. 1998). Each measurement channel consists of a silicon photodiode and an interference filter, which are temperature stabilized at 26°C, and a transimpedance amplifier. Refractive and reflective optical components image the source onto the six filtered photodiodes. The full-angle field of view is 2.5° and an alignment system ensures proper focus on objects from 85 cm to infinity. At the minimum focus, the diameter of the source area imaged by the SXR is approximately 45 mm.

The SXR was characterized and calibrated at NIST for relative spectral responsivity, linearity with radiant flux, point-spread responsivity, and stability. It was calibrated in 1994 and 1996 using a small integrating sphere which was calibrated for spectral radiance using the NIST Facility for Automated Spectroradiometric Calibrations (FASCAL).

The SXR is controlled, and data are logged, using a Macintosh computer running custom software which sequentially records signals from each channel as selected by the operator. The recorded measurements from the SXR were made with a single digital multimeter (DMM), a Hewlett-Packard (HP) model 34401A. The DMM was calibrated in June 1995 and July 1996. The SXR electronics and temperature control system, as well as the DMM, were warmed up for about 12 h before any measurements were made.

The SXR was used to measure the GSFC sphere during its calibration at NIST in April 1995, again in January 1997 to verify the operation of the sphere before shipment to OSC, and at OSC during the post-thermal vacuum calibration of SeaWiFS. Every measurement of the GSFC sphere by SeaWiFS was bracketed by measurements of the sphere with the SXR. For all measurements, the voltage gain was unity, the SXR was located about 135 cm from the exit aperture of the integrating sphere, and the lens focal setting was between 1.2 m and 1.3 m. For the majority of the measurements, the SXR was aligned to view the center of the exit aperture of the sphere at normal incidence. For the SeaWiFS linearity tests at OSC, the SXR was placed about 2 m from the sphere and aligned to view the center of the exit aperture at an angle of about 30° from normal.

The SXR can be rotated about the optical axis in increments of 90°. During the NIST calibration of the sphere in 1995 and the measurements at NIST of the sphere in January 1997, the orientation was *north* (one of the connectors on the back of the SXR is used to reference the orientation), but at OSC the orientation was *east*. The difference in orientation is not expected to affect the SXR measurement uncertainty (Johnson et al. 1998).

The SXR has a small, wavelength-dependent, size-of-source effect (SSE) that results in an overestimate of the spectral radiance of sources that are larger than the source used to calibrate the SXR. Two methods were used to account for the SSE in the measurements of the integrating sphere. For the sphere calibration in 1995 and the study in January 1997, (both at NIST) a model incorporating the normalized point-spread responsivity data was used to determine the correction. For the measurements at OSC, an on-axis circular black disc was placed in front of the exit aperture of the sphere and centered on the optical axis of the SXR. Measurements of the disc were used for the SXR instrument background, thus accounting for the amplifier offset and the extraneous signal from the finite response outside the instrument's nominal field of view.

The SXR parameters are given in Table 6. The SXR measurement wavelengths, λ_{SXR}, were calculated using a moment analysis which includes the relative spectral response (Johnson et al. 1998). The analysis does not include the spectral shape of the source that is measured:

$$\lambda_{\mathrm{SXR}} = \frac{\int \lambda\, R(\lambda)\, d\lambda}{\int R(\lambda)\, d\lambda}. \qquad (2)$$

Here, $R(\lambda)$ is the relative spectral responsivity for one of the six channels in the SXR. The SXR channels are narrow compared to the 20 nm and 40 nm bandwidths for the SeaWiFS bands, so the measurement wavelengths are not very sensitive to the relative spectral shape of the source (Johnson et al. 1998).

In Table 6, the calibration coefficients are negative because the output voltage from the SXR is negative for measurements of optical sources if the interconnecting cable

Table 6. SXR parameters at a voltage gain of unity. As an example of the combined relative standard uncertainty for SXR measurements of spectral radiance, values are given which correspond to measurements of the 1.07 m diameter GSFC sphere source with 16 lamps in operation.

Channel Number	λ_{SXR} [nm]	*Calibration Coefficient* [$V\,cm^2\,sr\,\mu m\,mW^{-1}$]	*Size-of-Source Correction GSFC Sphere* *Model*	*Black Disc*	*Relative Standard Uncertainty* [%]
1	411.222	−1.101185	0.9954	0.9972	0.99
2	441.495	−1.468061	0.9987	0.9958	1.19
3	486.938	−0.2442614	0.9988	0.9961	0.62
4	547.873	−0.2425734	0.9975	0.9969	0.65
5	661.718	−0.2604715	0.9948	0.9980	0.60
6	774.767	−0.03013285	0.9914	0.9930	0.68

is connected with the ground shield to the common input of the DMM. The SSE correction was calculated using the modeled point-spread measurements at NIST in April 1995, and was measured using the black disc at OSC in 1997. Both correction factors are given in Table 6; the agreement is within ±0.3%. The relative standard uncertainty is the root-sum squared of the individual components of uncertainty which correspond to the SXR measurements of the GSFC sphere source with 16 lamps operating (Johnson et al. 1998, and Tsai and Johnson 1998). These uncertainties are stated to illustrate the typical accuracy of the SXR for measurements of integrating sphere sources.

3.2 GSFC Integrating Sphere

The GSFC integrating sphere is 107 cm in diameter and coated with barium sulfate. It was manufactured by Optronic Laboratories Inc. for the National Oceanic and Atmospheric Administration (NOAA) and later transferred to the Space Geodesy Network and Sensor Calibration Branch at GSFC. The exit aperture is 39.5 cm in diameter and the sphere is internally illuminated by up to 16 baffled 45 W quartz halogen lamps. The lamps are positioned uniformly around the exit aperture. The lamps are divided into four sets of four, and each set is operated by a separate precision current source. Additional details can be found in Johnson et al. (1996) and Early and Johnson (1997).

In anticipation of the radiometric calibration measurements at OSC prior to the launch of the OrbView-2 satellite, and in support of the Fourth SeaWiFS Intercomparison Round-Robin Experiment (SIRREX-4, Johnson et al. 1996), the GSFC integrating sphere was calibrated at NIST in April 1995. The calibration used a standard strip lamp calibrated for spectral radiance, $L(\lambda)$, and a prism-grating monochromator (Early and Johnson 1997). The calibration was done at four radiance levels, with first 16 lamps, then 8, 4, and 1 lamp in operation. The strip lamp, which was calibrated using FASCAL, was used to determine the spectral radiance responsivity of the monochromator. The monochromator was used to determine the spectral radiance of the exit aperture of the sphere at the 16-lamp setting. Measurements at the other three radiance levels were referenced to the 16-lamp setting, because the dynamic range of the monochromator was insufficient for direct ratios to the strip lamp. The measured spectral radiance and the relative standard uncertainty were reported every 10 nm from 380–1,100 nm. The relative standard uncertainties, u_n^L, which is equal to $u\big(L(\lambda)\big)/L(\lambda)$, were from 0.3–2.6%, depending on the measurement wavelength and the number of lamps in operation. Table 7 summarizes the spectral radiance of the GSFC sphere as measured in April 1995 at NIST; more details are given in Early and Johnson (1997).

During the April 1995 measurements, the SXR was used to measure the spectral radiance at the center of the exit aperture of the GSFC sphere. The SXR and the NIST strip lamp and spectroradiometer system agreed to within 1.2% at the six measurement wavelengths of the SXR and all four sphere levels (Early and Johnson 1997). The agreement was within the combined uncertainties of the two methods for determining the spectral radiance of the sphere source. The SXR was also used to measure the spatial uniformity of the spectral radiance in the exit aperture of the sphere source at the same four radiance levels.

3.3 GSFC Spectroradiometer

The GSFC 746/ISIC spectroradiometer is a scanning single-grating monochromator which has a 10.2 cm diameter integrating sphere with a known entrance aperture as the collection optic. The 746/ISIC is calibrated prior to each measurement of an integrating sphere using a 1,000 W quartz-halogen standard irradiance lamp which is traceable to NIST. First, the irradiance responsivity is determined from measurements of the standard lamp. Then, the 746/ISIC is rotated to measure the spectral irradiance from the integrating sphere. The diameter of the exit aperture of the sphere, the diameter of the entrance aperture of the small sphere on the 746/ISIC, and the distance between the two apertures is used to convert the

Table 7. GSFC sphere radiances and relative standard uncertainties, $u_n^L = u\big(L(\lambda)\big)/L(\lambda)$, at the SeaWiFS design wavelengths for the lamp configurations studied by Early and Johnson (1997). The spectral radiance $L(\lambda)$ is given in units of $\mathrm{mW\,cm^{-2}\,sr^{-1}\,nm^{-1}}$ and the relative standard uncertainty is in percent.

λ_D	*16 Lamps*		*8 Lamps*		*4 Lamps*		*1 Lamp*	
[nm]	$L(\lambda)$	u_{16}^L	$L(\lambda)$	u_8^L	$L(\lambda)$	u_4^L	$L(\lambda)$	u_1^L
412	3.9096	0.51	1.8763	0.53	0.93162	0.54	0.23594	0.75
443	6.5185	0.47	3.1403	0.49	1.5616	0.49	0.39759	0.56
490	11.525	0.42	5.5805	0.42	2.7808	0.42	0.70939	0.44
510	13.960	0.40	6.7728	0.41	3.3771	0.41	0.86132	0.42
555	19.774	0.38	9.6299	0.38	4.8069	0.38	1.2253	0.39
670	33.762	0.33	16.548	0.33	8.2771	0.33	2.1060	0.33
765	41.605	0.31	20.433	0.31	10.233	0.31	2.5944	0.32
865	45.046	0.30	22.188	0.30	11.121	0.30	2.8096	0.32

measured spectral irradiance to the average spectral radiance for the exit aperture of the sphere. For the measurements at OSC on 6 March, the 746/ISIC measured from 400–900 nm with a bandwidth of about 4.8 nm and a step size of 10 nm. A single grating with 1,200 lines per millimeter, and blazed at 500 nm, was used, along with two order sorting filters which eliminated second order effects. On 7 March, the measurements covered the spectral range from 400–1,150 nm. The 746/ISIC system is sensitive to extraneous sources of radiation, since the field of view is the entire hemisphere. Table 8 indicates that scattered radiation is the major contributor to the uncertainty in the measurements of the 746/ISIC for wavelengths that are shorter than 440 nm.

Table 8. Estimated uncertainties for the 746/ISIC near a subset of the SeaWiFS bands (Johnson et al. 1997).

Wavelength [nm]	*Relative Standard Uncertainty* [%]
412	6.5
443	2.5
490	1.9
565	1.6
665	1.5

For the SeaWiFS calibration project, the 746/ISIC was used on 6–7 March to measure the spectral radiance of the GSFC sphere source in the OSC clean room. On 6 March, the SXR and the 746/ISIC measured the GSFC sphere with 16 lamps operating. Standard lamp F182, which was calibrated using FASCAL in August 1994, was used on 6 March to calibrate the 746/ISIC. Standard lamp F391, calibrated by Optronic Laboratories, was used on 7 March. On both days, the wavelength calibration of the 746/ISIC was determined using selected sources of standard emission lines.

3.4 SeaWiFS and OrbView-2

SeaWiFS was integrated with OrbView-2 in January 1994 and was shipped to VAFB in June 1997. During the January and April 1997 calibration, OrbView-2 was in the high-bay clean room at the OSC Germantown, Maryland facility. The instrument was controlled using the ground support equipment (GSE) at OSC, which was located just outside the clean room. In order to reduce sources of electronic noise, SeaWiFS and OrbView-2 were operated with battery power from the solar array simulators.

In SeaWiFS, the scan mirror rotates 360° at 6 Hz so that during portions of the scan, the view is through the instrument input aperture, while at other times, the inside of the instrument housing is observed. A second aperture provides a view of the SeaWiFS diffuse reflecting panel, which can be illuminated by the sun during the mission. Data can be archived for a selected portion of the complete scan, corresponding to 116.6°. These portions of the rotation of the scan mirror through the full cycle are named for convenience: *Earth mode* is when the scan mirror views the Earth from −58.3° to +58.3° about the nadir position (at 0° and the center of the telescope aperture), and *solar mode* is when the scan mirror views the interior of the instrument and the diffuse panel from 60–175° (Woodward et al. 1993). The electronic calibration pulse occurs during a portion of the solar mode, after the view of the on-board diffuser. During the work reported here, data were acquired for both the Earth and solar modes.

For both the Earth and solar modes, the zero offsets (or dark counts), for each channel are measured when the scan mirror views the interior of the instrument housing from 140–220° Woodward et al. (1993). The instantaneous field of view of one channel is $1.6 \times 1.6\,\mathrm{mrad}^2$. The four channels in each band are aligned along the direction of the moving image from the scan mirror. In either the 1:1 or the 4:1 TDI setting, the output of the four channels in each band are delayed before they are summed, so the resulting average corresponds to the same location on the

Earth's surface—this is termed a pixel. With the scan mirror rotating at 6 Hz, there are 1,285 pixels in one scan line, for either the Earth or the solar mode. For the dark count (DC) restore measurements, the average offset for the measurements over the scan angles from 140–220° is stored as pixel 0 and is used to correct the subsequent pixels in that scan line.

Real-time data acquisition at OSC in Germantown was used to control SeaWiFS and archive the data. In order to transfer the data files from the Germantown facility to the SeaWiFS Project in Greenbelt, Maryland, a second computer at the OSC site in Reston, Virginia was used. Computer security protocols at the Germantown facility prevented the direct transfer of the files. The transfer usually occurred during the evening hours, after the daily experiments were completed.

The environmentally-controlled clean room at OSC is inside the high-bay area. The environmental conditions in the clean room were recorded on 22 January 1997: the temperature was 21.1°C and the relative humidity was 34%. The filters for the clean room are located in the south wall, and the direction of air flow is from this wall to the opposite (or north) wall, which consists of many horizontal slats, or louvers. A metal roll-up door is located at the downstream end of the clean room in the east wall, so equipment and material can be moved from the high-bay area into the high-bay clean room. A row of windows is also situated in the east wall; these windows were covered with black paper during the calibration experiment. The overhead lights inside the clean room were turned off during all measurements. Although light could enter the clean room through the open louvers, it was not possible to close them and obstruct the air flow. Instead, all of the overhead lights in the high-bay area that illuminated the north wall were also turned off during all of the measurements.

4. MEASUREMENT PROCEDURES

The SeaWiFS calibration test occurred over a 4 month interval (Tables 1–3). The measurement procedures associated with the calibration of SeaWiFS can be divided into five functional areas:

1) Preparation and planning;
2) System verification;
3) Optical alignment and equipment operation;
4) Record keeping and archiving of the procedures and data; and
5) Executing measurements.

4.1 Preparation and Planning

Preparation and planning were a critical part of the calibration of SeaWiFS. On 9 September 1996, personnel from the SeaWiFS Project, OSC, and NIST met to discuss the experiment. The OSC facility was evaluated, and tasks were assigned to various teams or individuals. The dates of the calibration and the postvibration measurements were at the discretion of OSC, because the general prelaunch activities were assigned the highest priority.

During December 1996 and January 1997, prior to the calibration of SeaWiFS at the end of January, a test procedure was developed and documented in an internal SeaWiFS publication: *TP12001 SeaWiFS Post Thermal Vacuum Calibration Test Procedure*. The document was designed as a compilation of the documents that resulted from the experiment, of the methods of data analysis to be employed, and of the step-by-step experimental activities. TP12001 served as a pre-experiment planning document; once the experiment began, some of the procedures were modified and additional procedures were performed. Log sheets from the experiments are appendices in TP12001.

An attempt was made to plan for possible contingencies, such as, failed equipment or schedule conflicts with the NIST or SeaWiFS personnel. Spare parts, such as, seasoned 45 W lamps for the GSFC sphere source, were procured and taken to OSC. Additional personnel were made available in case the measurements at OSC came at inopportune times for the NIST or SeaWiFS personnel. Prior to the calibration, special data acquisition software for OrbView-2 was developed so that the SeaWiFS output counts could be reported in near-real time. Based on the November 1993 calibration of SeaWiFS (Tables 4–5) and the expected radiance of the GSFC sphere from the 1995 NIST calibration (Table 7), the anticipated output of SeaWiFS was determined. A spreadsheet was prepared so the new results could be compared to those based on the 1993 calibration. A spreadsheet was also prepared for the reduction of the SXR data, and the results from the April 1995 SXR measurements of the GSFC sphere were made available for rapid comparison.

Once the calibration experiment was underway, daily meetings were held to discuss the results acquired to date, and to review the plans for the next sequence of measurements. These daily review meetings usually occurred in the morning, while SeaWiFS and the GSFC sphere source were warming up. Departures from TP12001, which were generally in the experimental procedures, were discussed and noted as corrections to that document.

4.2 System Verification

Before a particular experiment was performed, and in some cases as part of the experiment, the instruments, data acquisition software, and laboratory environment were examined to determine the optimum experimental parameters to be used during the actual measurements. Usually, this consisted of performing additional measurements. These tests established the operating parameters of the instruments, allowed for the identification of sources of bias, and helped to familiarize personnel with the complete experimental system.

The first measurement of this nature occurred on 3 January 1997, at NIST. The GSFC sphere was operated with

a lamp configuration of 16, 8, 4, and then 1; measurements were made with the SXR. The results, when compared to the expected spectral radiance of the GSFC sphere (Early and Johnson 1997), indicated that for the same lamp configuration, the output had decreased as a function of wavelength (Sect. 1). It must be assumed that the SXR had remained in calibration over the interval from 1994–1997; this assumption is supported by a preliminary analysis of the second SXR calibration at NIST in 1996. This 3 January test also demonstrated that there were no gross equipment failures with either the GSFC sphere source or the SXR (lamp failure, power supply instabilities, etc.).

The second verification test occurred on 21 January 1997 in the OSC clean room in Germantown. The SXR measured the output of the GSFC sphere and the results were compared to the 3 January 1997 values. The results were in agreement, establishing that the equipment had not been altered by the transport from Gaithersburg to Germantown. Several measurements were made with various illumination conditions (especially the status of the overhead lights in the external high-bay area) so that extraneous sources of radiant flux would be minimized during the SeaWiFS calibration experiment. The final configuration is described in Sect. 3.4.

The third verification was on 22 January 1997, before the SeaWiFS calibration tests. SBRC personnel inspected the optics of SeaWiFS using visible and ultraviolet light sources. A few fibers and dust particles were observed inside the housing on a baffle, but no serious contamination was apparent. The few fibers were removed by vacuuming.

The voltage calibration pulse was used to determine gain ratios (Sect. 2.3) as an additional verification of SeaWiFS. The SeaWiFS output corresponding to a dark target, termed *background,* was another indicator of system stability. The voltage calibration pulse was used to verify SeaWiFS at OSC and at VAFB (Tables 1–3).

4.3 Alignment and Operation

The calibration experiment required that the SXR, the 746/ISIC, and SeaWiFS measure concentric areas in the exit aperture of the GSFC sphere source. Because the measurements were to take place at different times (e.g., before and after the SeaWiFS vibration tests), the alignment procedures and operation of the equipment were designed with repeatability in mind. All of the equipment was cleaned using lint-free cloths and alcohol before they were placed in the clean room.

On 21 January 1997, the GSFC sphere source was positioned so the separation between the sphere's exit aperture and SeaWiFS' entrance optic was about 2.5 m. The sphere was raised to the highest position possible, and positioned so the SeaWiFS nadir sample measured the center of the sphere's exit aperture at approximately normal incidence. The support frame of the GSFC sphere was made level, and the orientation of the plane of the exit aperture was checked using a bubble level. The support frame was readjusted until the exit aperture was plumb. Then, the adjustable feet of the sphere support frame were locked in place and the position of each of the feet was outlined on the floor using masking tape. The separation distance between the sphere and SeaWiFS was adequate for placement of the SXR and passage of personnel from the SXR operation station on the east side of the clean room to the exit door on the west side.

The SXR was mounted on its tripod, and positioned in its nominal position—1.35 m from the plane of the sphere's exit aperture to the face plate of the SXR, with the SXR aligned to view the center of the exit aperture at normal incidence. This separation distance corresponded to the configuration used at NIST in April 1995, and was chosen to achieve repeatability between the two measurements. With the aperture cover over the exit aperture of the sphere, the height, the location in the horizontal direction, and rotation about these two orthogonal axes of the SXR were adjusted until the SXR was aligned correctly to the GSFC sphere. Alignment was judged satisfactory when the SXR was level, at the correct distance from the sphere, and centered in the sphere's exit aperture. At the same time, the white alignment circle in the center of the aperture cover was centered in the SXR's field of view. (The SXR has an ocular alignment system that is co-aligned with the optical axis of the six measurement channels.) The position of the SXR tripod was recorded by outlining the position of the feet on the floor with tape. During measurements with SeaWiFS or the 746/ISIC, the SXR and its tripod were moved as a unit to an area away from the ongoing measurements.

The black disc used for recording the background counts for the various instruments (SXR, 746/ISIC, and SeaWiFS) was mounted on a second tripod. Using the visual sighting system in the SXR, this tripod was aligned to the optical axis of the SXR–GSFC sphere system and its location was also marked using tape. For most of the measurements, the *disc* tripod was left in place but the mount holding the disc was removed and the head of the tripod was lowered to a position below the lower edge of the exit aperture of the sphere.

On 22 January 1997, SeaWiFS was aligned to the GSFC sphere after the optics were inspected and cleaned. Using the controls on the mounting platform, OrbView-2 was rotated so that the motion of the SeaWiFS scan mirror resulted in measurements in the horizontal plane; this was the configuration used at SBRC in November 1993. With OrbView-2 level, the optical axis of SeaWiFS was too high and would have resulted in scans that were not centered in the sphere's exit aperture. Because the sphere was at the maximum height, OrbView-2 was pitched by about 1.1° using the hydraulic controls on the OrbView-2 mounting platform. OrbView-2 was moved until SeaWiFS appeared to view the center of the sphere's exit aperture with the nadir scan mirror position.

Because the alignment using tape measures was difficult, the final alignment involved measurements of the sphere exit aperture under conditions of partial obscuration. As one member of the team held a large, opaque target over a portion of the sphere's exit aperture, another member, situated at the control panel of the GSE, observed the output of a selected pixel. The target was moved from the edge to the center, in the horizontal and then the vertical directions. The final alignment corresponded to the optical axis of SeaWiFS about 2.5 cm from the center of the exit aperture of the sphere. The black disc used with SeaWiFS was aligned in a similar fashion. An undersized disc was chosen and the target was moved until the counts in the nadir pixel reached a minimum value. Then, the proper disc was put into place.

This sequence of alignment procedures established the alignment of the GSFC sphere, the SXR, and SeaWiFS for the 22–24 January set of measurements. Because SeaWiFS was moved in and out of the clean room for the vibration tests, the alignment procedure given above had to be repeated on 11 April 1997.

The GSFC sphere was operated as described in Johnson et al. (1996) and Early and Johnson (1997). The precision current supplies have a potentiometer for adjusting the current. On 21 January, the first time the GSFC sphere was operated at OSC, the potentiometers were adjusted so the digital display on the four separate power supplies read 6.500 A ±0.002 A. With 16 lamps operating, the sphere was allowed to warm up about 20 min before the final adjustment to the potentiometers. The power supplies contain an internal ramp-up circuitry so the current is varied from 0–6.5 A over an interval of about 2 min. This protects the filament in the lamp; however, there is no ramp-down circuitry. Because the position of the potentiometers can be difficult to reproduce, and because this was the standard operating practice for the GSFC sphere, the lamps were turned off by immediate cessation of the current. This may act to shorten the lamp lifetime, but it does result in enhanced repeatability of the GSFC sphere radiance. Compared to the operating values in April 1995 at NIST, the lamp currents for the sphere source at OSC in 1997 agreed within ±1 mA. The lamp voltages were the same within ±10 mV, except for lamp 10, which varied by up to ±150 mV during the 1995 calibration of the sphere.

For the January, March, and April set of measurements at OSC, the SXR was turned on and the filters and detectors were raised to 26°C using a thermoelectric element and a commercial temperature controller. Then the SXR was left in this configuration from 21–24 January, 6–7 March, and 10–11 April. SeaWiFS was turned on the day of the measurements, and generally, it was turned off during lunch. When SeaWiFS was on, there was power to the detector electronics and to the scan mirror motor. The batteries remained on trickle charge throughout. During the SeaWiFS mission, the detector electronics are turned off on the dark side of the orbit, about every 45 min. On 24 January, a special warm-up test of SeaWiFS was done, with SeaWiFS turned on after the SXR began its sequence of data acquisition.

4.4 Documentation

Various instrument record (or log) sheets were designed for use during SeaWiFS calibration. In addition, a laboratory notebook suitable for use in the clean room was used to record the actual sequence of events. Various personnel associated with the overall experiment kept other records in individual laboratory notebooks. These documents, along with this technical memorandum, form the record of the experiment.

Three test equipment log sheets were designed. The GSFC sphere log sheet was designed to record the output current from each of the four GSFC sphere power supplies, as indicated by the digital meters and the voltage across each lamp. This voltage is output to a fifth digital meter and a multiturn switch is used to select the lamp corresponding to the digital output. The lamps are connected in a four-wire configuration, and the displayed voltage corresponds to the voltage across the lamp. The organization of the GSFC sphere log sheet was made to coincide with the normal operation of the sphere source (Early and Johnson 1997). This involves measurements with a lamp configuration of 16, 8, 4, 1, and 0 lamps operating. The current output by each of the four power supplies, the voltage across each lamp, and the time and date of the measurement of these sphere parameters were recorded on the log sheet. Up to six separate measurements could be recorded on a single log sheet.

The SXR log sheet was used to record file name, time of the measurements, and the raw signals at various intervals in the measurements of the GSFC sphere source. For each of the six channels, the three possible types of data include the SXR output voltage for measurements with the lens cap on (*background*), the lens cap off and the SXR black disc in place (*ambient*), and the lens cap off and the black disc removed (*signal*). This latter configuration corresponds to direct measurements of the radiance in the exit aperture. Four sets of these data could be recorded on a single log sheet. Other information on the experimental parameters was entered into the computer data file.

The GSFC 746/ISIC log sheet followed the format developed at the SIRREX activities. Experimental parameters, such as the distance between the two apertures, the filename, the type of measurement, and the configuration of the 746/ISIC were recorded on the log sheets.

4.5 Measurements

Each of the experiments listed in Tables 1–2 followed a general format (Table 9). The format was finalized by first developing the TP12001 through discussions, then through trial and error (on 21 January 1997). Steps 1–6 were

done at the beginning of a set of experiments. In step 7, OrbView-2 and SeaWiFS were turned on, and housekeeping data were recorded. These data were used to determine if the spacecraft and instrument were operating normally. Step 3, where background counts or volts were recorded, was meant to monitor the instrument electronics, such as the transimpedance amplifiers, which have finite offset voltages.

The cords (step 12) were sections of flat cord, acceptable for use in the clean room, held across the center of the exit aperture. To position the cords, the aperture cover plate screws were used—the screws were installed in two pairs of opposing tapped holes around the circumference of the exit aperture. The intersection of the cords occurred at the center of the exit aperture and was apparent in the SXR's field of view.

Steps 9–27 describe measurements of the sphere with 16 lamps operating; the brightest sphere setting was always measured first. The subsequent measurements at the lower levels, however, did not alternate between the SXR and SeaWiFS, as Table 9 indicates, and the SXR was not always used first. Rather, the more efficient procedure of "A-B-B-A" was adopted, where A and B represent the two instruments. The first A-B pair corresponded to one sphere setting, and the next B-A pair corresponded to the following sphere setting. Which instrument began the sequence depended on which instrument was aligned to the sphere at that time. This sequence minimized the number of realignments of the SXR to the sphere. Finally, for measurements with the 746/ISIC, the general concept listed in Table 9 was followed, with the 746/ISIC substituting for SeaWiFS; however, only the 16-lamp level was measured.

4.5.1 Measurements on 21 January 1997

The objective on 21 January was to verify the operation of the GSFC sphere and the SXR (Sect. 4.2). After aligning the sphere and the SXR, tests were performed to determine which of the overhead lights in the external high bay area affected the measurements (Sect. 4.2). Data were acquired with a lamp operation of 16, 8, 4, and 1. A standard operating mode for the SXR was selected: two sets for the background data type, three sets for the ambient data type, and five sets for the signal data type. Each set consisted of 10 readings of the DMM for each channel, starting with channel 1 and ending with channel 6. It took about 45 s to acquire one set of SXR data.

4.5.2 Measurements on 22 January 1997

The objective of the measurements on 22 January was to determine preliminary values for the calibration coefficients of SeaWiFS. After the inspection and cleaning of the SeaWiFS optics (Sect. 4.2), the SeaWiFS alignment was verified as described above (Sect. 4.3). SeaWiFS was operated in the standard gain and TDI combination, $g = 1$ and the 4:1 TDI setting. The sphere was operated with 16, 8, 1, and 0 lamps in operation. A black disc 10 cm in diameter was used for the SXR ambient data type and a black disc 17.8 cm in diameter was used for SeaWiFS. For SeaWiFS, background data were acquired during the Earth and solar modes. The preliminary results indicated that the agreement with the 1993 calibration coefficients was within 5%, and extensive cleaning of the optics was not required.

4.5.3 Measurements on 23 January 1997

The objective of the measurements on 23 January was to determine the repeatability of the sphere–SXR and the sphere–SeaWiFS system by measuring the same illumination condition of the sphere in three separate measurements. The first warm-up interval for SeaWiFS was 1.5 h. The sphere was operated with a lamp configuration of 16, 8, 4, 1, and 0 (Table 9). SeaWiFS was operated with the standard gain and TDI setting. The first set was in the morning, and the black discs were used with both the SXR and SeaWiFS. Then, with the sphere off and the room lights off, SeaWiFS recorded background counts for the Earth and solar mode at two gain settings. SeaWiFS and the sphere were turned off during lunch, and the warm-up interval for both instruments after lunch was about 20 min. The second and third set of measurements of the five sphere levels took place during the afternoon of 23 January 1997.

4.5.4 Measurements on 24 January 1997

The objective of the measurements on 24 January was threefold:

1) Quantify the warm-up interval for SeaWiFS;
2) Perform the full calibration test for each of the 32 channels; and
3) Measure the linearity of SeaWiFS using the SXR as the reference instrument.

These latter data, however, were lost, either from human error or a computer malfunction; therefore, the linearity test was repeated on 11 April.

For the SeaWiFS warm-up test, the SXR was aligned to view the center of the exit aperture of the sphere at an angle of about 30° from the sphere–SeaWiFS optical axis. Lamps 3 and 4 in the sphere were turned on and allowed to stabilize for 50 min [the designations for the lamps are given in Early and Johnson (1997)]. Next, a 20 min SXR continuous measurement sequence was initiated, with measurements at all six channels. At the same time, SeaWiFS was turned on and measurements were made for about 20 min. Finally, both lamps in the sphere were turned off.

For the full SeaWiFS calibration, the sphere was operated with a lamp configuration of 16, 8, 4, 1, and 0. The measurement sequence began with SeaWiFS and the black discs were used to record ambient signals for both SeaWiFS and the SXR. At each sphere level, SeaWiFS was operated at all four gain settings and at the five TDI combinations. The measurements, therefore, included a repeat

Table 9. General format of the procedure for measurements of the GSFC sphere source at OSC using the SXR or SeaWiFS during 1997.

Step	*Data Type*	*Procedure*
1		Align the GSFC sphere and secure its position.
2		Align the SXR to the sphere and mark the location on the floor.
3		Align the second tripod and its black disc to the optical axis and mark location on floor.
4		Move the SXR and its tripod out of the way.
5		Align SeaWiFS to the sphere and secure its position.
6		Remove the dust cover from SeaWiFS.
7		Turn on SeaWiFS; initialize electronics and software.
8		Remove the sphere exit aperture cover and turn off all of the room lights.
9		Move the SXR with its tripod to the measurement location to view the sphere.
10	Background	Record the SXR or SeaWiFS output with all sources of radiant flux blocked (SXR) or turned off (SeaWiFS).
11		Remove the SXR lens cap.
12		Verify the alignment using two cords stretched across the exit aperture.
13		Install the SXR disc onto the second tripod.
14		Verify the alignment of the disc using a narrow visible object held across the disc center in the horizontal and vertical directions.
15		Replace the eyepiece cap on the SXR.
16		Turn on the sphere power supplies 1–4, for all 16 lamps operating.
17		Allow sphere to warm up at least 15 min.
18	Ambient	Measure the spectral radiance of the black disc with the SXR.
19		Record the sphere lamp currents and voltages.
20		Remove the SXR disc and the lower head of the second tripod.
21	Signal	Measure the spectral radiance of the sphere with the SXR.
22		Move the SXR out of the way.
23		Install the black disc for SeaWiFS on the second tripod; adjust the height.
24	Ambient	Measure the spectral radiance of the black disc with SeaWiFS.
25		Remove the SeaWiFS disc and lower head of the second tripod.
26	Signal	Measure the spectral radiance of the sphere with SeaWiFS.
27		Record the sphere lamp currents and voltages.
28		Turn off power supply 4 and 3, leaving 8 lamps operating.
29		Wait 5 min and continue measurements with 8, 4, 1, and 0 lamps.
30		Record the SeaWiFS background counts and then turn off SeaWiFS.

of the standard gain and TDI setting that was measured on 23 January.

4.5.5 Measurements on 6–7 March 1997

The objective of the measurements of the GSFC sphere with the 746/ISIC on 6–7 March was to determine the spectral radiance of the source as a function of wavelength. This information was required to quantify the wavelength-dependent degradation in the spectral radiance (observed at the six SXR wavelengths) in regions other than those of the SXR measurement wavelengths. The measurements took place in the OSC clean room. SeaWiFS and OrbView-2 were outside the room undergoing vibration testing.

On the morning of 6 March, the SXR and the 746/ISIC were turned on and aligned to the GSFC sphere. The wavelength calibration of the 746/ISIC was measured using a helium emission-line source. In the afternoon, standard irradiance lamp F182 was used to calibrate the 746/ISIC, which then measured the GSFC sphere with 16 lamps operating. An ambient measurement of the sphere was made using the 17.8 cm diameter black disc centered on the optical axis between the sphere source and the 746/ISIC. Then, the lamp was used a second time to calibrate the 746/ISIC. The 746/ISIC was moved from in front of the sphere and additional measurements of mercury and neon emission-line sources were performed. During this time, the SXR was used to measure the sphere.

On 7 March 1997, the measurements of the sphere with 16 lamps operating using the 746/ISIC and the SXR were repeated. First, the SXR measured the output of the sphere; then the 746/ISIC was aligned to the sphere and lamp F391 was used to calibrate the 746/ISIC. Next, the 746/ISIC measured the GSFC sphere, and then F391 was

used again to calibrate the 746/ISIC. Ambient measurements, with the direct beam blocked, were taken for both the measurements of the standard lamp and the sphere source. After this, the SXR was aligned to the sphere and a second measurement set was acquired. Finally, the sphere was turned off and several additional measurements with the 746/ISIC and the mercury and neon emission-line sources were made.

4.5.6 Measurements on 11 April 1997

The objective of the measurements on 11 April was to determine if the calibration coefficients or other measurable parameters (offset counts) had changed during the post-thermal vacuum vibration test of OrbView-2. Beginning with the raising of the sphere to its maximum height, the alignment procedures followed the steps taken on 21 January (Sect. 4.5.1), which are explained in Sect. 4.2. The partial occultation method was used to optimize the alignment of SeaWiFS to the exit aperture of the sphere. The sphere source was operated with a lamp configuration of 16, 8, 4, 1, and 0. As on 24 January, SeaWiFS made measurements at all four gain settings and at five TDI settings. By the time the measurements began, SeaWiFS had been on for 4 h and the SXR had been on for over 12 h. The black disc was used to record the ambient signal for both SeaWiFS and the SXR. Only one sequence of the various sphere levels was performed, starting with the SXR.

For the measurement of the SeaWiFS linearity, the SXR was relocated to the same off-axis position used during the warm-up test on 24 January. The sphere was operated at 16, 15, 14, ... 2, 1, and 0 lamps. The SXR recorded one data set (one set with the average of 10 readings for each channel) at each sphere level and SeaWiFS recorded data for 20 s. SeaWiFS was operated at the 4:1 TDI setting and measurements were made of each sphere level at gain 1 and gain 3.

5. SXR AND 746/ISIC RESULTS

The details of the analysis of the SXR and the 746/ISIC measurements of the GSFC sphere at OSC are described in this section. The analysis is necessary because, based on the SXR as a transfer radiometer, the GSFC sphere did not remain stable between April 1995 and January 1997, so the calibration by NIST in April 1995 was not valid in 1997. After the SXR and the 746/ISIC results are described, the method used to determine the spectral radiance of the sphere source for the calibration of SeaWiFS at OSC is explained.

5.1 SXR Measurements

The SXR was used to measure the GSFC sphere source in conjunction with the calibration of this source at NIST in April of 1995 (Early and Johnson 1997). The agreement between the NIST calibration, which was based on a standard lamp of spectral radiance and the SXR, was 1.2% or better (Table 6 in Early and Johnson 1997). As a function of the SXR measurement wavelength, the difference was very similar for each of the four lamp levels. The two largest differences were −1.1% at 442 nm, with the SXR giving a smaller value than the NIST calibration, and 1.2% at 548 nm, with the SXR giving a larger value than the NIST calibration. The spectral radiance of the GSFC sphere source measured by the SXR in 1995 is given in Table 10. The SXR measurements were corrected for the SSE using the model based on the measurements of the point spread response function (Johnson et al. 1998). The measurement wavelengths and calibration coefficients used to reduce the SXR data for this 1995 study coincided with those used in earlier publications (Mueller et al. 1996 and Johnson et al. 1996).

The average of the SXR spectral radiance measurements of the GSFC sphere at OSC from 21 January to 11 April 1997 are also given in Table 10. As explained above, the black disc was used to record the excess signal arising from the SSE in the SXR. In addition, revised SXR effective wavelengths and calibration coefficients (Table 6) were used to reduce the 1997 values. Therefore, the 1997 spectral radiances normalized by the 1995 values include differences resulting from these changes in the SXR measurement wavelengths and calibration coefficients.

The revised SXR measurement wavelengths were different from those used in 1995, because the definition in (2) was used instead of the previous definition, which was analogous to (1). The revised calibration coefficients were different, because the model used to interpolate the spectral radiance of the SXR calibration source was updated to one that gave smaller residuals. These changes are within the SXR uncertainties. The GSFC sphere spectral radiance measured by the SXR, normalized to the average value, from 21 January to 11 April are plotted in Fig. 1 for the 16 and 1 lamp levels. Because there is no obvious trend in these data, the average of all of the SXR results was determined. The standard deviation of the measurements at each wavelength and lamp level is one component in the SXR uncertainty budget (Tsai and Johnson 1998).

Because the ratios of the SXR-measured spectral radiances in Table 10 depend on the method used to assign the measurement wavelengths and calibration coefficients, the ratio of the net signals from the SXR were determined. The average net signal, corrected for SSE, for each SXR channel determined in 1997 at OSC, was divided by the corresponding value from the 1995 NIST calibration experiment. These ratios are plotted in Fig. 2a. The difference in the ratio of the net voltages to the ratios of the spectral radiances for the 1995 and 1997 SXR measurements agree to within ±0.5%, except for channel 2, where the two methods of determining the ratio differ by 1%.

Figure 2a indicates that for the 16, 8, and 4 lamp configuration, the relative decrease in the radiance of the GSFC sphere was the same at each SXR wavelength, with

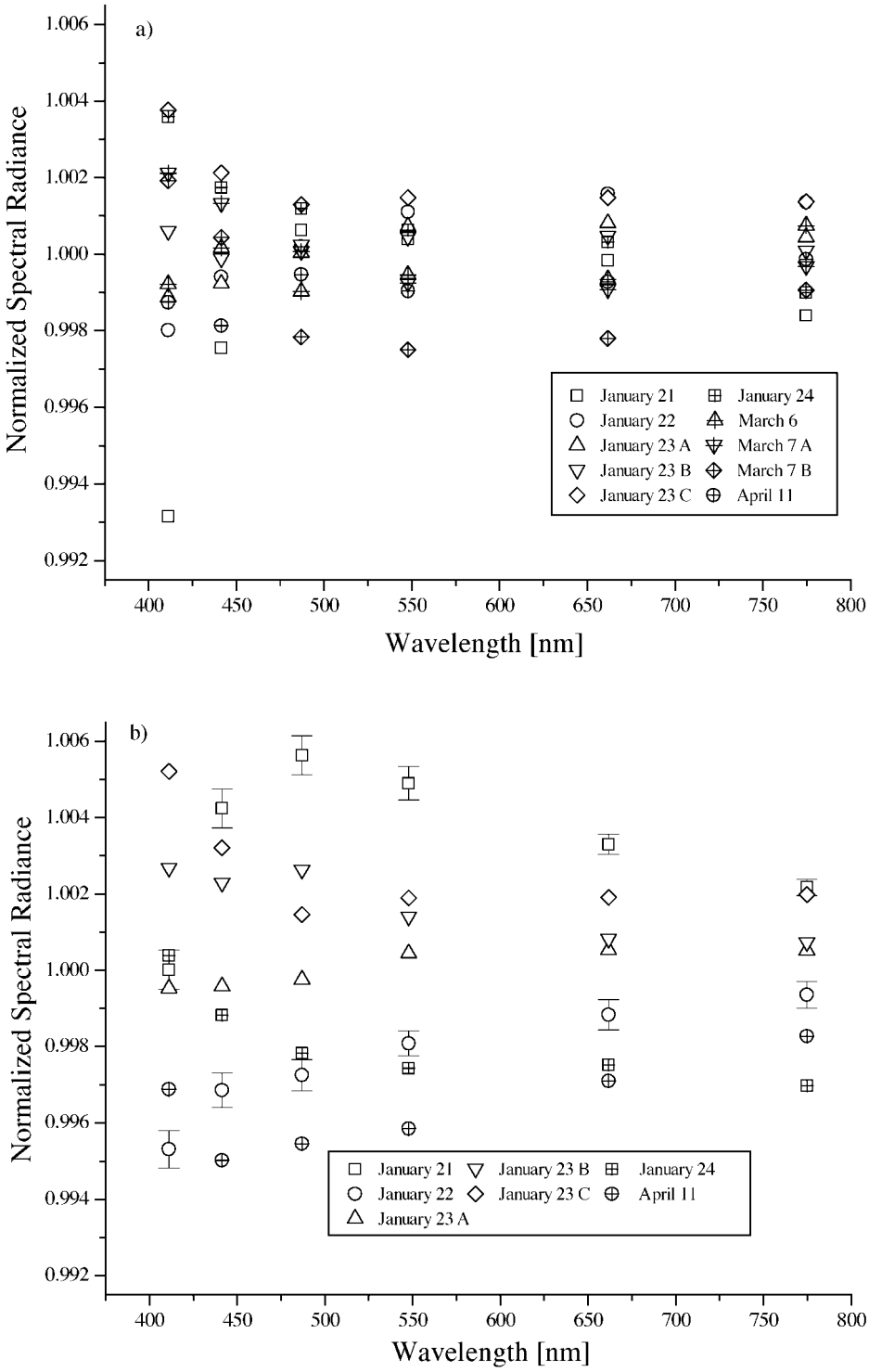

Fig. 1. Spectral radiances of the GSFC integrating sphere measured at OSC in Germantown, Maryland using the SXR. The results are normalized by the average values at each SXR measurement wavelength. Each symbol corresponds to a different day, as indicated in the legend. The relative standard deviations of each SXR measurement are illustrated using vertical lines only because these values are larger than, or comparable to, the size of the plotted symbols: **a)** radiances for the 16 lamp configuration, and **b)** radiances for the 1 lamp configuration.

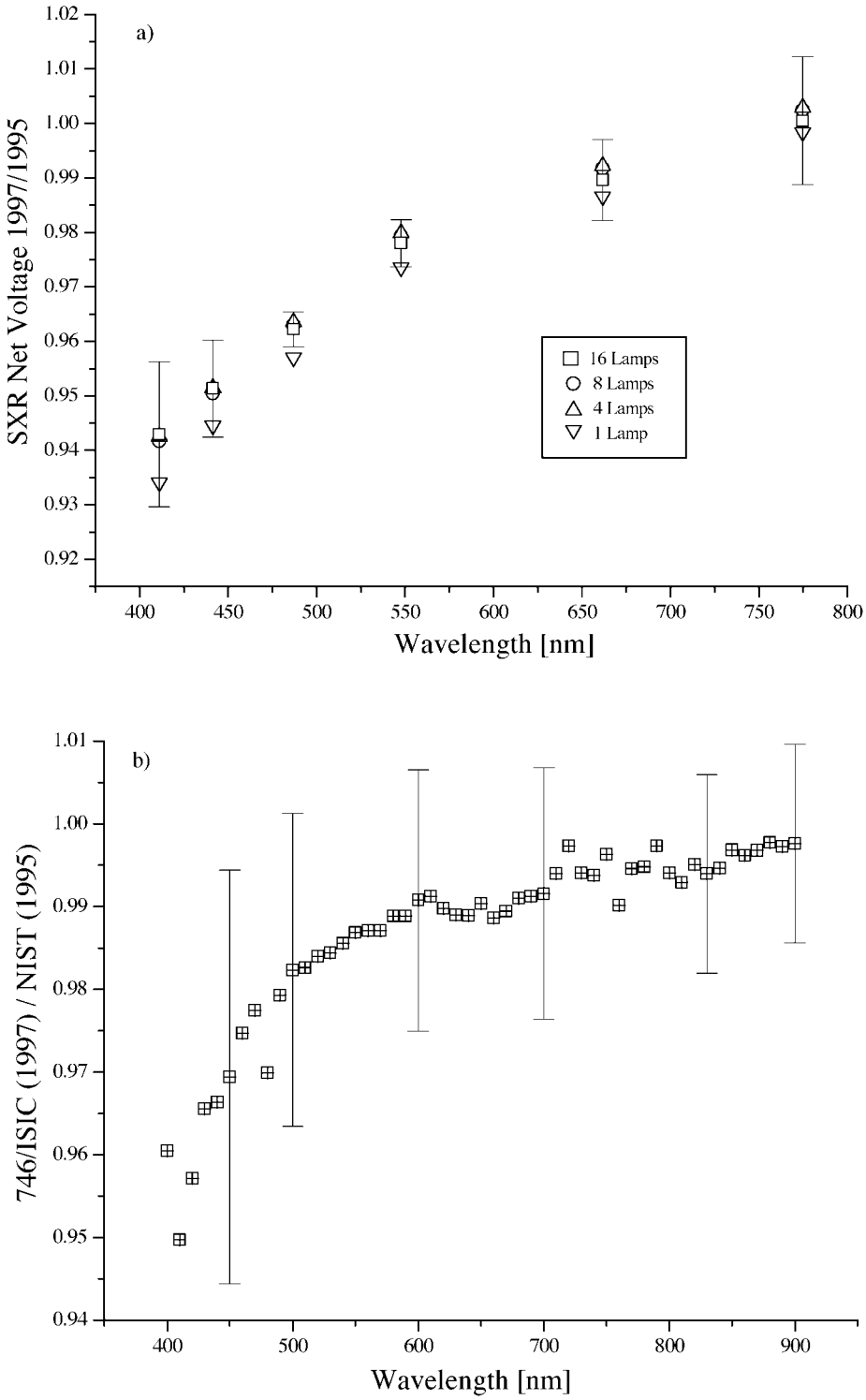

Fig. 2. The average net signals measured by the SXR and the 746/ISIC in 1997 for the GSFC integrating sphere at the different lamp settings normalized by the corresponding value from the NIST 1995 calibration of the sphere source. The vertical lines represent, for the 16 lamp configuration, the combined standard uncertainty for these ratios: **a)** measurements by the SXR, and **b)** measurements by the 746/ISIC (16 lamps).

Table 10. A comparison of the SXR spectral radiances measured for the GSFC sphere source in 1995 and 1997, and the ratio of these values. The SXR spectral radiances are in units of $\mathrm{mW\,cm^{-2}\,\mu m^{-1}\,sr^{-1}}$.

λ_{SXR}	*16 Lamps*			*8 Lamps*			*4 Lamps*			*1 Lamp*		
[nm]	1995	1997	97:95	1995	1997	97:95	1995	1997	97:95	1995	1997	97:95
411.2	3.853	3.646	0.946	1.848	1.746	0.945	0.9188	0.8690	0.946	0.2349	0.2202	0.937
441.5	6.317	6.074	0.962	3.040	2.920	0.961	1.512	1.454	0.962	0.3865	0.3689	0.954
487.0	11.22	10.84	0.966	5.422	5.244	0.967	2.702	2.614	0.967	0.6899	0.6631	0.961
547.9	19.08	18.57	0.973	9.269	9.034	0.975	4.626	4.511	0.975	1.180	1.143	0.969
661.7	32.81	32.40	0.988	16.05	15.88	0.989	8.026	7.947	0.990	2.040	2.009	0.985
774.8	42.36	42.60	1.006	20.82	20.97	1.007	10.42	10.51	1.009	2.642	2.651	1.003

the largest change observed at the shortest measurement wavelength. For the single lamp configuration, the spectral trend is the same, but the magnitude of the change is greater. Ancillary SXR data on the GSFC sphere, acquired at SIRREX-4 in May 1995, and during a special test in December 1995, were compared to the 1997 values and correlated with lamp operating hours and the total elapsed time. The observed change in the GSFC sphere depends on the total elapsed time, and not the total lamp operating hours. This indicates that a temporal change in the reflectance of the barium sulfate coating, which is a known effect, is the primary reason for the change in the output of the GSFC sphere between 1995 and 1997. The difference observed for the 16, 8, and 4 lamp configuration and the single lamp configuration may be due to the change in the color temperature of lamp 1, which is used for more hours than the other 15 lamps in the sphere.

The uncertainties shown in Fig. 2a reflect the use of the SXR as a transfer radiometer for measurements of the same source separated in time. There are four components to the uncertainty:

1) The stability of the SXR between the measurements of the GSFC sphere source;
2) The measurement uncertainty in 1995;
3) The measurement uncertainty in 1997; and
4) The uncertainty in the correction for the SSE.

To estimate the stability of the SXR from 1995 to 1997, the calibration coefficients that were used to reduce the 1997 OSC measurements (determined from the SXR calibration in September 1994) were compared to new values (preliminary results determined from the SXR calibration in the fall of 1996). For channels 1 and 3–5, the values agreed to within ±0.7%; for channels 2 and 6, the agreement was within −1.7% and 1.3%, respectively.

The standard deviations of the 1995 SXR measurements were not accessible for this work, so the SXR measurement uncertainties from the second set of measurements on 23 January 1997 at OSC were used to represent the SXR measurement uncertainties the day the sphere was calibrated at NIST (24 April 1995). The standard deviations of all of the SXR results at OSC (Fig. 1) were used to represent the measurement uncertainty for the SXR in 1997. These standard deviations, therefore, include the repeatabilities of the measurements for the GSFC sphere and the SXR, i.e., for the source–detector system. The uncertainty associated with the correction for the SSE was determined using the larger of either the estimated uncertainty in the correction from the model (Johnson et al. 1998) or the difference between the results predicted from the model and the results measured with the black disc. These uncertainties are from 0.1–0.3%, depending on the SXR measurement channel (Tsai and Johnson 1998). The combined relative standard uncertainty from these four sources of uncertainty is from 1.4–0.4% (Fig. 2a).

5.2 746/ISIC Measurements

The spectral scans of the gas discharge lamps were used to estimate the accuracy of the wavelength scale of the 746/ISIC. The 692.947, 724.517, and 966.542 nm lines in neon, and the 435.84, 546.07, and 1013.975 nm lines in mercury were measured, along with the helium-neon laser line at 632.82 nm. The center wavelength for each line shape was determined using the mean of the wavelengths for which the signal was 10% of the maximum value. The difference in these center wavelengths, plus the wavelength reading of the 746/ISIC, was fit to a second order polynomial and then used to correct the 746/ISIC measurements. The correction to the 746/ISIC wavelength scale, which read low, was between 0.52 nm at 400 nm and 0.89 nm at 850 nm.

For the measurements of the sphere, the net signals were determined using the scans of the sphere aperture with the black disc in place, and for the lamp, the net signals were determined with the direct beam blocked from the lamp to the 746/ISIC. The spectral radiances for the 6 March measurements with F182, where the lamp was measured before and after the sphere, were determined using the second lamp scan only, because the signals from the two lamp scans differed by about 0.5% and the second lamp scan was deemed more reliable (J. Cooper pers. comm.). The spectral radiances for the 7 March measurements using F391, where the lamp was measured before and after the two measurements of the sphere, resulted in consistent signals, so the average lamp signal from the three lamp scans and the average sphere signal were determined.

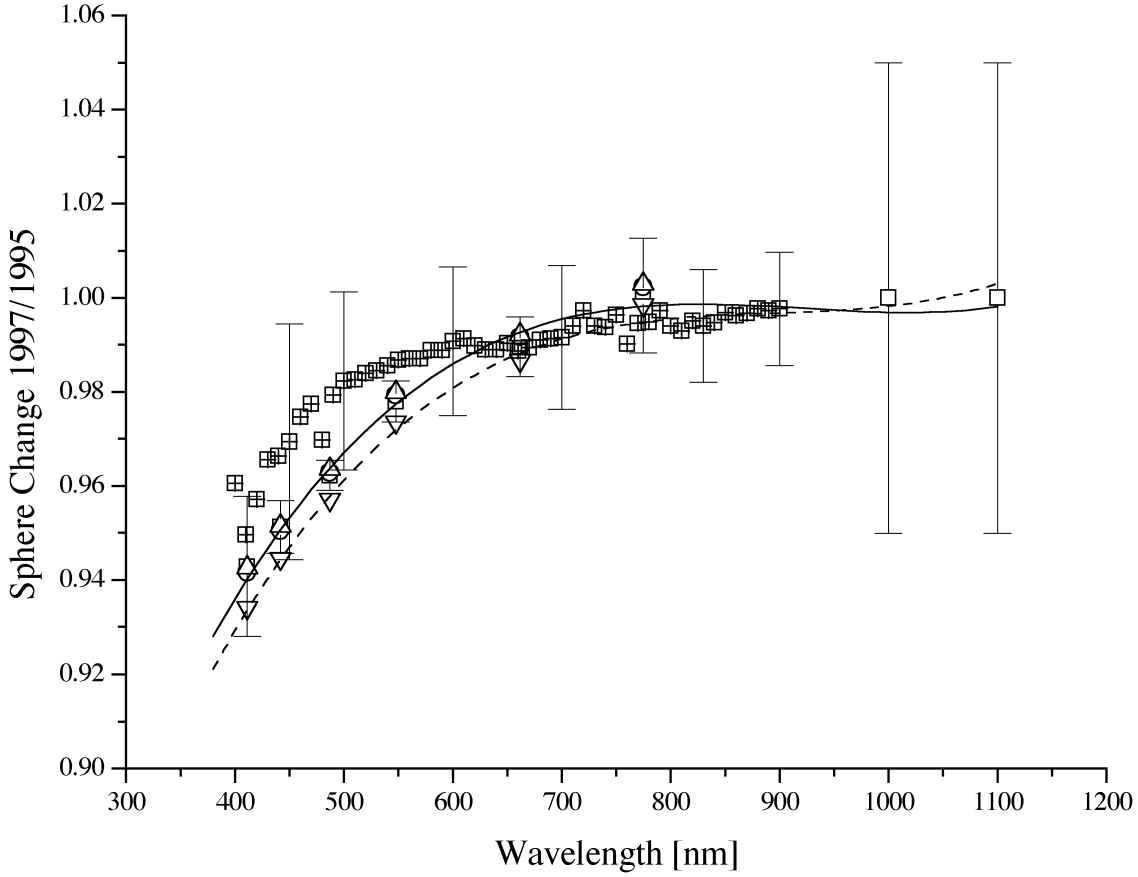

Fig. 3. Measurements of the relative change in the spectral radiance of the GSFC sphere source as measured in 1997 and normalized by the 1995 measurements at NIST. The SXR and 746/ISIC normalized results are plotted using the same symbols as in Fig. 2. The solid line is a third order polynomial fit for the 16, 8, and 4 lamp configuration, and the dashed line is a third order polynomial fit for the 1 lamp configuration. The vertical lines represent the combined uncertainties (Fig. 2), except for the two points at 1,000 nm and 1,100 nm.

The 6 March 746/ISIC measured radiances were not consistent with the 7 March values; the 7 March values were about 4% greater over the spectral range where the measurements could be compared (400–900 nm). A check of the records for F391 revealed more than 50 h of operation since its calibration. For this reason, it was concluded that F391 could not be used to reliably calibrate 746/ISIC. This is unfortunate, because F182 was only calibrated to 900 nm. The 6 March 746/ISIC data are presented in Fig. 2b as the ratio of the 6 March 1997 746/ISIC measurements of the GSFC sphere source with 16 lamps operating, normalized by the April 1995 NIST calibration (Early and Johnson 1997). It is possible to directly compare these results because both were measured with a 10 nm wavelength interval, nearly the same bandwidth, and at the same wavelengths.

5.3 Source Spectral Radiance

Comparison of Figs. 2a and 2b indicates that the sphere radiance for wavelengths beyond about 750 nm did not decrease significantly between April 1995 and the measurements in 1997. In the spectral region from 400–450 nm, however, the ratio of the SXR net voltages and the ratio of the spectral radiances determined using the spectroradiometers indicate the sphere radiance decreased by 4–6%, with the 746/ISIC predicting the smaller change. These ratios, which indicate the change in the radiance of the sphere as measured using the SXR and the 746/ISIC, are plotted together in Fig. 3. This change is consistent with the aging of the barium sulfate coating; Johnson et al. (1996) report the measurements of the GSFC sphere before and after it was recoated in April 1994.

The ratio of net signals is the correct factor to use for the SXR comparison of the 1995 and 1997 sphere radiance because this removes any sensitivity to the assigned values for the SXR calibration coefficients or measurement wavelengths. The SXR has demonstrated good stability, including transportation to a remote facility; measurements of a NIST sphere source before and after shipment to Japan resulted in an average difference of 0.05% (Johnson et al. 1997).

The ratio of spectral radiance assigned to the sphere source is the correct factor to use for the 746/ISIC measurements. The 746/ISIC cannot be used to determine signal ratios between the 1995 calibration and the 1997 SeaWiFS calibration because measurements were not made in 1995 using the 746/ISIC. In addition, the 746/ISIC is not stable; it requires calibration whenever it is used, so the results are always expressed in radiometric units.

The correction factors were determined by using only a part of the measurements from the two determinations of the relative change in the sphere radiance. The most reliable determination derives from the SXR measurements, but the results at the six SXR wavelengths are insufficient to determine the relative change in the sphere radiance over the required spectral region of 380–1,100 nm. The longest measurement wavelength of the SXR is 775 nm. The 746/ISIC measurements are sensitive to scattered light below about 450 nm (Johnson et al. 1997), and the relative standard uncertainty is comparable to the SXR-determined relative change in the sphere below about 550 nm. To estimate the correction for wavelengths greater than 775 nm, two values from the 746/ISC measurements of the 16 lamp configuration were included, at 830 and 900 nm (Fig. 3).

The lines in Fig. 3 are the result of modeling the decrease in the sphere radiance as a third order polynomial. Two fits were performed, one to represent the average relative change from April 1995 to the spring of 1997 for the GSFC sphere radiances corresponding to 16, 8, or 4 lamps operating, and the second for the 1 lamp configuration. In order to extend the polynomial fit to 1,100 nm without introducing any nonphysical behavior, the ratio was assigned to be unity at 1,000 and 1,100 nm, with a relative standard uncertainty of 5%. This is a reasonable approximation, because the reflectance of the sphere coating is expected to change more rapidly at shorter wavelengths rather than at longer wavelengths, and such changes are not expected to result in increased sphere radiances.

The coefficients for the two fits, a_0, a_1, a_2, and a_3, are given in Table 11. For the 16, 8, and 4 lamp configuration, the 18 results from the SXR were used, along with the two results from the 746/ISIC measurements and the two forced values. For the 1 lamp configuration, the six SXR results were used, along with the two results from the 746/ISIC measurements, even though they were for the 16 lamp configuration. The two forced values were also included. This was necessary to produce a reasonable fit over the desired spectral range of 380–1,100 nm. For each fit, the uncertainties indicated by the vertical lines in Fig. 3 were used to weight the data.

These polynomials represent the correction factor $F_n(\lambda)$, for the NIST 1995 spectral radiances used to determine the spectral radiance of the GSFC sphere source at OSC in 1997. The NIST 1995 spectral radiances are denoted $L_{n,95}(\lambda)$ and the final values used at OSC for the calibration of SeaWiFS in 1997 are denoted $L_{n,97}(\lambda)$:

$$F_n(\lambda) \;=\; a_0 \;+\; a_1\lambda \;+\; a_2\lambda^2 \;+\; a_3\lambda^3 \qquad (3)$$

and

$$L_{n,97}(\lambda) \;=\; F_n(\lambda)L_{n,95}(\lambda), \qquad (4)$$

where n corresponds to the number of lamps operating (the 16, 8, 4 or 1 lamp configuration). The coefficients for (3) are given in Table 11. The results for $L_{n,97}(\lambda)$ are shown in Fig. 4.

The uncertainties in the spectral radiance determined using the 1995 NIST calibration values and (4) were determined by summing in quadrature the uncertainties in the ratios used in the fit (Fig. 3) and the uncertainties in the NIST calibration (Early and Johnson 1997). The uncertainties in the ratios were estimated every 10 nm from 380–1,100 nm using a *smoothing* interpolation function in a standard data analysis package (KaleidaGraph from Synergy Software). The input values consisted of the uncertainties in the ratios at the six SXR wavelengths, as well as the values at 830, 900, 1,000, and 1,100 nm. The uncertainties in the spectral radiance of the GSFC sphere at OSC are about 1.6% for band 1, less than 1% for bands 2–6, and 1.2% for bands 7–8. There is a weak dependence on lamp configuration (Fig. 5).

As a verification of the spectral radiance determined for the GSFC sphere using the method described above, a cubic spline interpolation was performed at the SXR measurement wavelengths (Table 6) in these radiances (on a 10 nm grid). The results were compared to the average spectral radiances determined with the SXR in 1997 at OSC (Table 10). The agreement was good, with average differences of 0.9, 0.2, 0.7, 0.8, −0.7, and 1.3% for SXR channels 1–6, respectively.

5.4 Spectral Radiances for SeaWiFS

The spectral radiances $L_{n,97}(\lambda)$ from (4) are given at the same wavelengths that were measured during the NIST calibration of the GSFC sphere source in April 1995, i.e., from 380–1,100 nm every 10 nm. Two methods of using these values to determine the SeaWiFS calibration coefficients are described.

The first method is required to compare the results at OSC to the results obtained by the instrument manufacturer for their November 1993 measurements (Barnes et al. 1994b). For that work, the calibration coefficients were determined using the net counts from SeaWiFS and the corresponding spectral radiance at the nominal center wavelengths, λ_D (Table 4). To determine the spectral radiance at these wavelengths, a cubic spline interpolation in the $L_{n,97}(\lambda)$ values was used. The results are given in Table 12, along with the corresponding value for the standard uncertainty in these values, $u_n\big(L(\lambda_D)\big)$ (Fig. 5).

After the initial calibration of SeaWiFS in 1993 (at SBRC) was completed, the SeaWiFS Project concluded that band-averaged spectral radiances provided a better representation of the measurements (Barnes and Yeh 1996).

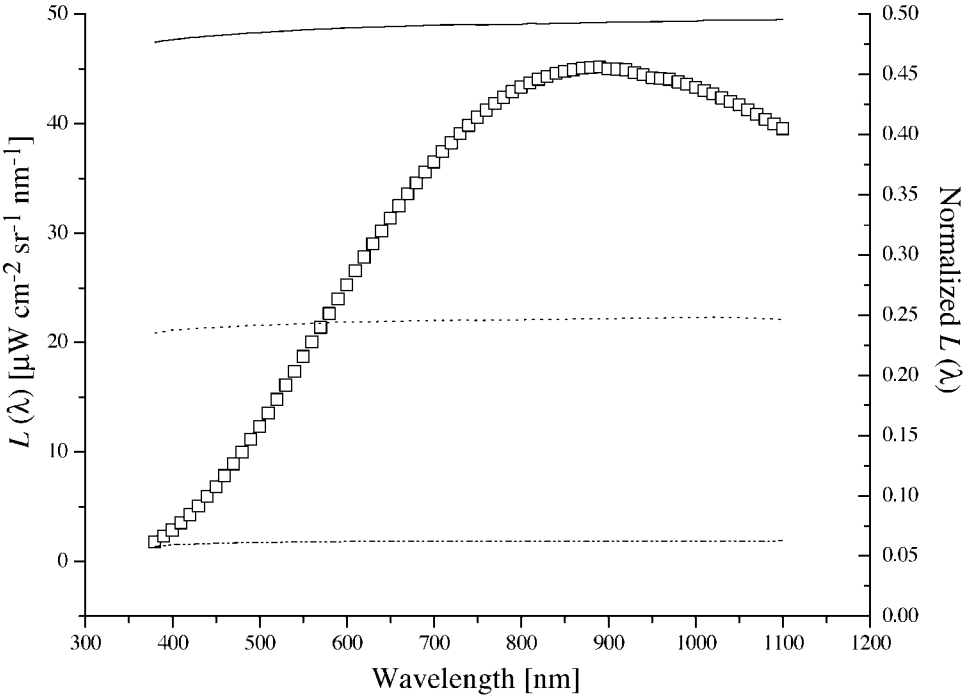

Fig. 4. Spectral radiance of the GSFC sphere source for the recalibration of SeaWiFS at OSC in 1997. The spectral radiance with 16 lamps operating is indicated with the open squares; the values correspond to the left ordinate. The spectral radiance with the 8, 4, and 1 lamp operation is illustrated using the solid, dot, and dash-dot-dot lines. These spectral radiances were normalized by the values for the 16 lamp configuration and these ratios correspond to the right ordinate.

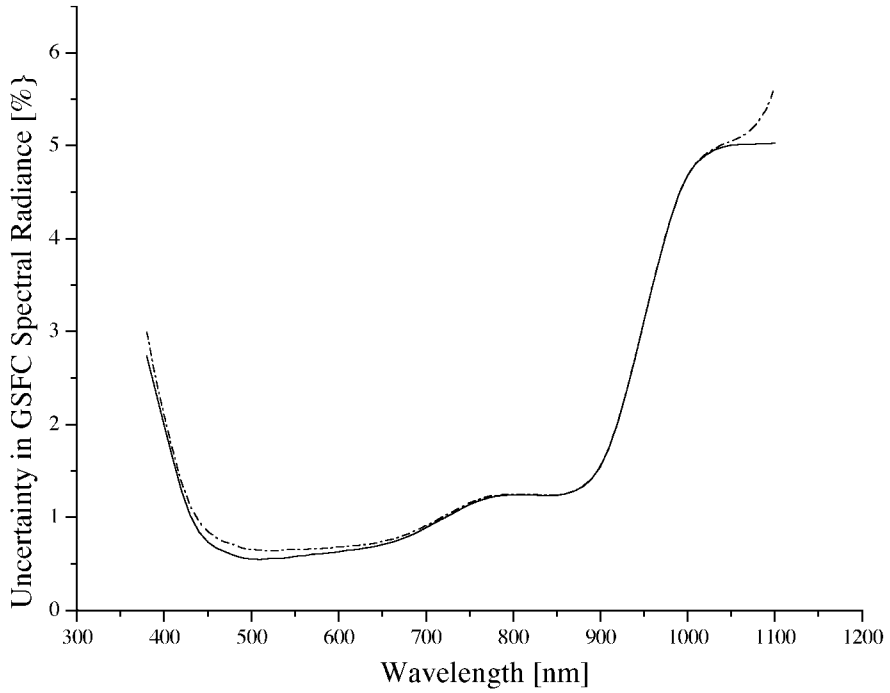

Fig. 5. Relative standard uncertainties, expressed in percent, of the spectral radiance of the GSFC sphere source at OSC in 1997 for the calibration of SeaWiFS. The solid line corresponds to the 16 lamp configuration, and the dash-dot line corresponds to the 1 lamp configuration.

Table 11. Polynomial coefficients for the correction factors used to determine the spectral radiance of the GSFC sphere at OSC in 1997 from the NIST 1995 calibration values. Two sets of values were determined, one for the sphere levels corresponding to 16, 8, and 4 lamps operating, and the other for the sphere levels corresponding to 1 lamp operating.

Coefficient	*Values*		*Unit*
	16, 8, 4 Lamps	1 Lamp	
a_0	0.630958	0.614468	Dimensionless
a_1	1.22001×10^{-3}	1.26463×10^{-3}	nm^{-1}
a_2	-1.33729×10^{-6}	-1.40356×10^{-6}	nm^{-2}
a_3	4.83255×10^{-10}	5.22699×10^{-10}	nm^{-3}

Table 12. Spectral radiances and relative standard uncertainties, $u_n^{\mathrm{D}}(\lambda_{\mathrm{D}}) = u_n\big(L(\lambda_{\mathrm{D}})\big)/L_{n,97}(\lambda_{\mathrm{D}})$ at the SeaWiFS nominal center wavelengths for the GSFC sphere source at OSC. The units of spectral radiance are $\mu\mathrm{W\,cm^{-2}\,sr^{-1}\,nm^{-1}}$ and the relative standard uncertainty is in percent.

λ_{D}	*16 Lamps*		*8 Lamps*		*4 Lamps*		*1 Lamp*	
[nm]	$L_{16,97}(\lambda_{\mathrm{D}})$	$u_{16}^{\mathrm{D}}(\lambda_{\mathrm{D}})$	$L_{8,97}(\lambda_{\mathrm{D}})$	$u_{8}^{\mathrm{D}}(\lambda_{\mathrm{D}})$	$L_{4,97}(\lambda_{\mathrm{D}})$	$u_{4}^{\mathrm{D}}(\lambda_{\mathrm{D}})$	$L_{1,97}(\lambda_{\mathrm{D}})$	$u_{1}^{\mathrm{D}}(\lambda_{\mathrm{D}})$
412	3.668	1.61	1.760	1.61	0.8740	1.61	0.2201	1.72
443	6.188	0.98	2.981	0.99	1.482	0.99	0.3754	1.10
490	11.10	0.61	5.376	0.61	2.679	0.61	0.6800	0.71
510	13.52	0.57	6.559	0.58	3.270	0.58	0.8300	0.67
555	19.33	0.59	9.416	0.59	4.700	0.59	1.193	0.66
670	33.51	0.78	16.42	0.78	8.215	0.78	2.083	0.81
765	41.49	1.16	20.38	1.16	10.20	1.16	2.580	1.18
865	44.96	1.35	22.15	1.35	11.10	1.35	2.800	1.35

Table 13. Band-averaged radiances and relative standard uncertainties, $u_n^{\mathrm{B}}(\lambda_{\mathrm{B}}) = u_n\big(L_{\mathrm{B}}(\lambda_{\mathrm{B}})\big)/L_{n,\mathrm{B},97}(\lambda_{\mathrm{B}})$. The units of band-averaged radiance are $\mu\mathrm{W\,cm^{-2}\,sr^{-1}\,nm^{-1}}$. The values of λ_{B} are for the 16 lamp configuration. They vary by less than 0.05 nm for the three other lamp configurations.

λ_{B}	*16 Lamps*		*8 Lamps*		*4 Lamps*		*1 Lamp*	
[nm]	$L_{16,\mathrm{B},97}$	$u_{16}^{\mathrm{B}}(\lambda_{\mathrm{B}})$	$L_{8,\mathrm{B},97}$	$u_{8}^{\mathrm{B}}(\lambda_{\mathrm{B}})$	$L_{4,\mathrm{B},97}$	$u_{4}^{\mathrm{B}}(\lambda_{\mathrm{B}})$	$L_{1,\mathrm{B},97}$	$u_{1}^{\mathrm{B}}(\lambda_{\mathrm{B}})$
415.55	3.837	1.86	1.842	1.87	0.9146	1.87	0.2301	1.98
444.79	6.303	0.98	3.037	0.99	1.511	0.99	0.3821	1.09
493.08	11.32	0.85	5.482	0.86	2.732	0.86	0.6927	0.96
511.02	13.55	0.58	6.573	0.58	3.277	0.58	0.8309	0.67
558.16	19.42	0.77	9.460	0.78	4.722	0.78	1.197	0.85
668.80	33.30	0.87	16.32	0.87	8.163	0.87	2.068	0.90
767.51	41.50	1.18	20.39	1.18	10.21	1.18	2.579	1.20
865.05	44.69	1.65	22.01	1.65	11.03	1.65	2.782	1.65

The band-averaged radiance is defined (Barnes 1996c) as

$$L_{n,\mathrm{B},97} = \frac{\int_{380}^{1100} L_{n,97}(\lambda)R(\lambda)d\lambda}{\int_{380}^{1100} R(\lambda)d\lambda}, \qquad (5)$$

where $R(\lambda)$ is the spectral responsivity for one SeaWiFS band (Barnes et al. 1994) and $L_{n,97}(\lambda)$ is the spectral radiance of the source. Note that the units of $L_{n,\mathrm{B},97}$ are the same as those for spectral radiance, but this is due to the choice of normalization; the physical interpretation of $L_{n,\mathrm{B},97}$ corresponds to radiance. The band-averaged spectral radiances calculated from (4) and (5) are given in Table 13. The calculation of the uncertainties in these values, $u_n(L_{\mathrm{B}})$, is described in Sect. 7. For the laboratory measurements, it is not necessary to associate a value for λ_{B} with $L_{n,\mathrm{B},97}$. For in-orbit measurements, it may be necessary to define λ_{B} for the algorithms that convert the SeaWiFS measurements to geophysical quantities.

6. SeaWiFS RESULTS

The methods used to reduce and analyze the SeaWiFS data are described in this section. The emphasis is on the measurements made on 24 January and 11 April 1997 in

the 1:1 TDI setting; these data are used to derive the calibration coefficients for SeaWiFS. Similar methods were used to analyze the SeaWiFS data from the other measurements (Tables 1–3).

6.1 Measurement Equation

The basic measurement equation, in the laboratory during the prelaunch calibration, or from orbit, is

$$S_x(g,c) \;=\; \frac{1}{\gamma_x(g,c)}\int_{380}^{1100} L_x(\lambda)\,R(\lambda)\,d\lambda, \qquad (6)$$

where $S_x(g,c)$ are the corrected net signals that depend on the measurement condition ($x =$ "lab" or "orbit"), g is the gain, and c is the channel. $L_x(\lambda)$ is the spectral radiance of the source for that measurement condition, and $\gamma_x(g,c)$ is a constant that depends on the measurement conditions and instrument parameters. The limits of the integral correspond to the spectral region where the instrument has sensitivity.

The center wavelength method used at SBRC approximates the integral in (6), effectively assuming that the functions $R(\lambda)$ for SeaWiFS are very narrow. Then, the measurement equation becomes

$$S_{\rm lab}(g,c) \;=\; \frac{L_{n,97}(\lambda_{\rm D})\,R(\lambda_{\rm D})\,\Delta\lambda}{\gamma_{\rm lab}(g,c)}, \qquad (7)$$

where $S_{\rm lab}(g,c)$ are the corrected net counts from SeaWiFS for the measurements of the GSFC sphere source (Sect. 6.2) and $\Delta\lambda$ is a bandwidth parameter. For the purpose of comparing the OSC results to the SBRC results, the calibration coefficient $K_2(g,c)$ is

$$\begin{aligned} K_2(g,c) &\equiv \frac{\gamma_{\rm lab}(g,c)}{R(\lambda_{\rm D})\,\Delta\lambda} \\ &= \frac{L_{n,97}(\lambda_{\rm D})}{S_{\rm lab}(g,c)}. \end{aligned} \qquad (8)$$

The center wavelength method does not allow for the finite bandwidth of $R(\lambda)$ and the fact that the relative spectral shape of the source depends on the measurement condition. For example, (Barnes 1996a) estimated that the GSFC sphere source, as measured at NIST in April 1995, had the same relative spectral shape as a 2,850 K blackbody. The relative spectral shape for the upwelling Earth radiance, however, was modeled in that document by a 12,000–38,000 K blackbody. The finite bandwidths and the large differences in the relative spectral shape of the source used to calibrate SeaWiFS, compared to the source that it measures from orbit, require that the analysis be based on (6).

The ratio of the corrected signals for the two measurement conditions is

$$\frac{S_{\rm orbit}(g,c)}{S_{\rm lab}(g,c)} \;=\; \frac{\gamma_{\rm lab}(g,c)}{\gamma_{\rm orbit}(g,c)}\,\frac{\displaystyle\int_{380}^{1100} L_{\rm orbit}(\lambda)\,R(\lambda)\,d\lambda}{\displaystyle\int_{380}^{1100} L_{\rm lab}(\lambda)\,R(\lambda)\,d\lambda}. \qquad (9)$$

The quantity of interest to the SeaWiFS science team is the band-averaged radiance from orbit. From (9) and (5),

$$\begin{aligned} \frac{\displaystyle\int_{380}^{1100} L_{\rm orbit}(\lambda)\,R(\lambda)\,d\lambda}{\displaystyle\int_{380}^{1100} R(\lambda)\,d\lambda} &= S_{\rm orbit}(g,c)\,\frac{\gamma_{\rm orbit}(g,c)}{\gamma_{\rm lab}(g,c)} \\ &\quad\times \frac{\displaystyle\int_{380}^{1100} L_{n,97}(\lambda)\,R(\lambda)\,d\lambda}{S_{\rm lab}(g,c)\displaystyle\int_{380}^{1100} R(\lambda)\,d\lambda}. \end{aligned} \qquad (10)$$

from which

$$\begin{aligned} K_2(g,c) &= \frac{\displaystyle\int_{380}^{1100} L_{n,97}(\lambda)\,R(\lambda)\,d\lambda}{S_{\rm lab}(g,c)\displaystyle\int_{380}^{1100} R(\lambda)\,d\lambda} \\ &= \frac{L_{n,{\rm B},97}}{S_{\rm lab}(g,c)}. \end{aligned} \qquad (11)$$

Either method (band-centered or band-averaged) results in a calibration coefficient with units of spectral radiance per count. The advantage of using the band-averaged radiances, both for the laboratory and on-orbit measurements, is that no error is introduced by approximating the integral, as is the case for the band-centered method [compare (9) with (8) and (10)]. If the $R(\lambda)$ functions are accurate, the band-averaged radiance and the signal will change by the same relative amount for sources with different spectral shapes; then $K_2(g,c)$ for the band-averaged method is independent of the source spectral shape.

For the SeaWiFS recalibration, measurements are expressed in terms of the ratio of the net counts obtained during the calibration to those obtained during an experiment. Also identified, through the ratio of the constants $g_x(g,c)$, are factors other than relative spectral shape that may be different between the calibration laboratory and the final measurement. Instrument factors that can be modeled using this approach include sensitivity to polarization, the spatial extent and variation of the source, or departures of gain ratios from nominal values. For example, Yeh et al. (1997) described a method for correcting the measurements of oceans for the excess signal caused by nearby bright sources, such as clouds. For the general SeaWiFS algorithm, the gains are incorporated into the calibration coefficient, $K_2(g,c)$, and several instrument factors are included in determining the corrected signals (Sect. 6.2).

6.2 Corrected Net Signal

In this section, the relationship between the raw counts and the corrected net signals is described. The presentation follows from the prelaunch radiometric characterization and calibration equations (Barnes et al. 1994b).

6.2.1 Model

The corrected net signals $S_x(g,c)$ are given by

$$S_x(g,c) = (C_{\rm out} - C_{\rm dark})\left[1 + K_3(T - T_{\rm ref})\right] \times K_4(Pxl)\, R_i\, CG(t - t_0) + CO. \quad (12)$$

In (12) above

- $C_{\rm out}$ is the value of the total output counts from the sensor in digital counts;
- $C_{\rm dark}$ is the value of the dark counts (or zero offsets) from the sensor in digital counts;
- K_3 is the correction factor for the temperature dependence of the photodiode responsivity in units of $\rm K^{-1}$;
- T is the focal plane temperature in Kelvin;
- $T_{\rm ref}$ is a reference temperature, $T_{\rm ref} = 293\,\rm K$;
- K_4 is a (dimensionless) correction factor for the scan modulation;
- Pxl is the value of the pixel (dimensionless) along the scan line;
- R_i is a dimensionless correction factor for the difference in reflectance between the two sides of the scan mirror;
- i is the dimensionless value (1 or 2) to denote the mirror side;
- CG is the time-dependent overall system gain in per unit time;
- t is the time of the SeaWiFS measurement;
- t_0 is the time of the SeaWiFS launch; and
- CO is a dimensionless calibration system offset.

The values for $C_{\rm dark}$ and R_i that are necessary to determine $S_{\rm lab}(g,c)$ were determined using the data acquired at OSC. The details of the calculations are given below. The time-dependent overall system gain and offset, CG and CO, respectively, allow for adjustments to the laboratory calibration as a function of time on orbit. The overall system gain or offset are expected to vary slowly with time and could be caused by degradation of the mirrors or other system components. During the mission, periodic solar or lunar measurements will be used to assess changes in these parameters. For the laboratory work reported here, $CG \equiv 1$ and $CO \equiv 0$.

The temperature correction factor, K_3, was derived by Eplee and Barnes (1997) for each of the eight bands. K_3 is small, from 0.00008–$0.00090\,\rm K^{-1}$. During the calibration of SeaWiFS at OSC, the maximum focal plane temperatures, T, were about 302 K. The resulting corrections, applied to each scan line, ranged from 0.07–0.8%.

The scan modulation correction factor, K_4, accounts for variations in the instrument response as a function of scan mirror position, i.e., for each pixel in a scan line. These corrections were determined during the characterization of SeaWiFS by SBRC (Barnes et al. 1994b), resulting in a quadratic model. Compared to the nadir pixel (in the center of the scan line), this correction can be up to 1.7% at the ends of the scan. Because only two pixels around the nadir pixel were used for the determination of $S_{\rm lab}(g,c)$, K_4 is unity to within ±0.0006%, so K_4 is equal to unity for the measurements reported here.

6.2.2 Measurements

During the measurements at OSC, SeaWiFS viewed the GSFC sphere at different radiance levels; for the radiometric calibration, there was a lamp configuration of 16, 8, 4, and 1. On 24 January and 11 April 1997, measurements were made for all gains for both TDI settings (4:1 and 1:1). This corresponded to five measurements at each radiance level, because in the 1:1 TDI setting, the output of SeaWiFS corresponds to one channel for each band, requiring four measurements to include all four channels. At each radiance level, the total counts, $C_{\rm out}$, were recorded for each channel and each gain for all eight bands. Each measurement for a fixed set of parameters consisted of acquiring 120 successive scan lines, which took about 20 s. The output of the channels in bands 2–8 saturated for some of the sphere radiance levels and gain combinations.

Table 14 gives the radiance level and gain combinations that did not saturate SeaWiFS in the 1:1 TDI setting. From Table 14, it is clear that the number of independent measurements of $K_2(g,c)$ for each band, channel, and gain combinations for this experiment varied between zero and four—compare band 8 ($c = 1$ and $g = 1$) to the corresponding values for band 1. The ocean channels were saturated at all lamp levels for band 6 at $g = 2$, and for bands 7 and 8 at $g = 1$ and $g = 2$, respectively. The calibration coefficients were, therefore, calculated using the gain ratios and the calibration coefficients for the unsaturated measurements. Determination of the gain ratios is described in Sect. 6.3.1.

For the analysis, only the central portion of each scan line was used. Because SeaWiFS was aligned with the exit aperture of the sphere source, counts from the nadir (0° scan angle) pixel corresponded to the central position in the exit aperture. The average value for the net corrected signal was determined for the five pixels centered on the nadir pixel using (12), which becomes

$$S_{\rm lab}(g,c) = \left\langle (C_{\rm out} - C_{\rm dark})[1 + K_3(T - T_{\rm ref})]R_i \right\rangle, \quad (13)$$

because $K_4(Pxl) = 1$, $CG = 1$, and $CO = 0$. For each set of measurement parameters (sphere level, band, channel, and gain), the average net corrected signal was determined for 600 measurements (5 pixels and 120 scans). For each sphere level, the final values for $S_{\rm lab}(g,c)$ were determined from the average of the 24 January and 11 April measurements.

6.2.3 Offset Counts

The values for $C_{\rm dark}$ were determined for each scan line using the corresponding dark count (DC) restore value

Table 14. Sphere radiance levels, denoted by the number of lamps operating, and SeaWiFS gain, $g = 1$–4, that did not result in saturated values for C_{out} for the measurements at OSC on 24 January and 11 April in the 1:1 TDI configuration. Combinations that resulted in the saturation of SeaWiFS are indicated by a dash (-).

Band Number	*Channel Number*	*Gain Setting* $g = 1$	$g = 2$	$g = 3$	$g = 4$
1	1	16, 8, 4, 1	16, 8, 4, 1	16, 8, 4, 1	16, 8, 4, 1
	2	16, 8, 4, 1	16, 8, 4, 1	16, 8, 4, 1	16, 8, 4, 1
	3	16, 8, 4, 1	16, 8, 4, 1	16, 8, 4, 1	16, 8, 4, 1
	4	16, 8, 4, 1	16, 8, 4, 1	16, 8, 4, 1	16, 8, 4, 1
2	1	16, 8, 4, 1	8, 4, 1	16, 8, 4, 1	8, 4, 1
	2	16, 8, 4, 1	8, 4, 1	16, 8, 4, 1	8, 4, 1
	3	16, 8, 4, 1	8, 4, 1	16, 8, 4, 1	8, 4, 1
	4	16, 8, 4, 1	16, 8, 4, 1	16, 8, 4, 1	16, 8, 4, 1
3	1	16, 8, 4, 1	16, 8, 4, 1	16, 8, 4, 1	16, 8, 4, 1
	2	8, 4, 1	4, 1	8, 4, 1	4, 1
	3	8, 4, 1	4, 1	8, 4, 1	4, 1
	4	8, 4, 1	4, 1	8, 4, 1	4, 1
4	1	8, 4, 1	4, 1	8, 4, 1	4, 1
	2	8, 4, 1	4, 1	8, 4, 1	4, 1
	3	8, 4, 1	4, 1	8, 4, 1	4, 1
	4	16, 8, 4, 1	16, 8, 4, 1	16, 8, 4, 1	16, 8, 4, 1
5	1	16, 8, 4, 1	16, 8, 4, 1	16, 8, 4, 1	16, 8, 4, 1
	2	4, 1	1	4, 1	1
	3	4, 1	1	4, 1	1
	4	4, 1	1	4, 1	1
6	1	1	-	4, 1	1
	2	1	-	4, 1	1
	3	1	-	4, 1	1
	4	16, 8, 4, 1	16, 8, 4, 1	16, 8, 4, 1	16, 8, 4, 1
7	1	8, 4, 1	16, 8, 4, 1	16, 8, 4, 1	16, 8, 4, 1
	2	-	-	1	1
	3	-	-	1	1
	4	-	-	1	1
8	1	-	-	1	1
	2	-	-	1	1
	3	-	-	1	1
	4	8, 4, 1	8, 4, 1	8, 4, 1	8, 4, 1

(Barnes et al. 1994a). This is the procedure used at SBRC and on orbit. In order to estimate the standard uncertainty in C_{dark}, the mean and standard deviation of the individual DC restore values acquired during the 120 DC restore scan lines was determined. In some cases, C_{dark} was very stable, resulting in zero for the standard deviation. In this case, the standard deviation was assigned the value $1/\sqrt{12}$, which arises from a resolution of 1 count and the assumption of a uniform, rectangular probability distribution function (International Organization for Standardization 1993). The average values of C_{dark} for the radiometric calibration analysis are given in Table 15, along with the standard uncertainty. The values for C_{dark} for 11 April and 24 January agreed to within ±0.5%.

As a separate investigation, the dark counts were measured using different techniques to compare them to the DC restore values. On 24 January and 11 April, following the measurements of the sphere with one lamp illuminated, this lamp was turned off and SeaWiFS measured the *dark* sphere. All four gains were measured, in the 1:1 and 4:1 TDI setting. As measured by the SXR, this produced a zero radiance source. For the 32 channels in the 1:1 TDI setting, the average of the difference between the counts from the dark sphere and the corresponding DC restore value was less than ±0.03 counts with a standard deviation of about 0.1 counts, independent of gain setting. For

Table 15. Average values of C_{dark}, in digital counts, from 24 January and 11 April for the SeaWiFS calibration analysis. The standard uncertainties $u(C_{\text{dark}})$ are also given in digital counts.

Band	*Channel*	*Gain 1*		*Gain 2*		*Gain 3*		*Gain 4*	
Number	*Number*	C_{dark}	$u(C_{\text{dark}})$	C_{dark}	$u(C_{\text{dark}})$	C_{dark}	$u(C_{\text{dark}})$	C_{dark}	$u(C_{\text{dark}})$
1	1	21.0	0.20	21.0	0.20	21.0	0.20	21.0	0.20
	2	23.2	0.13	23.5	0.20	23.3	0.17	23.4	0.19
	3	18.4	0.17	16.9	0.20	18.0	0.13	17.4	0.18
	4	20.9	0.11	19.0	0.18	20.2	0.14	19.6	0.19
2	1	18.5	0.18	17.4	0.18	18.1	0.09	17.8	0.15
	2	21.0	0.06	19.9	0.15	20.6	0.17	20.2	0.14
	3	15.8	0.13	12.4	0.17	14.8	0.14	13.4	0.18
	4	18.0	0.20	18.0	0.20	18.0	0.20	18.0	0.20
3	1	21.0	0.20	21.0	0.20	21.0	0.20	21.0	0.20
	2	22.1	0.12	23.0	0.10	22.0	0.06	22.9	0.13
	3	20.9	0.08	19.0	0.11	21.0	0.20	19.6	0.17
	4	19.0	0.07	17.1	0.13	19.0	0.20	17.7	0.15
4	1	21.4	0.17	21.4	0.17	21.5	0.18	21.4	0.17
	2	19.6	0.18	18.5	0.18	20.0	0.20	18.9	0.12
	3	19.3	0.17	19.9	0.13	19.1	0.11	19.8	0.14
	4	21.0	0.20	21.0	0.20	21.0	0.20	21.0	0.20
5	1	26.0	0.20	26.0	0.20	26.0	0.20	26.0	0.20
	2	22.3	0.16	23.4	0.18	22.0	0.20	23.0	0.09
	3	22.1	0.11	15.9	0.14	24.7	0.16	18.3	0.16
	4	17.1	0.09	11.9	0.16	19.0	0.20	14.1	0.11
6	1	21.7	0.17	13.2	0.26	27.0	0.20	24.5	0.18
	2	17.5	0.18	11.8	0.28	21.0	0.15	19.4	0.17
	3	33.1	0.15	36.3	0.27	31.0	0.20	32.0	0.07
	4	21.0	0.20	21.0	0.20	21.0	0.20	21.0	0.20
7	1	23.0	0.20	23.0	0.20	23.0	0.20	23.0	0.20
	2	20.2	0.13	11.0	0.20	27.0	0.20	24.1	0.09
	3	21.1	0.10	22.4	0.22	20.0	0.15	20.8	0.14
	4	26.6	0.18	24.4	0.21	28.0	0.20	27.3	0.16
8	1	19.0	0.13	16.3	0.26	21.0	0.20	20.1	0.11
	2	25.9	0.13	29.0	0.24	23.2	0.13	24.0	0.11
	3	16.2	0.15	13.3	0.25	18.4	0.17	17.9	0.08
	4	20.0	0.20	20.0	0.20	20.0	0.20	20.0	0.20

the 8 bands in the 4:1 TDI setting, the average difference was less than ±0.02 counts with a standard deviation of about 0.07 counts.

Also on 24 January and 11 April, the black disc was placed over the center of the exit aperture of the sphere when it was at each of the four radiance levels, and SeaWiFS measured the radiance of this dark source. A gain setting of $g = 1$ and the 4:1 TDI setting were used. For each lamp level, the bands that had no saturated channels (Table 14) were analyzed by comparing the black disc measurements to the values of C_{dark} from the DC restore measurement. The counts produced by the black disc were no more than 1.6 counts higher than the corresponding values of C_{dark}, and corresponded to a relative bias of from 0–0.5%, with the majority of the comparisons below 0.3%. These differences are not statistically significant given the values for $u(S_{\text{lab}})$. Also, it should be noted that interpretation of these results in terms of the documented stray light effects in SeaWiFS (Barnes et al. 1995) is difficult because the black disc was in the near field of the optical system, which is focused for objects at infinity.

6.2.4 Mirror Side Correction

For SeaWiFS, alternate scan lines correspond to measurements using the two sides of the half-angle mirror (Barnes et al. 1994b). Because the reflectance of the two sides may differ, the mirror side correction factor must be determined before calculating $S_{\text{lab}}(g, c)$ from (13). This is

possible by using only the average net counts for the alternate scan lines, because the GSFC sphere source is stable and uniform.

The net counts for the alternate scan lines are proportional to the reflectance of the mirror, ρ_1 or ρ_2. Defining the average reflectance of the mirror as $\bar{\rho} = (\rho_1 + \rho_2)/2$, the reflectance of each side is

$$\rho_1 \;=\; \left\langle \frac{2C_i}{C_1 \;+\; C_2} \right\rangle \bar{\rho}, \tag{14}$$

where C_i are the net counts, $C_{\rm out} - C_{\rm dark}$, for mirror side $i = 1$ or 2. The average corresponded to measurements of alternate scan lines for the data acquired on 24 January and 11 April. The average reflectance $\bar{\rho}$ is unity because its value is incorporated into the calibration coefficients $K_2(g, c)$. Therefore, the correction factors R_i are

$$R_i \;=\; \left\langle \frac{C_1 \;+\; C_2}{2C_i} \right\rangle. \tag{15}$$

Note that the sum of the two mirror side correction factors is unity.

The correction factors are given in Table 16 and indicate the reflectance of the two sides of the half-angle mirror is the same to less than 0.1% for bands 3–8; for bands 1 and 2, the difference is 0.14 and 0.1%, respectively. These values are comparable to those reported by Barnes et al. (1994b).

Table 16. Values for the mirror side correction factors determined from the measurements by SeaWiFS of the GSFC sphere source on 24 January and 11 April.

Band Number	R_1	R_2
1	1.0007079	0.9992921
2	1.0005341	0.9994659
3	0.9999844	1.0000156
4	1.0002266	0.9997734
5	0.9999985	1.0000015
6	1.0000016	0.9999984
7	1.0000002	0.9999998
8	1.0000085	0.9999915

6.3 Calibration

In this section, the corrected net signals (from Sect. 6.2) and the two methods of describing the radiance of the GSFC sphere—nominal center wavelength or band-averaged center wavelength (Sect. 6.1)—are used to determine the calibration coefficients for SeaWiFS. Because the ocean channels for three of the bands saturated for $g = 1$ or $g = 2$ for all four sphere levels measured, the measured gain ratios were required before determining the calibration coefficients.

6.3.1 Gain Ratios

The ratios of the variable gains of the SeaWiFS ocean channels were determined on 24 January, using the voltage calibration pulse. As explained in Sects. 2.3 and 4.2, the gain ratios are measured by operating SeaWiFS in the solar calibration mode and recording the response, in counts, to a constant voltage which is input to each channel's voltage amplifier. During the voltage pulse, the gain for each channel is varied from $g = 1$ to $g = 4$. The input to the voltage amplifier is the sum of this calibration voltage and the output of the transimpedance amplifier. Because the scan mirror observes the dark interior housing of the SeaWiFS instrument during this measurement, the voltage from the channel's preamplifier circuit is small compared to the calibration voltage, but it was accounted for with the DC restore measurement. For each channel in each band, the gain ratios were determined from the ratio of the net counts for $g = 2$, $g = 3$, or $g = 4$ relative to the counts for $g = 1$.

The final values, given in Table 17, are the average of 60 pixels and 120 scan lines. The nominal value for the gain ratios for all gain settings ($g = 2$, $g = 3$, or $g = 4$) for the cloud channels (channel 1 for bands 1, 3, 5, and 7, and channel 4 for bands 2, 4, 6, and 8) is unity. The nominal value for the gain ratios for the ocean channels, $g = 2$, is 2. The other values are given in Table 17; $g = 3$ was designed for the on-orbit lunar measurements, and $g = 4$ was designed for the on-orbit measurements of reflected sunlight using the diffuser panel. The relative standard uncertainty in the gain ratios is also given in Table 17 and explained in Sect. 7.3.

6.3.2 Calibration Coefficients

The calibration coefficients for SeaWiFS were determined for each of the 32 channels using the data acquired in the 1:1 TDI configuration. Independent determinations of the values for $K_2(g, c)$ result from measurements of the different radiance levels of the sphere source (Table 14). The procedure used at OSC was similar to the original calibration at SBRC, except that six sphere levels were used (Barnes and Eplee 1997). The OSC measurements for gains other than $g = 1$ can be used to verify the gain ratio values determined from the electronic measurements. As explained above, all four levels of the GSFC sphere saturated the ocean channels in band 6 for $g = 2$ and in bands 7 and 8 for $g = 1$ and $g = 2$; for these 15 values of $K_2(g, c)$, therefore, this verification was not possible.

In the 4:1 TDI configuration, the output for each band is the average of the output of the four channels (this is the standard mode from orbit), so the data acquired with the 4:1 TDI should agree with the weighted average of the 1:1 data, using the $K_2(g, c)$ values for the weights. Thus, the 4:1 data acquired for each sphere radiance level on 24 January and 11 April can be used to verify the values of $K_2(g, c)$ (Sect. 8.3).

Table 17. Results of the determination of the gain ratios from the internal voltage calibration pulse for SeaWiFS at OSC in 1997. The gain at $g = 2$, 3, or 4 is normalized to the gain at $g = 1$. The relative standard uncertainty in the gain ratios for $g = 2$, 3, and 4 is given in the fifth, seventh, and last columns.

Band Number	*Channel Number*	*Gain 1*	*Gain 2*	*Uncertainty* [%]	*Gain 3*	*Uncertainty* [%]	*Gain 4*	*Uncertainty* [%]
1	1	1	1.0156	0.27	1.0051	0.29	1.0105	0.27
	2	1	1.9865	0.20	1.3228	0.21	1.6818	0.20
	3	1	1.9862	0.21	1.3201	0.21	1.6806	0.21
	4	1	1.9925	0.18	1.3194	0.18	1.6796	0.18
2	1	1	1.9916	0.16	1.3192	0.16	1.6819	0.16
	2	1	1.9841	0.15	1.3189	0.18	1.6810	0.16
	3	1	1.9889	0.17	1.3172	0.18	1.6828	0.17
	4	1	1.0242	0.46	1.0081	0.47	1.0161	0.46
3	1	1	1.0509	0.67	0.9999	0.66	1.0309	0.88
	2	1	1.9887	0.17	0.8949	0.17	1.6811	0.17
	3	1	1.9886	0.13	0.8968	0.13	1.6811	0.14
	4	1	1.9901	0.14	0.8957	0.16	1.6799	0.14
4	1	1	1.9901	0.15	0.7869	0.23	1.6814	0.15
	2	1	1.9878	0.15	0.7883	0.19	1.6818	0.15
	3	1	1.9882	0.15	0.7882	0.16	1.6836	0.15
	4	1	1.0435	0.82	0.9855	0.84	1.0290	0.83
5	1	1	1.0441	0.83	0.9853	0.86	1.0294	0.84
	2	1	1.9908	0.17	0.6414	0.18	1.5964	0.17
	3	1	1.9894	0.16	0.6431	0.25	1.5964	0.17
	4	1	1.9895	0.15	0.6419	0.16	1.5942	0.15
6	1	1	1.9910	0.19	0.3630	0.24	0.6629	0.28
	2	1	1.9876	0.21	0.3649	0.31	0.6650	0.27
	3	1	1.9905	0.19	0.3642	0.26	0.6652	0.25
	4	1	1.0333	0.63	0.9667	0.56	0.9794	0.69
7	1	1	1.0492	0.92	0.9666	0.89	0.9682	0.92
	2	1	1.9879	0.19	0.3101	0.28	0.5755	0.23
	3	1	1.9886	0.17	0.3130	0.32	0.5758	0.29
	4	1	1.9905	0.18	0.3109	0.32	0.5769	0.28
8	1	1	1.9917	0.17	0.2603	0.46	0.4989	0.21
	2	1	1.9891	0.18	0.2613	0.40	0.4995	0.20
	3	1	1.9913	0.18	0.2600	0.48	0.4982	0.22
	4	1	1.0411	0.78	0.9589	0.81	0.9726	0.80

Using the 1:1 TDI configuration, $K_2(g, c)$ was determined for each channel using the band-centered and band-averaged methods, see (8) and (10). Because the four channels in each band have the same $R(\lambda)$ (Sect. 2.1), the same sphere radiance applies to each channel within a band. As an example, for $g = 3$ and $c = 4$ for the 4 lamp configuration, there are eight equations (one for each band) with the form:

$$K_2(3,4) = \frac{L_{4,97}(\lambda_{\rm D})}{S_{\rm lab}(3,4)}, \qquad (16)$$

(band-centered method) or

$$K_2(3,4) = \frac{\int_{380}^{1100} L_{4,97}(\lambda)\, R(\lambda)\, d\lambda}{S_{\rm lab}(3,4) \int_{380}^{1100} R(\lambda)\, d\lambda} = \frac{L_{4,{\rm B},97}}{S_{\rm lab}(3,4)}, \qquad (17)$$

(band-averaged method), where $R(\lambda)$ or $\lambda_{\rm D}$ depends on the band. In this case, there are four measurements of $K_2(3,4)$ for bands 1, 2, 4, and 6 from the 16, 8, 4, and 1 lamp configuration; three measurements for bands 3 and 8

from the 8, 4, and 1 lamp configuration; two measurements for band 5 from the 4 and 1 lamp configuration, and one measurement for band 7 from the one lamp configuration.

Some of the band-averaged results are illustrated in Figs. 6 and 7. Figure 6 shows the $K_2(g,c)$ values for $g = 1$ and their combined standard uncertainty for the single cloud channel in each band. This corresponds to the first channel in bands 1, 3, 5, and 7 and the fourth channel in bands 2, 4, 6, and 8. The independent values obtained for each sphere radiance level are shown; some of the data for the one-lamp configuration do not agree with the results at the other sphere levels. Figure 7 illustrates the $K_2(g,c)$ values at $g = 1$ for one of the ocean channels in each band (channel 2). The $K_2(g,c)$ values for bands 7 and 8 are not shown because these were not measured directly. The agreement among the calibration coefficients from the multiple sphere levels is good.

For the calculation of the $K_2(g,c)$ values for which the GSFC sphere source always saturated the channels (ocean channels at $g = 1$ for bands 7 and 8; ocean channels for $g = 2$ for bands 6, 7, and 8), the derived $K_2(g,c)$ values for other gains and the four and one lamp level were used. If the gain ratios in Table 17 are written as $G(g,c)$, then

$$K_2(1,c) \;=\; K_2(g,c)\,G(g,c), \tag{18}$$

because the gain ratios are with respect to $g = 1$. The coefficients for the ocean channels in band 6, $g = 2$, were derived from the one lamp measurements at $g = 1$, $g = 3$, and $g = 4$, and the four lamp measurements at $g = 3$ (Table 14). The ocean channels in bands 7 and 8 at $g = 1$ and $g = 2$ were derived from the one lamp measurements at $g = 3$ and $g = 4$.

The final values are reported in Table 18 (band-centered method) and Table 19 (band-averaged method). In each case, the final value is the weighted average of the results obtained at the different sphere levels. The weighting factors used were the uncertainties $u(K_2)$ which were obtained for each sphere level. The determination of these uncertainties is discussed in Sect. 7. The uncertainties in the weighted averages were determined according to the procedures outlined for determining combined standard uncertainty for correlated input quantities (International Organization for Standardization 1993).

As in Barnes et al. (1994b), the 32 values of $K_2(g,c)$, in conjunction with the value of $C_{\rm dark}$, were used to predict the net signal at saturation, $S_{\rm sat}(g,c)$—this is simply (12) with $C_{\rm out}$ = 1,023 counts. Using the $K_2(g,c)$ values determined from the band-averaged radiances (Table 19), the saturation radiance, $L_{\rm sat}(g,c)$, was calculated for each channel, $L_{\rm sat}(g,c) = S_{\rm sat}(g,c)K_2(g,c)$. In each band, the saturation radiance for the cloud channel will be much greater than that for the ocean channels.

The net corrected signals (or counts) for each channel in a band, evaluated at the radiance values where each channel saturates, are termed "knees." Knee 1 corresponds to the smallest of the four saturation radiances, and knee 2 corresponds to the next smallest. Knee 3 occurs between knee 2 and the radiance at which the band completely saturates. At each knee, the average of the predicted net counts for the four channels in each band corresponds to the counts at the knee when SeaWiFS is operated in the standard 4:1 TDI configuration. For all eight bands and each of the four gain settings, the radiance and net counts at the three knees and saturation are given in Table 20. Figure 8 illustrates the relationship between radiance and SeaWiFS output for the 4:1 TDI setting for band 1 and gain 1.

6.4 Linearity

In order to test the linearity of the net corrected signals from SeaWiFS with respect to radiant flux, the SXR and SeaWiFS measured the flux from the GSFC sphere at 17 different radiance levels, from 16–0 lamps, on 11 April 1997. The measurements started with 16 lamps illuminated; at each successive level one lamp was switched off. The 4:1 TDI setting and $g = 1$ was used, because this is the typical measurement configuration for SeaWiFS ocean color measurements. Gain 3 ($g = 3$) was included to provide additional radiance levels that produced fewer than the knee 1 counts in Table 20. For the test, the SXR was positioned to view the center of the exit aperture of the GSFC sphere from an angle of about 30° from the normal vector to the exit aperture. SeaWiFS was aligned to view the center of the exit aperture with the nadir pixel corresponding to the central position. For each sphere level, the SXR acquired one data set at all six channels, with 10 measurements at each channel. SeaWiFS recorded data for 120 scan lines.

The data were analyzed by determining the net voltages for each SXR channel and the net corrected counts from SeaWiFS, plotting the SeaWiFS counts as a function of SXR voltage, and fitting the result to a straight line. For each SeaWiFS band, the slope of the line is inversely proportional to the calibration constant, which can be determined for the 4:1 TDI setting from the data in Table 20 (Barnes et al. 1994b). The SXR black disc was not used; instead, for each channel, the voltage offset measured with the lens cap in place was subtracted from the total signal and this result was corrected for the average SSE as measured over the course of the entire experiment at OSC. The SeaWiFS net corrected counts $S_{\rm lab}(g,c)$ were determined as described above. The uncertainty determined from the standard deviations in the $S_{\rm lab}(g,c)$ values was used to weight the data in the linear regression.

Because a one-to-one correspondence does not exist in measurement wavelengths between the SXR and SeaWiFS, the spectral variation in the sphere as a function of lamp configuration was investigated. For each channel in the SXR, and band in SeaWiFS, the ratio of the output signals for successive lamp levels was compared to the value

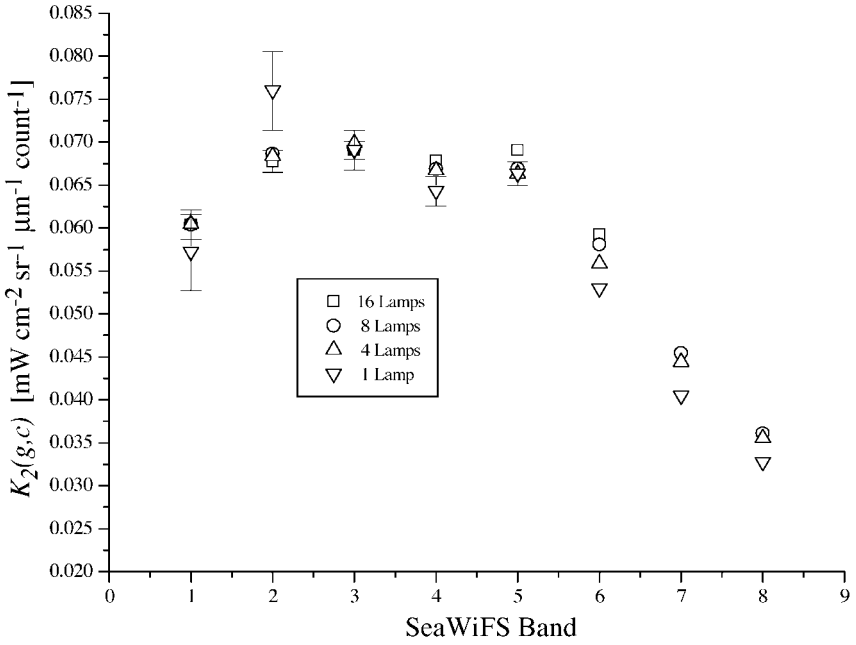

Fig. 6. Band-averaged $K_2(g, c)$ values for the single cloud channel in each band at $g = 1$ as a function of the radiance level of the GSFC sphere source. The symbols correspond to the different lamp configurations. The vertical bars correspond to the combined standard uncertainty in the calibration coefficients as described in Sect. 7 (16 and 1 lamp level only which are not shown if they are comparable or smaller than the size of the plotted symbol). Similar results were obtained at the other gain settings for the cloud channels. For each set of results, the weighted averages gave the final values (Table 19).

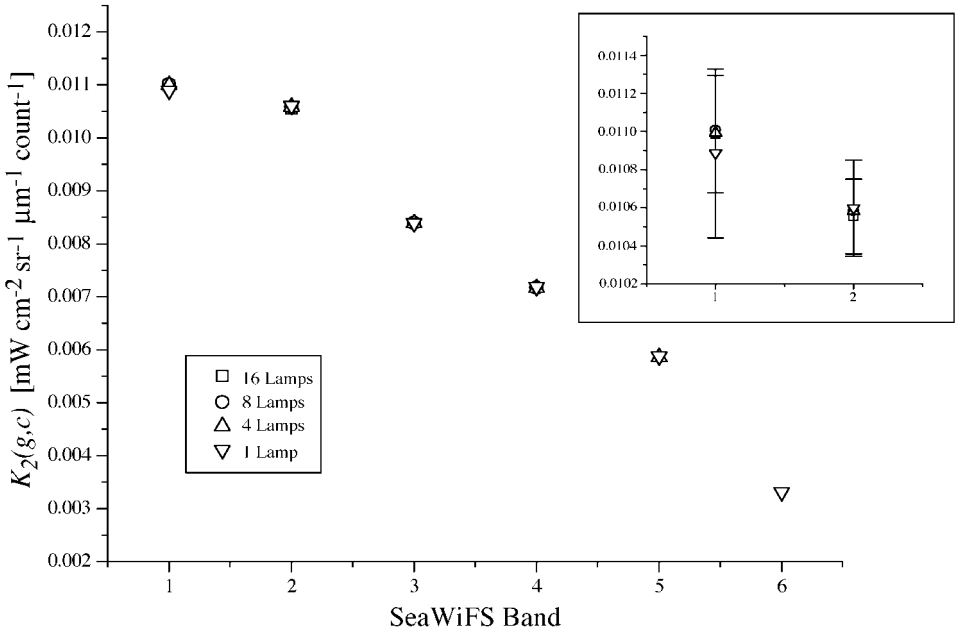

Fig. 7. Band-averaged $K_2(g, c)$ values for one ocean channel in each band at $g = 1$ as a function of the radiance level of the GSFC sphere source. The symbols correspond to the different lamp configurations. Similar results were obtained at other gain settings and ocean channels. The insert is an expanded view of the results for bands 1 and 2; the vertical bars correspond to the combined standard uncertainty in the calibration coefficients as described in Sect. 7 (16 and 1 lamp level only).

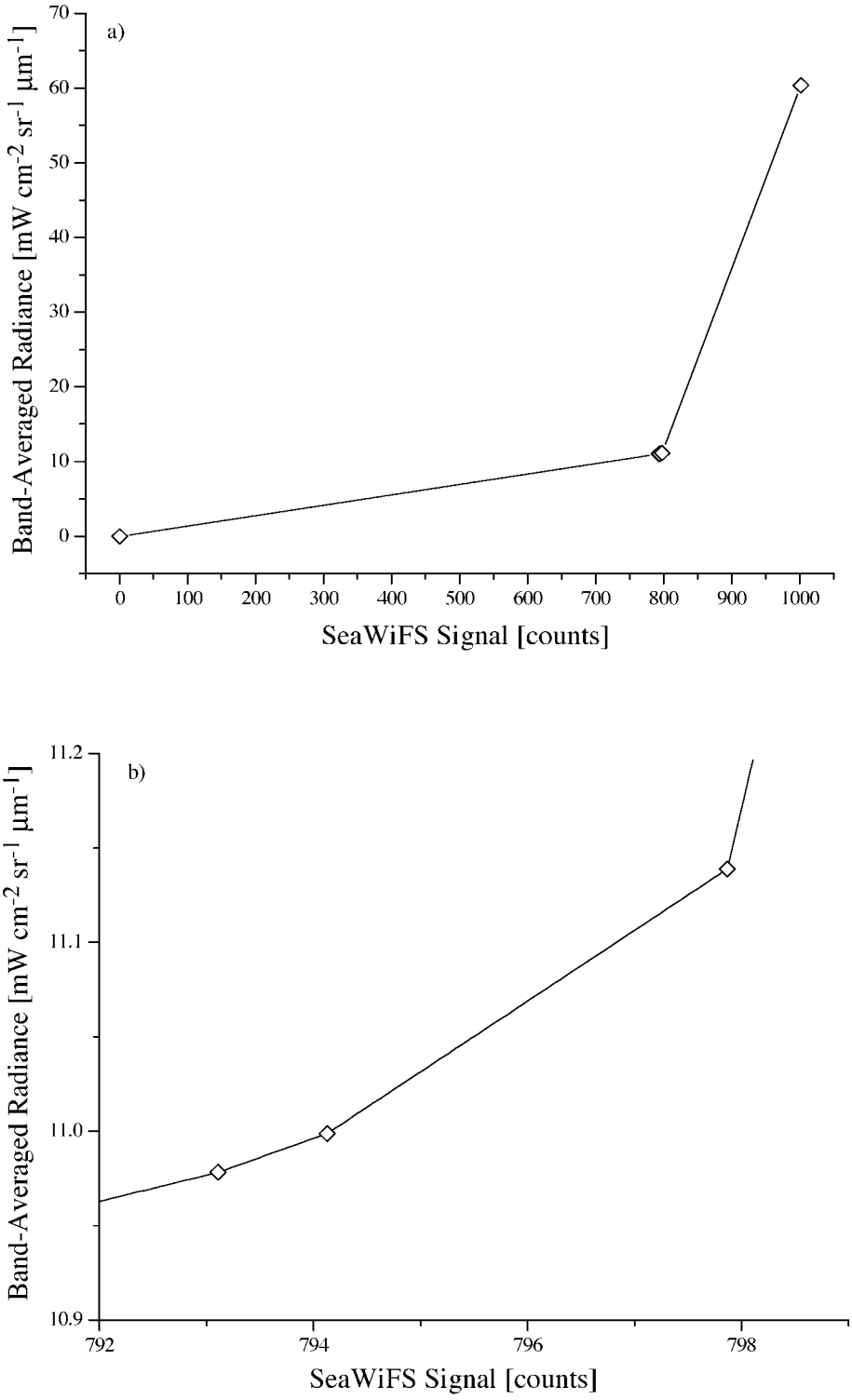

Fig. 8. The relationship between band-averaged radiance and corrected net output from SeaWiFS band 1 in the standard configuration ($g = 1$, 4:1 TDI setting): **a)** measurements over the entire dynamic range of the band, and **b)** measurements in the region of the three knees. The slopes of the lines are equal to the band 1 calibration coefficient $K_2(1)$ in the various regions.

Table 18. Values of $K_2(g,c)$ determined from $L_{n,97}(\lambda_D)$ values: the band-center method. The units of $K_2(g,c)$ are $\mathrm{mW\,cm^{-2}\,sr^{-1}\,\mu m^{-1}\,count^{-1}}$ and the relative standard uncertainty is given in percent. Each result is the weighted average of the results at the different lamp levels. The uncertainties are the average of the uncertainties in $K_2(g,c)$ obtained at the different sphere levels.

Band	*Channel (c)*	*Gain 1*		*Gain 2*		*Gain 3*		*Gain 4*	
Number	*Number*	$K_2(g,c)$	$u(K_2)$	$K_2(g,c)$	$u(K_2)$	$K_2(g,c)$	$u(K_2)$	$K_2(g,c)$	$u(K_2)$
1	1	0.05760	3.12	0.05512	3.08	0.05664	3.15	0.05587	3.10
	2	0.01050	2.88	0.005290	2.86	0.007947	2.88	0.006247	2.87
	3	0.01060	2.90	0.005338	2.86	0.008031	2.86	0.006303	2.87
	4	0.01049	2.87	0.005259	2.86	0.007943	2.87	0.006237	2.86
2	1	0.01038	2.01	0.005216	2.03	0.007872	1.98	0.006178	2.03
	2	0.01038	1.99	0.005228	2.02	0.007865	2.00	0.006170	2.03
	3	0.01042	2.01	0.005236	2.03	0.007905	1.99	0.006189	2.03
	4	0.06720	2.17	0.06414	2.16	0.06636	2.16	0.06491	2.21
3	1	0.06799	1.55	0.06520	1.53	0.06843	1.55	0.06619	1.54
	2	0.008227	1.44	0.004141	1.47	0.009194	1.44	0.004900	1.47
	3	0.008168	1.44	0.004106	1.47	0.009106	1.44	0.004857	1.48
	4	0.008164	1.44	0.004100	1.47	0.009113	1.44	0.004857	1.48
4	1	0.007146	1.31	0.003594	1.33	0.009085	1.32	0.004254	1.34
	2	0.007154	1.31	0.003601	1.34	0.009088	1.31	0.004258	1.34
	3	0.007129	1.31	0.003589	1.33	0.009044	1.31	0.004238	1.33
	4	0.06681	1.40	0.06486	1.40	0.06764	1.42	0.06525	1.40
5	1	0.06707	1.20	0.06556	1.19	0.06792	1.19	0.06585	1.20
	2	0.005840	1.17	0.002941	1.23	0.009104	1.17	0.003668	1.24
	3	0.005856	1.17	0.002950	1.24	0.009119	1.18	0.003676	1.24
	4	0.005859	1.17	0.002952	1.24	0.009133	1.17	0.003684	1.23
6	1	0.003347	1.15	0.001680	1.15	0.009205	1.08	0.005053	1.15
	2	0.003328	1.15	0.001676	1.16	0.009138	1.08	0.005006	1.15
	3	0.003400	1.14	0.001709	1.15	0.009340	1.09	0.005116	1.14
	4	0.05717	1.08	0.05544	1.08	0.05847	1.07	0.05776	1.09
7	1	0.04343	1.37	0.04357	1.34	0.04508	1.34	0.04471	1.34
	2	0.002373	1.41	0.001193	1.42	0.007655	1.38	0.004121	1.38
	3	0.002385	1.42	0.001199	1.43	0.007639	1.38	0.004131	1.38
	4	0.002371	1.41	0.001191	1.43	0.007622	1.38	0.004113	1.38
8	1	0.001699	1.57	0.0008531	1.57	0.006530	1.53	0.003405	1.52
	2	0.001720	1.56	0.0008648	1.57	0.006591	1.53	0.003440	1.53
	3	0.001698	1.57	0.0008528	1.58	0.006533	1.53	0.003408	1.53
	4	0.03494	1.50	0.03495	1.50	0.03587	1.50	0.03552	1.50

Table 19. Values of $K_2(g,c)$ determined from (11), which is the band-averaged method. The units of $K_2(g,c)$ are $\mathrm{mW\,cm^{-2}\,sr^{-1}\,\mu m^{-1}\,count^{-1}}$ and the relative standard uncertainty is given in percent. Each result is the weighted average of the results at the different lamp levels. The uncertainties are the average of the uncertainties in $K_2(g,c)$ obtained at the different sphere levels.

Band	*Channel (c)*	*Gain 1*		*Gain 2*		*Gain 3*		*Gain 4*	
Number	*Number*	$K_2(g,c)$	$u(K_2)$	$K_2(g,c)$	$u(K_2)$	$K_2(g,c)$	$u(K_2)$	$K_2(g,c)$	$u(K_2)$
1	1	0.06025	3.28	0.05767	3.24	0.05925	3.32	0.05844	3.27
	2	0.01098	3.04	0.005534	3.01	0.008314	3.03	0.006536	3.03
	3	0.01109	3.05	0.005584	3.02	0.008402	3.02	0.006594	3.03
	4	0.01098	3.03	0.005502	3.02	0.008310	3.02	0.006525	3.02

Table 19. (cont.) Values of $K_2(g,c)$ determined from (11), which is the band-averaged method. The units of $K_2(g,c)$ are $\mathrm{mW\,cm^{-2}\,sr^{-1}\,\mu m^{-1}\,count^{-1}}$ and the relative standard uncertainty is given in percent. Each result is the weighted average of the results at the different lamp levels. The uncertainties are the average of the uncertainties in $K_2(g,c)$ obtained at the different sphere levels.

Band	*Channel (c)*	*Gain 1*		*Gain 2*		*Gain 3*		*Gain 4*	
Number	*Number*	$K_2(g,c)$	$u(K_2)$	$K_2(g,c)$	$u(K_2)$	$K_2(g,c)$	$u(K_2)$	$K_2(g,c)$	$u(K_2)$
2	1	0.01057	2.01	0.005313	2.02	0.008018	1.98	0.006293	2.03
	2	0.01058	1.98	0.005325	2.02	0.008011	1.99	0.006284	2.03
	3	0.01061	2.01	0.005333	2.02	0.008052	1.99	0.006304	2.03
	4	0.06845	2.17	0.06534	2.15	0.06760	2.16	0.06613	2.20
3	1	0.06932	1.68	0.06649	1.66	0.06977	1.68	0.06749	1.67
	2	0.008387	1.57	0.004221	1.59	0.009373	1.56	0.004994	1.60
	3	0.008327	1.56	0.004185	1.60	0.009283	1.57	0.004951	1.60
	4	0.008323	1.56	0.004179	1.60	0.009290	1.57	0.004951	1.60
4	1	0.007159	1.31	0.003600	1.34	0.009102	1.32	0.004261	1.34
	2	0.007167	1.32	0.003607	1.34	0.009105	1.31	0.004265	1.34
	3	0.007142	1.31	0.003595	1.34	0.009061	1.31	0.004245	1.34
	4	0.06694	1.40	0.06499	1.41	0.06778	1.42	0.06538	1.41
5	1	0.06735	1.31	0.06581	1.31	0.06820	1.31	0.06609	1.32
	2	0.005865	1.28	0.002952	1.35	0.009143	1.29	0.003681	1.35
	3	0.005882	1.28	0.002961	1.35	0.009159	1.29	0.003689	1.35
	4	0.005884	1.28	0.002963	1.35	0.009172	1.28	0.003698	1.34
6	1	0.003323	1.21	0.001668	1.22	0.009143	1.15	0.005017	1.21
	2	0.003304	1.21	0.001664	1.23	0.009076	1.15	0.004969	1.21
	3	0.003376	1.21	0.001697	1.22	0.009277	1.15	0.005079	1.21
	4	0.05676	1.15	0.05499	1.15	0.05808	1.14	0.05737	1.16
7	1	0.04343	1.38	0.04357	1.36	0.04509	1.36	0.04472	1.36
	2	0.002372	1.42	0.001193	1.43	0.007652	1.40	0.004119	1.40
	3	0.002384	1.43	0.001199	1.44	0.007636	1.40	0.004130	1.40
	4	0.002370	1.43	0.001191	1.44	0.007619	1.40	0.004111	1.40
8	1	0.001688	1.83	0.0008476	1.84	0.006487	1.79	0.003383	1.79
	2	0.001709	1.82	0.0008592	1.83	0.006548	1.80	0.003418	1.79
	3	0.001687	1.83	0.0008472	1.84	0.006491	1.80	0.003386	1.79
	4	0.03470	1.77	0.03471	1.77	0.03564	1.77	0.03528	1.78

Table 20. The net counts from SeaWiFS bands 1–8, as a function of radiance for all four of the gain settings, determined using the values of $K_2(g,c)$ in Table 19. The net counts for each band are the average of the net counts for the four detectors in that band (the 4:1 TDI setting). At each knee, one of the detectors saturates. The radiance is given in units of $\mathrm{mW\,cm^{-2}\,sr^{-1}\,\mu m^{-1}}$ and the output of the SeaWiFS band is in net corrected counts.

Band	*Gain (g)*	*Knee 1*		*Knee 2*		*Knee 3*		*Saturation*	
Number	*Setting*	*Radiance*	*Output*	*Radiance*	*Output*	*Radiance*	*Output*	$L_{\mathrm{sat}}(g,c)$	$S_{\mathrm{sat}}(g,c)$
1	1	10.98	793.11	11.00	794.13	11.14	797.87	60.37	1002.15
	2	5.524	771.83	5.531	772.51	5.618	776.76	57.79	1002.91
	3	8.311	782.33	8.334	783.77	8.444	787.52	59.37	1002.39
	4	6.533	775.85	6.547	776.98	6.631	780.52	58.56	1002.66
2	1	10.60	789.53	10.62	790.68	10.69	792.45	68.80	1004.67
	2	5.342	772.98	5.342	773.04	5.390	775.46	65.67	1006.09
	3	8.031	780.04	8.057	781.80	8.118	783.91	67.94	1005.14
	4	6.302	774.83	6.325	776.79	6.364	778.46	66.46	1005.65

Table 20. (cont.) The net counts from SeaWiFS bands 1–8, as a function of radiance for all four of the gain settings, determined using the values of $K_2(g,c)$ in Table 19. The net counts for each band are the average of the net counts for the four detectors in that band (the 4:1 TDI setting). At each knee, one of the detectors saturates. The radiance is given in units of mW cm^{-2} sr^{-1} μm^{-1} and the output of the SeaWiFS band is in net corrected counts.

Band	*Gain (g)*	*Knee 1*		*Knee 2*		*Knee 3*		*Saturation*	
Number	*Setting*	*Radiance*	*Output*	*Radiance*	*Output*	*Radiance*	*Output*	$L_{\rm sat}(g,c)$	$S_{\rm sat}(g,c)$
3	1	8.345	780.00	8.356	780.74	8.394	782.02	69.46	1002.24
	2	4.202	767.01	4.203	767.22	4.221	768.34	66.62	1002.96
	3	9.302	782.27	9.327	783.72	9.382	785.36	69.91	1002.24
	4	4.968	768.75	4.977	769.73	4.995	770.69	67.62	1002.69
4	1	7.169	778.07	7.171	778.21	7.192	779.03	67.08	1002.67
	2	3.606	764.87	3.607	765.02	3.624	766.26	65.12	1002.82
	3	9.096	784.11	9.115	785.25	9.133	785.79	67.92	1002.61
	4	4.259	766.61	4.268	767.69	4.282	768.61	65.51	1002.74
5	1	5.869	770.79	5.887	772.36	5.919	773.85	67.15	1001.13
	2	2.951	759.18	2.982	764.55	2.996	765.83	65.61	1003.69
	3	9.143	782.29	9.152	782.82	9.209	784.58	67.99	1000.07
	4	3.681	762.27	3.707	765.81	3.731	767.52	65.89	1002.66
6	1	3.322	761.97	3.327	762.79	3.342	763.89	56.87	999.67
	2	1.674	756.69	1.683	759.32	1.685	759.57	55.10	1002.41
	3	9.094	783.38	9.107	784.10	9.203	787.10	58.20	997.99
	4	4.987	766.66	5.009	768.90	5.033	770.20	57.48	998.77
7	1	2.362	759.40	2.378	762.94	2.388	764.05	43.43	1000.30
	2	1.189	753.65	1.199	758.02	1.207	759.72	43.57	1002.79
	3	7.581	786.61	7.622	789.54	7.659	790.96	45.09	998.50
	4	4.094	768.13	4.115	770.76	4.139	772.35	44.72	999.21
8	1	1.695	762.30	1.699	763.42	1.704	764.27	34.81	1002.74
	2	0.8532	757.83	0.8540	758.30	0.8555	758.75	34.81	1003.34
	3	6.500	794.62	6.521	796.36	6.547	797.55	35.74	1002.36
	4	3.393	773.47	3.403	774.98	3.415	775.93	35.39	1002.48

expected if every lamp had identical output and identical spectral shape; the results are shown in Fig. 9. The values are close to unity, with variability increasing as the number of lamps decrease, as expected.

Table 21. Number of lamps illuminated during the SeaWiFS linearity test with the 4:1 TDI setting using the GSFC sphere source that resulted in measurements below knee 1 of the bilinear gain curve (Table 20 and Fig. 9).

Band	*Lamp Configuration*	
Number	$g=1$	$g=3$
1	16	16
2	16	16
3	12	13
4	8	11
5	5	7
6	1	4
7	0	3
8	0	2

The results are essentially the same, whether the SXR net voltages or the SeaWiFS net counts are used. For example, both instruments indicate the radiance change between the two-lamp and the three-lamp configuration was larger than the expected value of 1.5, with the bluer wavelengths showing the greatest change. This indicates the variation was caused by the lamps and not other factors, such as the uniformity of the spectral radiance in the exit aperture. he SeaWiFS linearity estimates for bands 4 and 8 (at 510 nm and 865 nm), were therefore, analyzed using the SXR channels 3 and 6 (at 487 nm and 775 nm).

With the data presented this way, it is easy to see which SeaWiFS bands were *below the knee* on the bilinear gain curve, i.e., none of the ocean channels were saturated. Above the knee, the SeaWiFS output for a band in the 4:1 TDI setting does not increase as rapidly with increasing radiance, so the normalized ratios are greater than unity. These points are off the scale in Figs. 9b and 9c. The number of lamps that resulted in measurements below the knee of the bilinear gain curves are given in Table 21 for $g=1$

and $g = 3$. The net corrected signals in digital counts for the two gain settings are given in Tables 22–23.

For $g = 1$, the net SeaWiFS counts for bands 1–5 were fit to a straight line. The independent variable for each curve fit is the net SXR voltages for the channel with the measurement wavelength closest to the SeaWiFS band. For $g = 3$, the SeaWiFS counts for bands 1–7 were analyzed the same way. As an example, the SeaWiFS counts and the fitted model for band 1 at $g = 1$ are plotted as a function of SXR channel 1 voltage in Fig. 10. The results of the linear fits were satisfactory in all cases. The constant offset b_0 was less than one count and the ratio of the fitted slopes for $g = 3$ and $g = 1$ for the same band agreed to within 1.5% of the expected gain ratios. The linear correlation coefficients were nearly unity, indicating the probability that the data were not correlated was less than 0.001 for all but the band 7, $g = 3$ case, where the probability was 0.0042. The standard deviations of the fits ranged from about 0.3 counts for band 1, to 4.1 counts for band 7. As an additional test, the data for bands 1 and 2 with $g = 1$ were fit to a quadratic curve in the SXR data—the net channel 1 voltage; the improvement in the fit was not statistically significant.

To illustrate the degree of linearity, the slope was determined for each SeaWiFS count, y_n, and SXR voltage, x_n, data pair: $(y_n - b_0)/x_n$. The subscript n refers to the number of lamps operating. The result was compared to the average slope for the linear regression for each fit. The results are shown in Fig. 11. The dispersion in the normalized slopes is less than ±0.6% and the standard deviation is about 0.2%.

Above knee 3, the data can also be analyzed using the simple linear regression model. The calibration constant for the 4:1 TDI setting above knee 3 is a constant for each band that depends on the spectral radiance and the net counts at saturation and knee 3 (Table 20 and Barnes et al. 1994b). Bands 3–8 with $g = 1$ were analyzed using the SXR data for channels 3–6, again using the SXR channel that was closest in wavelength to the SeaWiFS band. The results were also satisfactory, with the probability that the data were uncorrelated less than 0.001 in all cases except for band 3, where the probability was 0.0033. The standard deviations of the fits varied from 0.6–1.8 counts.

6.5 Warm Up and Repeatability

The temporal stability of the output from SeaWiFS was investigated on 24 January 1997 using the GSFC sphere source with two lamps illuminated. The SXR was aligned to view the center of the exit aperture of the sphere from an angle of about 30° from normal. The sphere was allowed to warm up for 1 h and then the SXR and SeaWiFS measured the sphere for about 20 min. The SXR was fully warmed up, but the power for the detector electronics and the scan motor in SeaWiFS were off until the measurements started. At 412 nm, the relative SXR output was stable to better than 0.1% over the 20 min interval. SeaWiFS was configured for the 4:1 TDI setting with $g = 2$ for bands 1–5, $g = 3$ for bands 7 and 8, and $g = 4$ for band 6. The counts were stable with time, and the standard deviations for the 20 min set for each band were less than 1 count.

Repeatability is the level of agreement between results obtained for successive measurements carried out under the same conditions (International Organization for Standardization 1993). Reproducibility is the level of agreement between the results for changed conditions of measurements. The SeaWiFS Project has defined short-term repeatability in terms of measurements made within a two week interval (Barnes et al. 1994a), and long-term repeatability in terms of longer time intervals. The successive measurements of the same radiance levels in the 1:1 TDI setting on 24 January and 11 April were repeatable to between 0.1–0.2%, depending on the radiance level. These values were determined by calculating the standard deviation of the ratio of the $S_{\rm lab}(g, c)$ values for the January and April measurements. The standard deviation was determined from the ratios corresponding to all unsaturated bands at a particular gain setting for each lamp level. There was no dependence with gain, so the average standard deviation for each lamp level was calculated and used to estimate the uncertainty component associated with the long-term repeatability of SeaWiFS.

The short-term repeatability for the $K_2(g, c)$ values was estimated from several measurements of the GSFC sphere source using the 4:1 TDI setting in January 1997. Although all gains were used, the majority of the data were for $g = 1$, and these results were used for the short-term repeatability analysis. On 23 January, the four radiance levels were measured three times (Table 1), and on 24 January the four radiance levels were measured once. On 22 January, three radiance levels were measured once (corresponding to the 16, 8, and 1 lamp illumination). For each band, the relative standard deviation (that is, the standard deviation of the separate measurements normalized by the mean) was determined. The result was between 0.01% (band 8, all four radiance levels) and 0.6% (band 1, 1 lamp).

Other measures of the repeatability of SeaWiFS are the result of a comparison of the three sets of gain ratios: 24 January and 23 April at OSC, and 16 June at VAFB. The gain ratios agreed to within ±0.5%, or within 1 count. Finally, the stability of the ratios of the calibration coefficients from two bands was evaluated. The SeaWiFS bio-optical algorithms are a function of such band ratios. For example, band 2 divided by band 5, and band 3 divided by band 5 are used for the chlorophyll concentration algorithm; and band 7 divided by band 8 is used for the atmospheric algorithm. These three color ratios varied by less than 0.4% for the 24 January and 11 April measurements.

Table 22. Values for $S_{\mathrm{lab}}(g, c)$ during the SeaWiFS linearity test for $g = 1$ on 11 April 1997. Results that are below the knee of the bilinear gain curve are shown in the columns with the actual band numbers. Results that are above the curve are in columns marked with the prime symbol ($'$).

Lamps	*Band*											
	1	2	3	3′	4	4′	5	5′	6	6′	7	8
16	278	472		797		805		825		891	976	1004†
15	255	433		792		802		820		881	961	1004†
14	237	404		790		799		816		872	947	1004†
13	219	374		787		796		811		864	932	1000
12	201	343	776			793		807		855	918	981
11	185	315	711			790		803		846	904	962
10	167	284	643			786		798		838	890	942
9	150	256	580			783		794		829	877	925
8	132	226	512		713			790		821	863	906
7	116	199	450		627			786		813	850	887
6	99	170	385		536			782		804	836	868
5	81	139	316		441		769			795	822	849
4	66	113	256		356		620			787	809	831
3	48	83	188		263		459			778	795	812
2	33	57	129		180		313			770	781	793
1	16	28	65		90		157		475		767	775

† Results where the band saturates.

Table 23. Values for $S_{\mathrm{lab}}(g, c)$ during the SeaWiFS linearity test for $g = 3$ on 11 April 1997. Results that are below the knee of the bilinear gain curve are shown in the columns with the actual band numbers. Results that are above the curve are in columns marked with the prime symbol ($'$).

Lamps	*Band*													
	1	2	3	3′	4	4′	5	5′	6	6′	7	7′	8	8′
16	362	615		795		806		824		889		975		1003†
15	332	564		792		802		819		879		959		1003†
14	309	526		790		799		815		870		946		1003†
13	286	487	759			795		810		862		931		999
12	263	447	697			792		806		853		917		980
11	241	410	640		786			802		844		903		961
10	218	370	578		710			797		835		888		941
9	196	333	521		641			793		827		875		924
8	173	294	461		566			788		819		861		905
7	152	259	405		498		711			811		848		886
6	130	221	346		426		608			802		834		867
5	106	181	284		350		501			793		820		848
4	86	146	230		283		404		704			807		830
3	63	108	169		209		299		523		789			810
2	44	74	116		143		204		355		535		679	
1	22	37	58		72		102		178		268		340	

† Results where the band saturates.

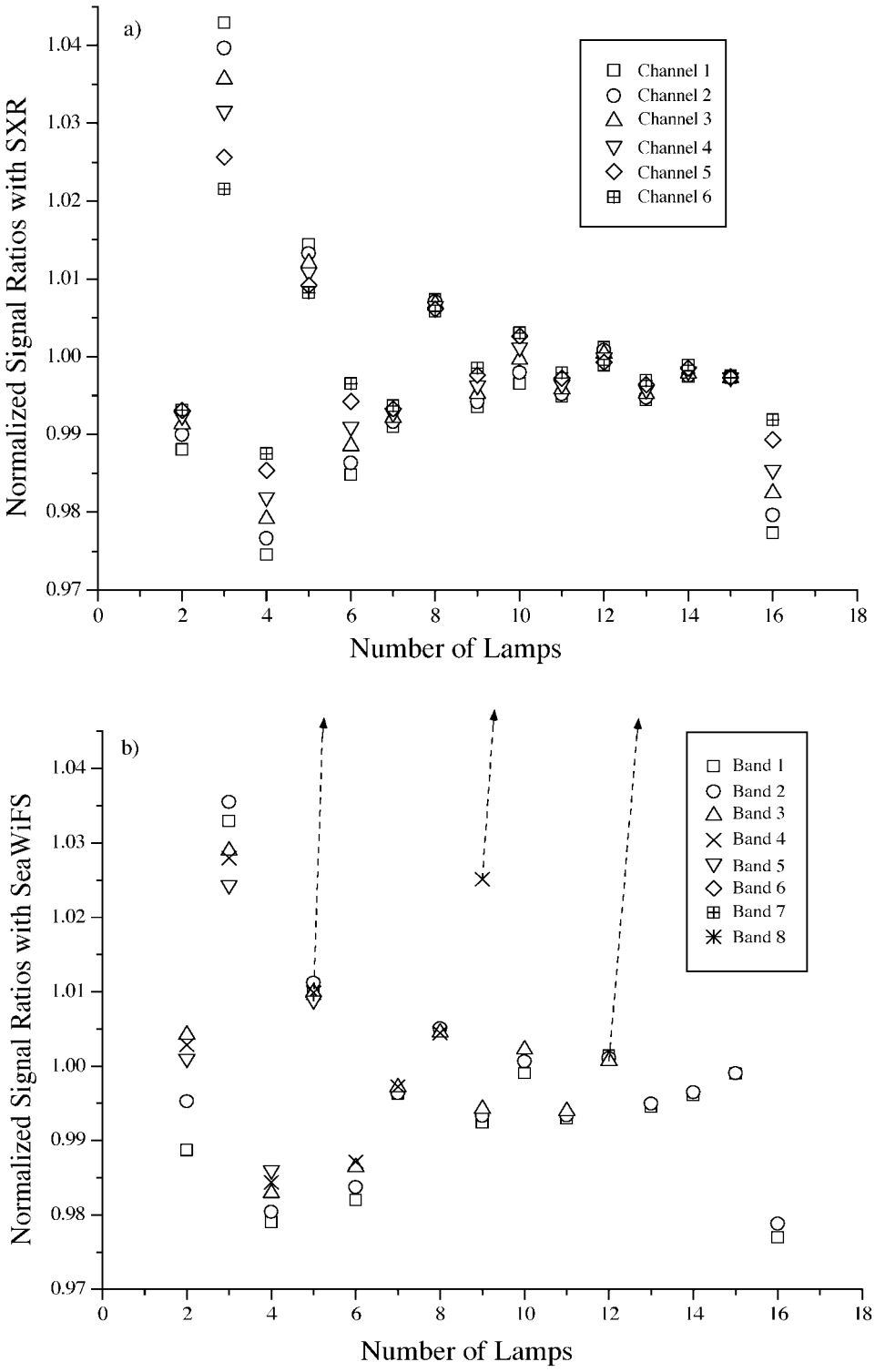

Fig. 9. The net signal, using the SXR and SeaWiFS, for the lamp configuration with $n-1$ lamps illuminated divided by the net signal for the lamp configuration with n lamps illuminated, multiplied by the factor $n/(n-1)$: **a)** Net signal ratios from the SXR. The symbols represent the SXR instrument channels. **b)** Net signal ratios from SeaWiFS at $g = 1$. The symbols represent the SeaWiFS bands. The dotted lines with arrows indicate the bands that crossed the knees in the bilinear gain curves (Table 22).

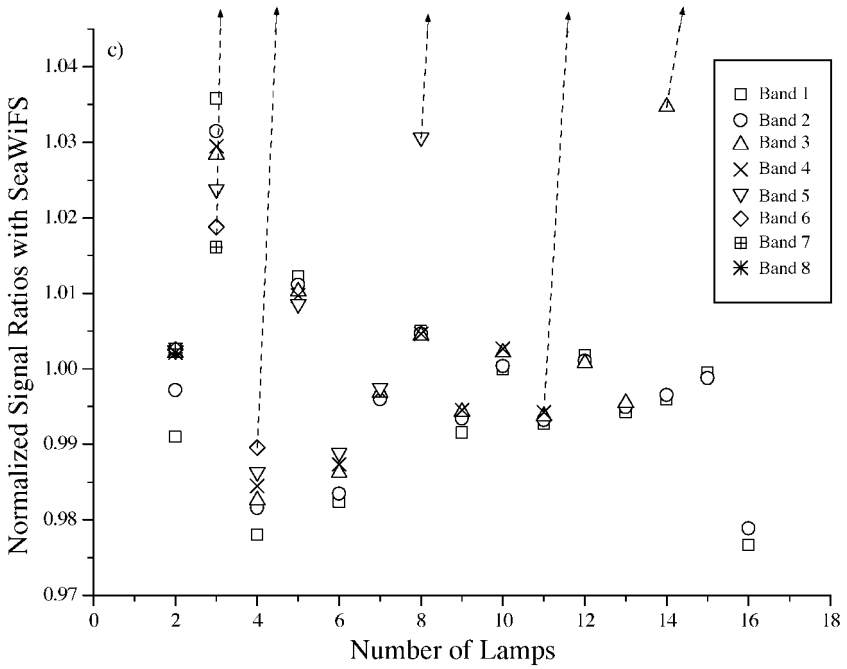

Fig. 9. (cont.) The net signal, using the SXR and SeaWiFS, for the lamp configuration with $n-1$ lamps illuminated divided by the net signal for the lamp configuration with n lamps illuminated, multiplied by the factor $n/(n-1)$: **c)** Net signal ratios from SeaWiFS at $g = 3$. The symbols represent the SeaWiFS bands. The dotted lines with arrows indicate the bands that crossed the knees in the bilinear gain curves (Table 23).

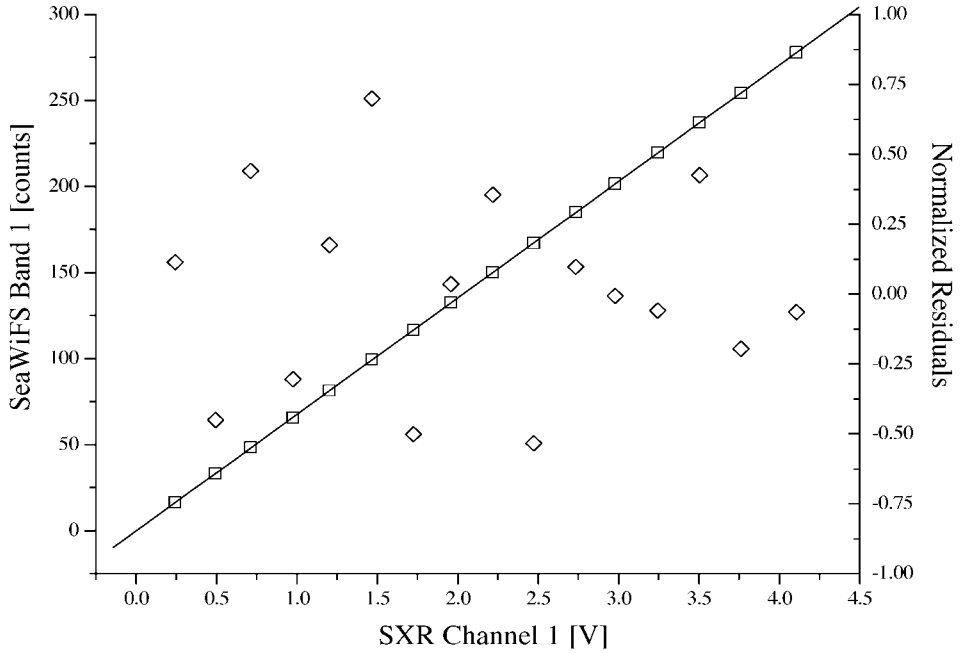

Fig. 10. The net corrected counts from SeaWiFS for band 1 and $g = 1$ plotted as a function of the net voltage of channel 1 of the SXR (open squares). The data were acquired on 11 April 1997, as the sphere was operated with 16, 15, 14, ... 2, and 1 lamp illuminated. The uncertainties in the SeaWiFS counts cannot be illustrated clearly because they are small compared to the symbols. The solid line is a linear fit to the data. Also shown, are the residuals to the fit, normalized by the uncertainties (open diamonds).

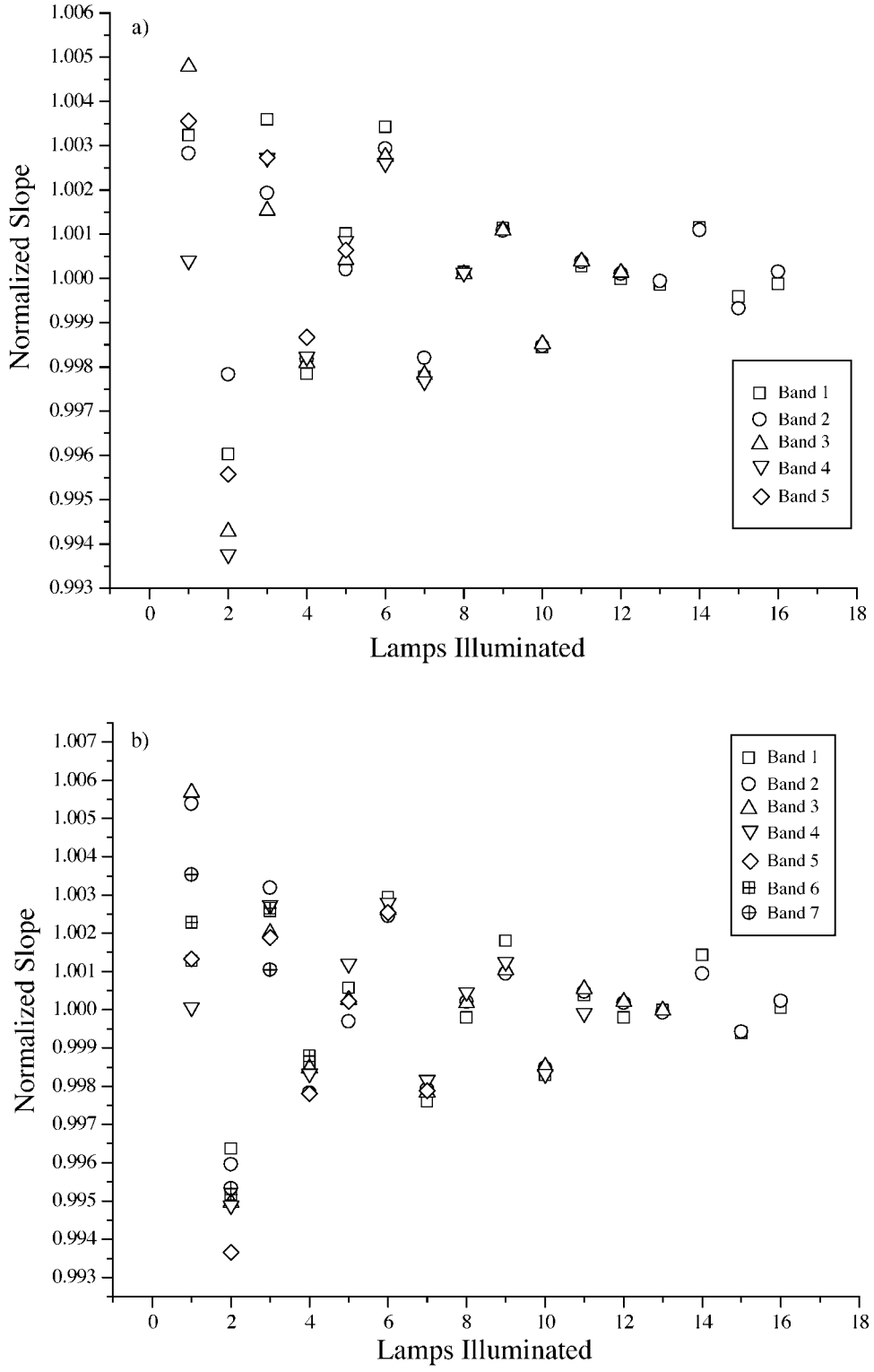

Fig. 11. Normalized slopes for the SeaWiFS linearity test for $g = 1$ and $g = 3$. The slope for each data pair, $(y_n - b_0)/x_n$, where b_0 was the fitted intercept, was normalized by the fitted slope. The symbols correspond to the SeaWiFS bands: **a)** slopes for $g = 1$, and **b)** slopes for $g = 3$.

7. UNCERTAINTY ANALYSIS

The uncertainty analysis follows from the method of propagation of uncertainties applied to the measurement equations described in Sect. 6. The combined uncertainty in the independent calibration coefficients $K_2(g,c)$, $u(K_2)$, is determined from

$$u^2(K_2) = \sum_{j=1}^{J} \left[\frac{\partial}{\partial z_j} K_2(g,c)\right]^2 u^2(z_j) + 2\sum_{j=1}^{J-1}\left[\sum_{k=j+1}^{J} \frac{\partial}{\partial z_j} K_2(g,c)\, \frac{\partial}{\partial z_k} K_2(g,c) u(z_j,z_k)\right]. \quad (19)$$

(Taylor and Kuyatt 1994) where $K_2(g,c)$ depends explicitly on the set of parameters z_j, which have standard uncertainties $u(z_j)$, and where j and k are indicies of summation. There are J parameters in (19), and the estimated covariance for pairs of parameters is $u(z_j,z_k)$. The partial derivative of $K_2(g,c)$ with respect to z_j are termed sensitivity coefficients. The sensitivity coefficients can be determined analytically from the measurement equation [(8) or (11), and (13)], or from experimental measurements.

Inspection of the measurement equation, (8) or (11), indicates two obvious uncertainty components: the radiance (either the band-centered or band-averaged values) or the net corrected signals. Other components include the linearity and repeatability of SeaWiFS, as well as terms associated with the GSFC sphere source.

7.1 Radiance

Let $L(\lambda)$ represent either the spectral radiance of the GSFC sphere source at the nominal SeaWiFS center wavelengths (band-centered spectral radiance) or the normalized integral of the spectral radiance of the sphere source, with the relative spectral responsivities of the SeaWiFS bands as weighting factors (band-averaged radiance). From (8) or (11)

$$\frac{\partial K_2(g,c)}{\partial L(\lambda)}\, u\big(L(\lambda)\big) \;=\; K_2(g,c)\, \frac{u\big(L(\lambda)\big)}{L(\lambda)}, \quad (20)$$

so it is necessary to determine the relative standard uncertainty in the radiance, $u\big(L(\lambda)\big)$.

7.1.1 Band-Centered Method

The method of determining the spectral radiance of the GSFC sphere source for the SeaWiFS measurements was described in Sect. 5. The sources of uncertainty are described in Sects. 5.1 and 5.3, as well as in Tsai and Johnson (1998). The relative standard uncertainties at the SeaWiFS nominal center wavelengths are given in Table 12 and illustrated in Fig. 5.

7.1.2 Band-Averaged Method

The uncertainty in the band-averaged radiance for each band depends on the uncertainty in the spectral radiance of the sphere, $u\big(L(\lambda)\big)$, and the uncertainty in the relative spectral response for each SeaWiFS band, $u\big(R(\lambda)\big)$. The uncertainty in the band-averaged radiance, $u_n(L_\mathrm{B})$, was evaluated by treating the uncertainties $u\big(L(\lambda)\big)$ and $u\big(R(\lambda)\big)$ as if the random portions were negligible. This is not really the case; Fig. 1 indicates that the random uncertainty in the spectral radiance can be up to 0.3%. This approximation, however, results in a conservative estimate for $u_n(L_\mathrm{B})$ and also simplifies the calculations. In the case of systematic uncertainties, the correlation coefficient (which is proportional to the covariance) is unity, and (19) is simplified to

$$u_n^2(L_\mathrm{B}) \;=\; \left[\sum_{j=1}^{J} \frac{\partial}{\partial z_j} L_{n,\mathrm{B},97}\; u(z_j)\right]^2. \quad (21)$$

Evaluating (21) involves approximating the integral expressions in (5) as sums and then determining the partial derivatives. The value of J was 2, corresponding to spectral radiance and relative spectral responsivity.

The values for $u\big(L(\lambda)\big)$ were the same as for the band-centered approach (Sect. 5.3). They were determined every 1 nm using cubic spline interpolation. Figure 5 illustrates these relative values in units of percent, $100\, u\big(L(\lambda)\big)/L(\lambda)$. The values for $u\big(R(\lambda)\big)$ were determined by comparing the results from the two independent measurements of these quantities at SBRC during the characterization of SeaWiFS. One method involved measurements of the separate components in the SeaWiFS optical train: spectral reflectance of the mirrors, spectral transmittance of the filters and beamsplitters, and spectral responsivity of the channels. The results, which covered the spectral interval from 380–1,150 nm, were multiplied together to determine relative spectral responsivity for each band in SeaWiFS.

The other method involved measurements of the system responsivity using a monochromatic source (Barnes et al. 1994b). Within ±30 nm of the nominal center wavelengths, the extent of the system level measurements, the two methods differed by no more than 6%. As a conservative estimate, the values for $u\big(R(\lambda)\big)$ for the spectral region, bounded by the 1% response (referenced to the peak response), were assigned a relative standard uncertainty of 6%. For regions where this comparison could not be made, an uncertainty of 50% was assigned to $u\big(R(\lambda)\big)$. The final results for the relative standard uncertainty in the band-averaged radiances are in Table 13.

7.2 Corrected Net Signal

The basic equation for the net corrected signal is (13), which indicates that $S_\mathrm{lab}(g,c)$ depends on a number of

parameters: $C_{\rm out}$, $C_{\rm dark}$, K_3, T, and R_i. Propagation of uncertainty for these parameters gives:

$$\frac{\partial S_{\rm lab}(g,c)}{\partial C_{\rm out}}\,u(C_{\rm out}) = \frac{S_{\rm lab}(g,c)}{\Delta C}\,u(C_{\rm out}) \approx u(C_{\rm out}), \quad (22)$$

$$\frac{\partial S_{\rm lab}(g,c)}{\partial C_{\rm dark}}\,u(C_{\rm dark}) = \frac{S_{\rm lab}(g,c)}{\Delta C}\,u(C_{\rm dark}) \approx u(C_{\rm dark}), \quad (23)$$

$$\frac{\partial S_{\rm lab}(g,c)}{\partial K_3}\,u(K_3) = \left[S_{\rm lab}(g,c) - \Delta C\,R_i\right]\frac{u(K_3)}{K_3} \approx \Delta T\,S_{\rm lab}(g,c)\,u(K_3) \quad (24)$$

$$\frac{\partial S_{\rm lab}(g,c)}{\partial T}\,u(T) = \frac{S_{\rm lab}(g,c) - \Delta C\,R_i}{\Delta T}\,u(T) \approx K_3\;S_{\rm lab}(g,c)\,u(T), \quad (25)$$

and

$$\frac{\partial S_{\rm lab}(g,c)}{\partial R_i}\,u(R_i) = \frac{S_{\rm lab}(g,c)}{R_i}\,u(R_i), \quad (26)$$

where $\Delta C = C_{\rm out} - C_{\rm dark}$ and $\Delta T = T - T_{\rm ref}$.

In (22)–(26), the standard uncertainty in $C_{\rm out}$, $C_{\rm dark}$, K_3, T, and R_i are denoted $u(C_{\rm out})$, $u(C_{\rm dark})$, $u(K_3)$, $u(T)$, and $u(R_i)$, respectively. The values for $C_{\rm out}$ were not readily available for analysis because the quantity ΔC was determined for each scan line. The corrections for temperature and mirror side reflectivity are small, however, so the quantity $S_{\rm lab}(g,c)/\Delta C$ differs from unity by no more than $\pm 0.8\%$ for focal plane temperatures up to 302 K. This sensitivity coefficient can, therefore, be ignored in (22) and (23) without causing the uncertainty component to be in error by more than 1%. The standard deviation of the 600 measurements of $S_{\rm lab}(g,c)$ was used to estimate $u(C_{\rm out})$. The standard deviation of the 120 measurements of $C_{\rm dark}$, was used to estimate $u(C_{\rm dark})$. The sensitivity coefficients in (24) and (25) involve the difference $[S_{\rm lab}(g,c) - \Delta C\,R_i]$, which is $K_3\,\Delta T\,R_i\,\Delta C \approx K_3\,\Delta T\,S_{\rm lab}(g,c)$ because the R_i is unity on average and $S_{\rm lab}(g,c) \approx \Delta C$. In (24), the relative standard uncertainty in K_3 is assumed to be 10%. In (25), $u(T)$ is determined assuming a uniform rectangular distribution function with a resolution of 0.267°C, resulting in a value of 0.077°C. The maximum temperature difference on 24 January was 8.6°C, and this value was used for estimating the uncertainty components for the measurements on 24 January and 11 April. Finally, in (26), the relative uncertainty in R_i, $u(R_i)/R_i$, was estimated assuming a uniform, rectangular distribution function for R_i bounded by R_1 and R_2. The uncertainty components arising from the uncertainty in K_3, T, or R_i are given in Table 24 for each SeaWiFS band. Most of the values are negligible, especially for bands 3–8.

Two independent determinations of $S_{\rm lab}(g,c)$ were made: on 24 January and 11 April 1997. These are denoted $S_{\rm lab}(g,c)_{\rm Jan}$ and $S_{\rm lab}(g,c)_{\rm Apr}$, respectively. On each day, $S_{\rm lab}(g,c)$ was determined for each set of experimental parameters (sphere radiance level, band, gain, and channel) from the average of 600 measurements. The average value of $S_{\rm lab}(g,c)$ was used in (8) or (11) to determine the calibration coefficients $K_2(g,c)$. The combined uncertainty in $S_{\rm lab}(g,c)$, $u(S_{\rm lab})$, is the quadrature sum of the components in Table 25. The two independent measurements of $S_{\rm lab}(g,c)$ reduce the uncertainty associated with these random components.

Table 24. The values for the uncertainty components (in percent), in relative units, which are independent of gain and sphere level. These are conservative values, in that the maximum focal plane temperature of 8.6°C was used for evaluating (24).

Band Number	*Uncertainty Components*		
	$u(K_3)$	$u(T)$	$u(R_i)$
1	0.077	0.007	0.041
2	0.050	0.005	0.031
3	0.036	0.003	0.001
4	0.034	0.003	0.013
5	0.034	0.003	0.000
6	0.013	0.001	0.000
7	0.009	0.001	0.000
8	0.007	0.001	0.000

7.3 Gain Ratios

The uncertainties (Table 17) were determined from the standard deviations of the net counts for the two gains that comprise a gain ratio by the propagation of uncertainty method. The gain ratio for gain g is

$$G(g,c) = \frac{S_{\rm lab}(g,c)}{S_{\rm lab}(1,c)}, \quad (27)$$

where $S_{\rm lab}(g,c)$ are net corrected counts. For the channels that were not saturated by the GSFC sphere, the combined uncertainty is the quadrature sum of the components listed in Table 26. As above, the standard deviations reported for $S_{\rm lab}(g,c)$ were used to estimate $u(C_{\rm out})$. The effect of the uncertainty in $C_{\rm dark}$ was accounted for using the value for the measurement uncertainty. The terms associated with the uncertainty in the focal plane temperature and the temperature coefficient were estimated as explained above, with the maximum temperature difference of 8.6°C; these terms are small (Table 24). Because no correction was applied for the mirror side reflectivity, there is no component of uncertainty from this term.

For the 15 channel and gain combinations that were always saturated by the GSFC sphere source (Table 14), the $K_2(g,c)$ values were determined using the gain ratios (Sect. 6.3.2). Because of the uncertainty in the gain ratios (Table 17), there are additional uncertainty components in these calibration coefficients corresponding to these factors.

Table 25. Direct uncertainty components for the net corrected signals from SeaWiFS. The combined uncertainty is the quadrature sum of the separate components. Type A uncertainty components are estimated using statistical means, and Type B components are estimated using other means (Taylor and Kuyatt 1994).

Source of Uncertainty	*Expression* [counts]	*Type*	*Experiment Variables*
C_{out}	$\frac{1}{2}\Big(u^2\big(S_{\text{lab}}(g,c)_{\text{Jan}}\big) + u^2\big(S_{\text{lab}}(g,c)_{\text{Apr}}\big)\Big)^{\frac{1}{2}}$	A	Sphere level, band, channel, gain
C_{dark}	$\frac{1}{2}\big(u^2(C_{\text{dark,Jan}}) + u^2(C_{\text{dark,Apr}})\big)$	A	Band, channel, gain
K_3	$\Delta T\, S_{\text{lab}}(g,c)\, u(K_3)$	B	Band
T	$K_3\, S_{\text{lab}}(g,c)\, u(T)$	B	Band
R_i	$S_{\text{lab}}(g,c)\, u(R_i)/1$	B	Band

Table 26. Direct uncertainty components for the gain ratios. The combined uncertainty in the gain ratios is the quadrature sum of the separate components.

Source of Uncertainty	*Expression (Relative Standard Uncertainty)*	*Type*	*Experiment Variables*
C_{out} at $g = 2$, 3, or 4	$u\big(S_{\text{lab}}(g,c)\big)/S_{\text{lab}}(g,c)$	A	Band, channel, gain
C_{dark} at $g = 2$, 3, or 4	$\big(S_{\text{lab}}(g,c)\sqrt{12}\big)^{-1}$	B	Band, channel, gain
C_{out} at $g = 1$	$u\big(S_{\text{lab}}(1,c)\big)/S_{\text{lab}}(1,c)$	A	Band, channel, gain
C_{dark} at $g = 1$	$\big(S_{\text{lab}}(1,c)\sqrt{12}\big)^{-1}$	B	Band, channel, gain
K_3	$\Delta T\, u(K_3)$	B	Band
T	$K_3\, u(T)$	B	Band

7.4 Other Components

There are several other factors that affect the uncertainty in the values for $K_2(g,c)$ which are implicit to the measurement equation. These include the linearity of response, repeatability, uniformity of the spectral radiance in the exit aperture of the sphere source, and the effect of wavelength errors in the relative spectral responsivities for each SeaWiFS band.

7.4.1 Linearity

For the SeaWiFS linearity test, the number of radiance levels was limited, and it was not possible to cover the full range of the linear portion of the bilinear gain curve for all bands and all gains. For $g = 1$ and bands 3, 4, and 5, the linearity measurements cover the full range of their responses below the knee; including the $g = 3$ results, the coverage is also good for bands 2 and 6. Figure 11 shows the responses in each band to be almost linear at the increased radiance levels (more than approximately eight lamps illuminated). The increased scatter in the normalized slopes with decreasing radiance is due to fewer SeaWiFS counts in the measurements. In general, however, the good agreement with the linear model using the SXR to measure the flux indicates that SeaWiFS performs as a linear instrument.

The SXR was shown to be linear using an optical beam-conjoiner, and the uncertainty associated with linearity is about 0.11% (Johnson et al. 1998). The relative standard uncertainty introduced by spectral variations in the sphere radiance that were difficult to quantify using the limited set of wavelengths from the SXR is small— probably less than 0.4% (Fig. 9).

Below the knee, the variation in the normalized slope with lamp level (Fig. 11), indicates that the linearity is bounded by 1.006 and 0.994, resulting in a relative standard uncertainty of 0.35%, assuming a uniform probability distribution. All of these uncertainty components were combined in quadrature, resulting in a relative standard uncertainty of 0.54% for the departure from linearity in SeaWiFS. This value was used for the uncertainty component associated with linearity for the $K_2(g,c)$ values for the 1:1 TDI setting.

Above the knee, where all three ocean channels are saturated, the relative standard uncertainty associated with linearity is estimated to be 1.0%. SeaWiFS measurements

Table 27. The values for the relative standard uncertainty components, in units of percent, associated with linearity and repeatability. The numbers in the second row refer to the number of lamps illuminated in the GSFC sphere source.

Band Number	*Linearity*	*Long-Term Repeatability*				*Short-Term Repeatability*			
		16	8	4	1	16	8	4	1
1	0.54	0.11	0.15	0.09	0.17	0.29	0.27	0.41	0.59
2	0.54	0.11	0.15	0.09	0.17	0.14	0.15	0.34	0.42
3	0.54	0.11	0.15	0.09	0.17	0.06	0.11	0.27	0.23
4	0.54	0.11	0.15	0.09	0.17	0.05	0.11	0.24	0.21
5	0.54	0.11	0.15	0.09	0.17	0.05	0.04	0.21	0.24
6	0.54	0.11	0.15	0.09	0.17	0.02	0.02	0.01	0.19
7	0.54	0.11	0.15	0.09	0.17	0.01	0.01	0.01	0.01
8	0.54	0.11	0.15	0.09	0.17	0.01	0.01	0.01	0.01

above the knee will be used primarily for stray light correction of ocean color data, and corrections for nonlinearity at this level of uncertainty are not significant.

7.4.2 Repeatability

The short-term and long-term repeatability measurements were described in Sect. 6.4. The uncertainty component for long-term stability was determined using the ratio of the measurements on 24 January and 11 April for the 1:1 TDI setting. The average (over gain settings) standard deviation (all 32 channels at the same gain) for ratios at the same radiance was used to estimate the uncertainty component associated with the long-term repeatability of SeaWiFS (Table 27). More data were available for the short-term repeatability analysis, from the multiple sets of the measurements at $g = 1$ and the 4:1 TDI setting. For each band, the uncertainty component associated with short-term repeatability was estimated using the standard deviation of the separate measurements at the same sphere level. The results are given in Table 27.

7.4.3 Sphere Uniformity

During the calibration, SeaWiFS and the SXR viewed the center of the exit aperture of the GSFC sphere source. For the SXR, the imaged area was about 7.2 cm in diameter, and the SXR was offset no more than about 0.5 cm from the center of the exit aperture. For SeaWiFS, flux was collected from an area about 8.4 cm in diameter (the aperture stop was 7.62 cm in diameter, with 1.6 mrad field of view and a distance of 2.5 m). This region was offset from the center of the exit aperture by about 2.2 cm.

The spatial uniformity of the spectral radiance of the GSFC sphere source's exit aperture was measured just before the 1995 NIST calibration using the SXR (Early and Johnson 1997). The spatial nonuniformity, expressed as the peak-to-valley variability in spectral radiance over the entire exit aperture, are given in Early and Johnson (1997) for the four sphere levels measured by SeaWiFS. The variation of the radiance uniformity with wavelength was not significant compared to the variation in the uniformity with the number of lamps illuminated.

The spatial mapping in 1995 at NIST was done at five SXR measurement wavelengths, corresponding to channels 1, 2, 3, 4, and 5. For the SeaWiFS calibration, with the SXR and SeaWiFS aligned to the center of the exit aperture and measuring nearly the same target area, the uncertainty caused by variations in spectral radiance is small compared to the uniformity values reported for the entire exit aperture. The peak-to-valley variability over the central 10 cm was used to estimate the uncertainty, assuming a uniform probability distribution function. For the 16, 8, 4, and 1 lamp configurations, this relative standard uncertainty is less than 0.4% (Table 28). It is assumed that the radiance uniformity of the GSFC sphere had not changed between the characterization in 1995 and the SeaWiFS calibration in 1997.

7.4.4 Wavelength

The uncertainty in the wavelength accuracy, $u(\lambda)$, of the relative spectral responsivity for the SeaWiFS bands, $R(\lambda)$, affects the accuracy of measurements with SeaWiFS. For either method of determining the calibration coefficients (band-centered or band-averaged), the magnitude of the uncertainty depends on the local slope of the source's spectral radiance according to

$$\frac{u\big(K_2(g,c)\big)}{K_2(g,c)} = \frac{u(\lambda)}{\lambda}\,\frac{\partial L(\lambda)}{\partial \lambda}\,\frac{\lambda}{L(\lambda)}. \qquad (28)$$

With an estimate of 1 nm for the uncertainty in the wavelength accuracy of the relative spectral response measurements, the uncertainty component for the calibration coefficients is from 0.02–2.03%, depending on the SeaWiFS band (Table 28). The values vary strongly with wavelength because the relative slope of the GSFC sphere's radiance varies strongly with wavelength.

Table 28. The values for the relative standard uncertainty components, in units of percent, associated with radiance uniformity in the exit aperture of the GSFC sphere and the possible wavelength error in the SeaWiFS relative spectral responsivity functions. The numbers in the second row refer to the number of lamps illuminated in the GSFC sphere source.

Band	*Source Uniformity*				*Wavelength Uncertainty*			
Number	16	8	4	1	16	8	4	1
1	0.09	0.12	0.2	0.4	1.98	1.99	2.00	2.03
2	0.09	0.12	0.2	0.4	1.46	1.48	1.48	1.49
3	0.09	0.12	0.2	0.4	1.05	1.06	1.07	1.07
4	0.09	0.12	0.2	0.4	0.92	0.93	0.93	0.93
5	0.09	0.12	0.2	0.4	0.69	0.69	0.70	0.70
6	0.09	0.12	0.2	0.4	0.31	0.32	0.32	0.32
7	0.09	0.12	0.2	0.4	0.15	0.15	0.15	0.15
8	0.09	0.12	0.2	0.4	0.02	0.03	0.03	0.03

7.4.5 Modeling Effects

The estimation of the band-averaged radiance was done independently by personnel at GSFC and NIST. Slight differences were observed, so the ratio of the two results was included in the uncertainty budget to account for modeling errors; the values were small (Table 29).

Table 29. The values for the relative standard uncertainty component, in units of percent, associated with modeling errors. The numbers in the second row refer to the number of lamps illuminated in the GSFC sphere source.

Band	*Modeling Errors*			
Number	16	8	4	1
1	0.207	0.207	0.212	0.060
2	0.166	0.165	0.170	0.041
3	0.121	0.121	0.122	0.009
4	0.110	0.112	0.112	0.016
5	0.098	0.096	0.098	0.002
6	0.086	0.086	0.086	0.005
7	0.072	0.072	0.073	0.002
8	0.027	0.027	0.027	0.000

7.5 Discussion

Not tabulated are values for the uncertainty associated with the net corrected signal, $u(S_{\mathrm{lab}})$, because there are 512 values—one for each band, channel, gain, and sphere radiance level. The components of $u(S_{\mathrm{lab}})$ that only depend on the SeaWiFS band are given in Table 24. The remaining components are associated with the output counts: $u(C_{\mathrm{out}})$ and $u(C_{\mathrm{dark}})$. These values were larger than the other three components given in Table 25, so $u(S_{\mathrm{lab}})$ was determined by the measurement precision. As a function of experimental parameters, $u(S_{\mathrm{lab}})$ was generally greater for the cloud channels than for the ocean channels, but was not very sensitive to the gain setting. The values for $u(S_{\mathrm{lab}})$ increased as the sphere radiance decreased (Figs. 6 and 7). Finally, the $u(S_{\mathrm{lab}})$ values were generally greater for the shorter SeaWiFS measurement wavelengths.

The uncertainties in the weighted averages were determined according to the procedures outlined for determining combined standard uncertainty for correlated input quantities (International Organization for Standardization 1993).

Figures 6 and 7 illustrate the combined standard uncertainty in $K_2(g,c)$ for $g = 1$ for a portion of the band-averaged results. As mentioned in Sect. 6.3.2, the values for $u(K_2)$ in Tables 18–19 were determined using the procedure for determining combined standard uncertainty for correlated input quantities (International Organization for Standardization 1993). As with $u_n(L_{\mathrm{B}})$, this treats the uncertainties for the individual $K_2(g,c)$ for each sphere level as systematic uncertainty. (Remember that the final values for each $K_2(g,c)$ are weighted averages of the values corresponding to each sphere level.) This approach was taken because many of the uncertainty components arise from systematic sources. The more correct procedure of assigning a portion of the uncertainty to random and systematic sources before using (21) would be very tedious and time consuming, thus, this approach results in a conservative estimate.

Comparing Tables 13 and 19 (or Tables 12 and 18) indicates that the uncertainty in the radiance is a significant contributor to the combined uncertainty; however, for the measurements below 600 nm with one lamp illuminated, $u(S_{\mathrm{lab}})$ is greater than the radiance uncertainty component. The uncertainty associated with the uniformity of the radiance in the GSFC sphere's exit aperture is important for the 1 lamp level (Table 28). The nonlinearity uncertainty component (Table 27) is important for bands 3–6, where the radiance uncertainty component is smallest. The wavelength error uncertainty component increases with decreasing wavelength (Table 28). The components associated with the short-term repeatability and modeling errors are also largest at the shorter wavelengths, but they are not significant sources of uncertainty (Tables 27–28).

8. CALIBRATION COMPARISON

In this section, the different calibrations of SeaWiFS are compared. This includes the dark counts, gain ratios, calibration coefficients, and the ratios of calibration coefficients among bands. The previous results are the manufacturer's calibration of SeaWiFS from the November 1993 measurements.

8.1 Dark Counts and Gain Ratios

Table 9 in Barnes et al. (1994b) is analogous to Table 20 in this report, except that in the Barnes et al. paper, the radiance values were corrected for out-of-band response. Comparing the counts at saturation for $g = 1$ shows that the agreement is better than 0.3 counts. This indicates that the dark counts in the standard setting ($g = 1$ and 4:1 TDI setting) remained stable within ±0.3 counts from November 1993 to April 1997. Barnes et al. (1994b) reported the same value of the counts at saturation, independent of gain, while this work reports a unique value at each gain. At $g = 2$, $g = 3$, or $g = 4$, the difference between Barnes et al. 1994b and this work is within ±1.3 counts for bands 1–4 and within ±2.4 counts for bands 5–8.

In Fig. 12, the gain ratios from Table 17 are compared to the previous values in Barnes et al. (1994b). The new gain ratios for $g = 2$, $g = 3$, and $g = 4$ are divided by the previous values, with the cloud channels shown separately from the ocean channels. All of the new gain ratios for the ocean channels agree with the previous values to within ±0.3%, which is within the estimated uncertainties stated in Table 17. The gain ratios for the cloud channels agree with the previous values to within about ±4%, which is greater than the estimated uncertainty for the gain ratios in this work.

The final values for the calibration coefficients determined in this work were used to calculate gain ratios, see (18), and were compared to the values determined from the voltage calibration pulse. For the ocean channels, the ratios of the $K_2(g, c)$ coefficients (Table 19) agreed with the corresponding gain ratios in Table 17 to within ±0.3%. For the cloud channels, the agreement was worse. For $g = 3$ and $g = 4$, the differences are ±2%, and for $g = 2$, the differences are as large as ±5% for bands 7 and 8.

8.2 Calibration Coefficients

Assuming the sphere sources used at SBRC in 1993 and at OSC in 1997 were calibrated accurately for spectral radiance, then the two experimental calibrations are an indicator of the reproducibility of SeaWiFS for measurements of a laboratory calibration source. Discrepancies greater than those expected from the estimated uncertainties in the spectral radiances of the sources and the resolution of SeaWiFS, would indicate that there are differences between the sources, or that SeaWiFS did not remain stable from its initial calibration in 1993 until the recalibration 1997. Parameters that can change in SeaWiFS include the shape and wavelength of the relative spectral responsivities. The comparison is restricted to $g = 1$. The values based on the SBRC calibration are given in Table 4, and the new values are in Tables 18–19. The new values, divided by the old values, are illustrated in Fig. 13 for the band-averaged method. For the ocean channels, the ratio varies between −3% to +4% as a smooth function of wavelength. The dispersion of the ratios for the three ocean channels in each band is small, from 0.1–0.5%. The cloud channels follow the same pattern, but with a greater dispersion. This is caused by the reduced sensitivities for these channels. A similar trend is observed if the band-centered calibration coefficients, $K_2(g, c)$, are compared, except that the difference is increased by about 1% for band 1 and 0.5% for band 2. Given that the relative standard uncertainty of the original calibration by SBRC was 5%, the results are in agreement within the combined uncertainty of the two methods of calibration.

As a verification of the analysis in this work and the relationship between the predicted and observed output from SeaWiFS in the 1:1 and 4:1 TDI setting, a comparison was done for those channels that were below knee 1 for $g = 1$. For each band, the output in the 4:1 TDI setting depends on the calibration coefficients for each channel, with an effective calibration coefficient $K_2(g)$ given by

$$\frac{1}{K_2(g)} = 0.25\left[\frac{1}{K_2(g,1)} + \frac{1}{K_2(g,2)} + \frac{1}{K_2(g,3)} + \frac{1}{K_2(g,4)}\right]. \quad (29)$$

The agreement for bands 2–6 was better than ±0.2%, and for band 1, the agreement was better than ±0.5% for the three brightest sphere levels (16, 8, and 4 lamps illuminated). The agreement for the 1 lamp configuration was 0.9%.

The significance of the stability of the calibration coefficient ratios among the various bands, or color ratios, was mentioned in Sect. 6.5. Figure 13 indicates that these color ratios are different for the 1993 SBRC calibration and the 1997 OSC calibration. For $g = 1$ and the band-averaged method (Table 4), the band-2–to–band-5 ratio decreased by about 2.6%, the band-3–to–band-5 ratio decreased by about 1.3%, and the band-7–to–band-8 ratio decreased by about 0.8%.

9. DISCUSSION

For the ocean channels, the gain ratios are in good agreement with the values determined by SBRC. In Barnes et al. (1994b), the three gain ratios for each ocean channel in a band were averaged, and a single value was reported (compare Tables 5 and 17). Also for the ocean channels,

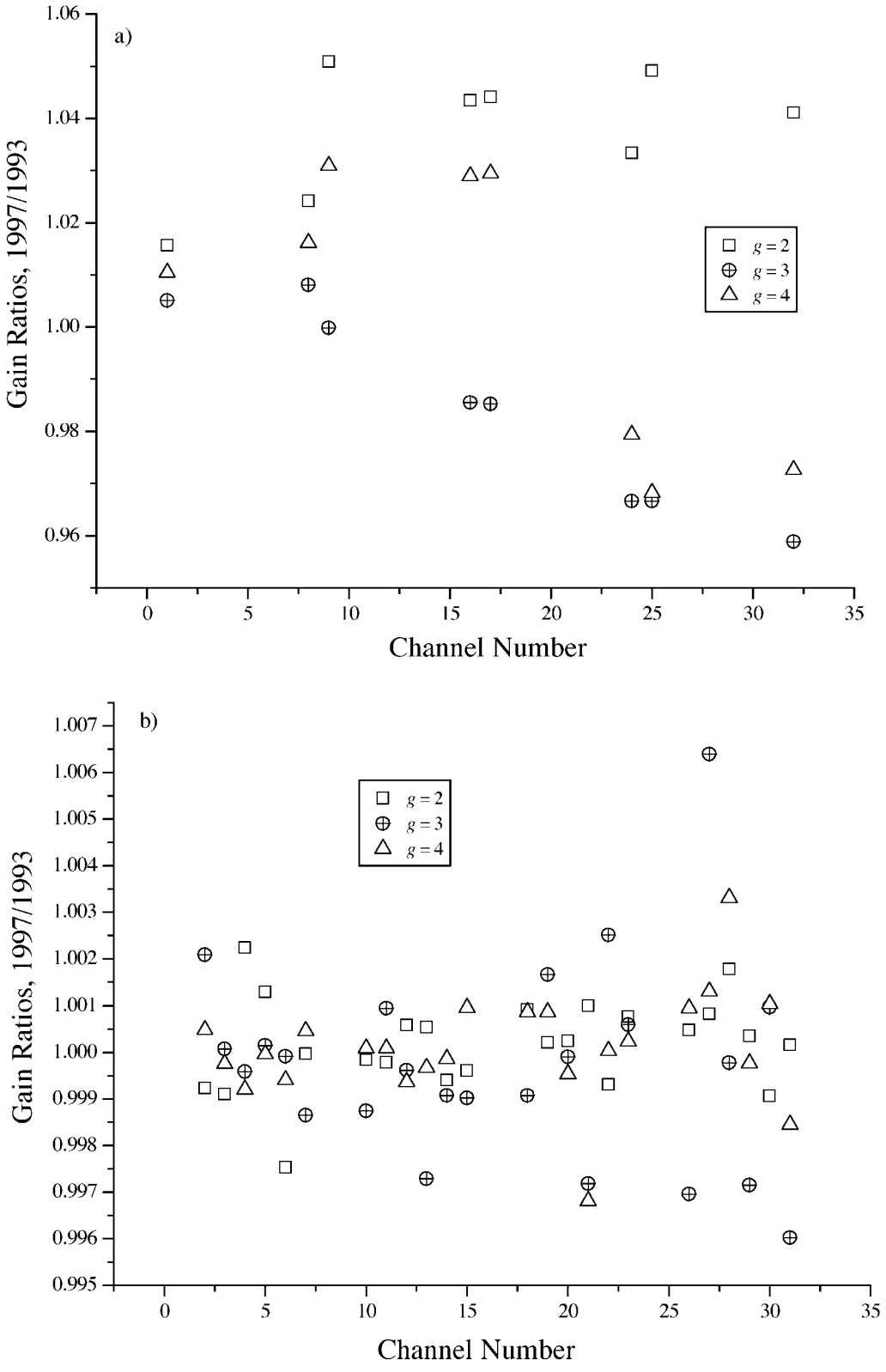

Fig. 12. Gain ratios for the cloud and ocean channels for $g = 2$, $g = 3$, and $g = 4$ normalized by the previous values (Barnes et al. 1994b). The channels for each band are numbered consecutively 1–32, beginning with band 1, channel 1 and ending with band 8, channel 4: **a)** gain ratios for the cloud channels, and **b)** gain ratios for the ocean channels.

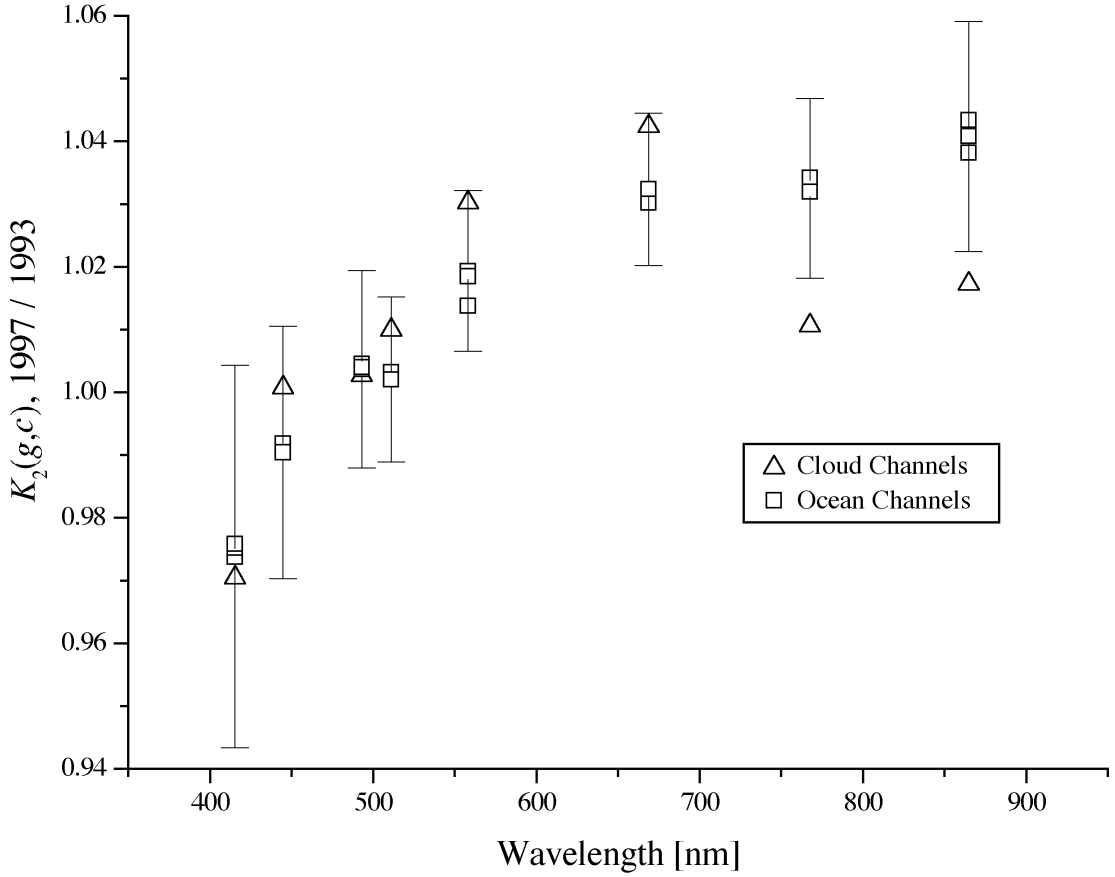

Fig. 13. Comparison of the calibration coefficients determined using the band-averaged spectral radiances between this work and the 1993 SBRC calibration for $g = 1$. The new values are normalized by the previous results. The vertical bars are the uncertainties $u(K_2)$ for one of the ocean channels in each band. The relative standard uncertainty in the original calibration is not illustrated, but it was estimated to be about 5%.

the values obtained in this work with the voltage calibration pulse agree with those derived from the calibration coefficients. For the cloud channels, the lack of agreement between the SBRC gain ratios and those determined in this work using the voltage calibration pulse is because Barnes et al. (1994b) set the gain ratios to be unity. The justification was the instrument design and the small signal-to-noise ratios, with values of about 75. It is now understood that the gain selection for the cloud channels involves different resistors, and that these resistors are imperfectly matched; therefore, the values for the gain ratios determined in this work are more accurate.

The relative disagreement of 2–5% for the cloud channels with the gain ratios determined from the voltage calibration pulse and the band-averaged calibration coefficients is understood in terms of the signal-to-noise ratios (as small as 10–20) that resulted from measurements of the GSFC sphere, especially for lamp level 1. The scatter in the calibration coefficients among sphere radiance levels shown in Fig. 6 is typical of the other gain settings. Even with this amount of scatter, the overall agreement in the gain ratios for the cloud channels (determined using the two methods) is better than the agreement between the SBRC and the new values determined from the voltage calibration pulse.

The linearity of SeaWiFS was measured on two occasions by SBRC (Sect. 2.4 and in Barnes et al. 1994a) in the standard configuration ($g = 1$ and the 4:1 TDI setting). If the single radiance level that resulted in anomalous results is excluded, the agreement with the new linearity measurements is good; compare Tables 24–25 in Barnes et al. (1994a) with Fig. 11 in this document. The 1997 calibration described here also reports results for the linearity of SeaWiFS for the case where the ocean channels are saturated.

For both the SBRC and the OSC measurements of the linearity and calibration coefficients of SeaWiFS, the dynamic range and relative spectral shape of the laboratory sources of spectral radiance limited the results. SeaWiFS was designed to determine the upwelling ocean radiance from measurements of the Earth's radiance from orbit. The difference in the relative spectral shape of the calibration source and the Earth's ocean–atmosphere system

is equivalent to the difference between a 12,000 K blackbody and a 2,850 K blackbody (Barnes 1996a, and Barnes and Yeh 1996). Therefore, at OSC (as well as SBRC), the short-wavelength bands were not studied above the knee, and at $g = 1$, the ocean channels in bands 7 and 8 were not studied below the knee. The overall result is that the linearity of the longer wavelength bands must be inferred from the results for the shorter wavelength bands. The calibration coefficients for the longer wavelength bands must be inferred from measurements at $g = 4$ and the lowest sphere radiance level.

The agreement with the new calibration coefficients and the SBRC values can only be assessed for $g = 1$ (Table 4). The new $K_2(g, c)$ values, divided by the SBRC values, are shown in Fig. 13 for the band-averaged results. Although the agreement is within the combined uncertainties of the two determinations, there is an obvious spectral dependence—the new calibration coefficients for bands 5–8 are greater than the SBRC values, while those for bands 1 and 2 are less.

As in this work, the SBRC determination of the calibration coefficients for the ocean channels in bands 7 and 8 involved radiometric measurements at $g = 4$ and electronic measurements of the gain ratios. The difference in the gain ratios (Table 5 and Table 17), however, cannot explain the 4% difference in the calibration coefficients for the ocean channels.

The measurement and modeling of the GSFC sphere source that resulted in the spectral radiance values used to determine the calibration coefficients in this report could be the cause of the discrepancy between this work and the SBRC measurements. The sphere was measured with low uncertainty in 1995 by direct comparison to a standard of spectral radiance (Early and Johnson 1997), and the SXR was used to relate the 1995 radiances to the 1997 values. The stability of the SXR over this time interval is, therefore, critical; it was established by comparing two separate calibrations of the SXR (Sect. 5.1). The additional measurements of the GSFC sphere using the SXR at SIRREX-4 in May 1995 and in December 1995 support the argument that the GSFC sphere changed spectrally with time because of changes in the reflectance of the inner surface. The independent measurements of the GSFC sphere at OSC using the 746/ISIC agree with the SXR results within the combined uncertainties (Fig. 3).

Another source of the discrepancy is the spectral radiance of the sphere source used at SBRC to calibrate SeaWiFS in 1995. For example, if the spectral radiance at SeaWiFS bands 1 and 2 was overestimated, while for bands 6, 7, and 8 it was underestimated, the results would be as in Fig. 13. Aging of the SBRC sphere source is not a likely source of the discrepancy because the sphere was calibrated just before the measurements with SeaWiFS. There have been independent assessments of the SBRC methods using the 746/ISIC, the SXR, and other portable transfer radiometers. In October 1992, the 746/ISIC measured the SBRC integrating sphere source that was used to calibrate SeaWiFS. Two sphere levels were studied; the first was comparable to the GSFC sphere with 16 lamps illuminated, and the second was more than twice the radiance. The agreement of the 746/ISIC results with the SBRC results was within 3% (Appendix B in Mueller 1993). At the same experiment, however, direct comparisons of lamp standards of spectral irradiance from SBRC and GSFC were not consistent given the combined uncertainties, and neither was an SBRC calibration of the GSFC integrating sphere source (Mueller 1993).

In August 1996, the 746/ISIC, the SXR, and several other transfer radiometers measured the SBRC sphere at four radiance levels (Butler and Johnson 1996). The internal agreement among the various transfer radiometers was from 1–2%, but not all of the measurements could be compared to SBRC values because they had not calibrated the sphere prior to the intercomparison. During the post-comparison calibration at SBRC, some of the lamps failed, leaving only the lowest radiance level available for comparison.

A second intercomparison was held in May 1998; this time, the Visible Transfer Radiometer, which was built by NIST for the NASA Earth Observing System (EOS) was used. A future paper will describe the results of both experiments.

Another independent verification of the calibration of the SBRC sphere source is the prelaunch solar-based radiometric calibration using SeaWiFS and its onboard diffusely reflecting panel (Biggar et al. 1994 and Biggar et al. 1995). For these measurements, in October 1992 and November 1993, SeaWiFS was taken outdoors and aligned so the sun illuminated the pane, as it does on orbit. Using ancillary data for the exoatmospheric solar irradiance, and correcting for the effects of the atmosphere, calibration coefficients were determined. The solar-based calibration was compared to the SBRC calibration by calculating the SeaWiFS output for the solar calibration during flight. The agreement was within −2% to +4%, except for band 8 in the 1992 experiment (Fig. 11 in Biggar et al. 1995). No corrections were made for the sensitivity of SeaWiFS to the relative spectral shape of the source (the out-of-band corrections). If the corrections given in Barnes et al. (1994b) are applied to the sphere-based values, then the agreement is within −1% to +2.5% for the 1993 measurements. The sign of the difference is positive if the sphere-based calibration resulted in increased predicted output from SeaWiFS, which would occur if the SBRC sphere radiance was underestimated. In general, there was no obvious dependence of the differences with wavelength.

Several times since its launch in August 1997, SeaWiFS measured the radiance of the solar-illuminated onboard panel. The observed counts are compared to those predicted from the ground-based solar measurements performed in November 1993 (Biggar et al. 1995). Preliminary analysis indicates that the actual measurements agree with the predicted values to within 3%.

10. SUMMARY

An ocean color satellite, SeaWiFS, was calibrated prior to launch at the spacecraft integrator facility before and after the final vibration test. An integrating sphere source, which had been calibrated by NIST almost two years before, was used as the laboratory standard of spectral radiance. The output of the source was observed to have degraded, based on measurements using a portable filter radiometer. The sphere radiance was also measured using a portable monochromator that was calibrated *in situ* using a lamp standard of spectral irradiance.

The measurement equation for SeaWiFS is presented and the sources of uncertainty for the laboratory calibration are clearly identified. For the on-orbit measurements, a similar analysis would apply, but in some cases, additional corrections and the uncertainties associated with them may have to be considered. An example is the size-of-source correction. None of the new results were corrected for the relative spectral shape of the source; they are referenced to the laboratory calibration source, as in (9). Likewise, no atmospheric corrections were applied.

For $g = 1$ and the 1:1 TDI setting, the 1997 calibration coefficients reported in this work agree with the initial 1993 values to within ±4%. This is within the mutual combined relative standard uncertainties, which are from 5.1–6%. The results of the 1997 calibration are being used for the SeaWiFS data processing algorithms. There appears to be a spectral dependence in comparing the SBRC and the new calibration coefficients. The source of this spectral dependence is not known. The response of the SeaWiFS channels in each band is linear to better than 1%. As well as could be determined, the associated radiometric parameters, such as, the mirror side correction, dark counts, and gain ratios agree with the manufacturer's calibration. Factors that could not be studied in the new work, which were quantified by SBRC, include the polarization sensitivity, the relative spectral responsivity, and the wavelength scale.

Acknowledgments

Many people contributed to this effort. Alan Holmes (formerly of SBRC, now with Santa Barbara Instrument Group) provided overall advice and assistance during the SeaWiFS calibration experiment, and helped to align SeaWiFS to the sphere source. Steve Brown and Howard Yoon of NIST assisted with the data acquisition, documentation, and operation of the SXR; Brown also analyzed the 746/ISIC wavelength calibration data. Chris Eyerman directed the OSC operation of SeaWiFS, and Joe Nvotka and Tim Wiegand operated the SeaWiFS and OrbView-2 systems. Several other OSC personnel provided valuable assistance, including James Eitnier, Steve Hood, John McCarthy, Howard Runge, and Eric Stucky. John Cooper (formerly of Hughes STX, currently with Kajax Engineering, Inc.) operated the 746/ISIC and provided preliminary results for that instrument. Steven Smith (Jackson and Tull, Inc.) and Jack Xiong (Science Systems Applications, Inc.) assisted with the data acquisition. Gene Feldman and Watson Gregg of the SeaWiFS Project assisted with archiving the SeaWiFS results. NIST's participation was made possible by NASA Interagency Agreement S-64096-E.

Glossary

A/D	Analog-to-Digital
DC	Dark Current
DMM	Digital Multimeter
GSE	Ground Support Equipment
GSFC	Goddard Space Flight Center
HP	Hewlett-Packard
FASCAL	Facility for Automated Spectroradiometric Calibrations
FEL	Not an acronym, but a lamp designator.
ISIC	Integrating Sphere Irradiance Collector
NASA	National Aeronautics and Space Administration
NIST	National Institute of Standards and Technology
NOAA	National Oceanic and Atmospheric Administration
OrbView-2	Not an acronym, but the current name for the SeaStar satellite.
OSC	Orbital Sciences Corporation
SBRC	Santa Barbara Research Center (Raytheon)
SeaStar	Not an acronym, but the former name of the satellite on which SeaWiFS was launched, now known as OrbView-2.
SeaWiFS	Sea-viewing Wide Field-of-view Sensor
SIRREX	SeaWiFS Intercalibration Round-Robin Experiment
SIS	Spherical Integrating Source
SSE	Size-of-Source Effect
SXR	SeaWiFS Transfer Radiometer
VAFB	Vandenberg Air Force Base

Symbols

a_0	Polynomial coefficient for the chage in the sphere radiance.
a_1	Polynomial coefficient for the change in the sphere radiance.
a_2	Polynomial coefficient for the change in the sphere radiance.
a_3	Polynomial coefficient for the change in the sphere radiance.
b_0	Constant for SeaWiFS linearity analysis.
C_{dark}	Output of SeaWiFS in counts used for the zero offsets.
C_i	Net counts for SeaWiFS for mirror side i.
C_{out}	Total output of SeaWiFS in counts.
CG	Time-dependent overall system gain for SeaWiFS.
CO	Calibration system offset for SeaWiFS.
c	Integer to represent a SeaWiFS channel in a given band (values 1, 2, 3, or 4).
$F_n(\lambda)$	Correction factor for GSFC sphere radiance for n lamps operating.

g Integer to represent SeaWiFS gain (values are either 1, 2, 3, or 4).
$G(g,c)$ Gain ratios (the gain at setting g normalized by the gain at $g = 1$ and for channel c).

i Integer to represent SeaWiFS scan mirror side (values 1 or 2).

j Integer index for summation.
J Total number of parameters.

k Integer index for summation.
$K_2(g,c)$ Calibration coefficient for a SeaWiFS band, gain setting g and channel c for either the band-centered or band-averaged radiance method, depending on context.
$K_2(g)$ Calibration coefficient for a SeaWiFS band and gain setting g in the 4:1 TDI setting for either the band-centered or band-averaged radiance method, depending on context.
K_3 Correction factor for SeaWiFS focal plane temperature.
K_4 Correction factor for SeaWiFS scan modulation.

$L(\lambda)$ Spectral radiance.
$L_{\mathrm{lab}}(\lambda)$ Spectral radiance for the laboratory measurement.
$L_{n,95}(\lambda)$ Spectral radiance of the GSFC sphere source at NIST in 1995 for n lamps operating.
$L_{n,97}(\lambda)$ Spectral radiance of the GSFC sphere source at OSC in 1997 for n lamps operating.
$L_{n,97}(\lambda_{\mathrm{B}})$ Band-averaged spectral radiance of the GSFC sphere at OSC in 1997 for n lamps operating.
$L_{n,97}(\lambda_{\mathrm{D}})$ Band-centered spectral radiance of the GSFC sphere at OSC in 1997 for n lamps operating.
$L_{n,\mathrm{B},97}$ Band-averaged radiance of the GSFC sphere source at OSC in 1997 for n lamps operating.
$L_{\mathrm{orbit}}(\lambda)$ Spectral radiance for the measurement on orbit.
$L_{\mathrm{sat}}(g,c)$ Saturation radiance for a SeaWiFS configuration (band, gain, and channel).
$L_{\mathrm{SBRC}}(\lambda)$ Spectral radiance of the sphere source at SBRC.
$L_x(\lambda)$ Spectral radiance for measurement condition denoted x (x = lab or orbit).

n Integer to represent number of lamps illuminated in the sphere source.

Pxl Pixel number, i.e., the numerical designation of a pixel in a scan line.

$R(\lambda)$ Spectral responsivity of an optical instrument.
R_i Correction factor for the difference in the reflectance between the two sides of the SeaWiFS scan mirror, $i = 1$ or 2.

$S_{\mathrm{lab}}(g,c)_{\mathrm{Apr}}$ Average corrected net counts for a SeaWiFS band, gain g, and channel c for 11 April 1997.
$S_{\mathrm{lab}}(g,c)_{\mathrm{Jan}}$ Average corrected net counts for a SeaWiFS band, gain g, and channel c for 24 January 1997.
$S_{\mathrm{orbit}}(g,c)$ Corrected net counts for a SeaWiFS band, gain, and channel on orbit.
$S_{\mathrm{sat}}(g,c)$ Corrected net counts for a SeaWiFS band, gain, and channel at saturation.
$S_x(g,c)$ Corrected net counts for a SeaWiFS band, gain g, and channel c for the measurement condition denoted x (x = lab or orbit).

t Time of the SeaWiFS measurement (refers to on-orbit measurements).
t_0 Time of the SeaWiFS launch.
T Focal plane temperature for SeaWiFS.
T_{ref} Reference value for SeaWiFS focal plane temperature.

u Standard uncertainty.
$u(C_{\mathrm{out}})$ Standard uncertainty in the SeaWiFS output counts when observing an illuminated source.
$u(C_{\mathrm{dark}})$ Standard uncertainty in the SeaWiFS output counts when observing a dark source.
$u(K_2)$ Standard uncertainty in the SeaWiFS calibration coefficient.
$u(K_3)$ Standard uncertainty in the SeaWiFS temperature correction coefficient.
$u(L(\lambda))$ Standard uncertainty in spectral radiance.
$u_n(L_{\mathrm{B}})$ Standard uncertainty in the band-averaged spectral radiance for n lamps operating.
$u_n^{\mathrm{B}}(\lambda_{\mathrm{B}})$ Relative standard uncertainty for $L_{n,97}(\lambda_{\mathrm{B}})$.
$u_n(L_{\mathrm{D}})$ Standard uncertainty in the band-averaged spectral radiance for n lamps operating.
$u_n^{\mathrm{D}}(\lambda_{\mathrm{D}})$ Relative standard uncertainty for $L_{n,97}(\lambda_{\mathrm{D}})$.
u_n^L Relative standard uncertainty for $L(\lambda)$.
$u(R_i)$ Standard uncertainty in the mirror side correction.
$u(R(\lambda))$ Standard uncertainty in the SeaWiFS relative spectral responsivity.
$u(S_{\mathrm{lab}})$ Standard uncertainty in the corrected net counts from SeaWiFS.
$u(T)$ Standard uncertainty in the SeaWiFS focal plane temperature.
$u(z_j)$ Standard uncertainty in parameter z_j.
$u(z_j, z_k)$ Covariance associated with parameters z_j and z_k.
$u(\lambda)$ Standard uncertainty in the wavelength accuracy of the $R(\lambda)$ values.

x_n Net voltage for the SXR for n lamps operating (for the SeaWiFS linearity analysis).

y_n Corrected net counts for SeaWiFS for n lamps operating (for the SeaWiFS linearity analysis).

z_j Parameter j in the SeaWiFS measurement equation.

$\gamma_x(g,c)$ Measurement constant for a SeaWiFS band, gain g, and channel c for the measurement condition denoted x (x = lab or orbit).

ΔC Defined as $C_{\mathrm{out}} - C_{\mathrm{dark}}$.
ΔT Defined as $T - T_{\mathrm{ref}}$.
$\Delta\lambda$ Bandwidth parameter.

λ Wavelength.
λ_{B} Band-averaged center wavelength for SeaWiFS.
λ_{SXR} Measurement wavelength for the SXR.

$\bar{\rho}$ Average reflectance of the SeaWiFS scan mirror.
ρ_i Reflectance of the side i of the SeaWiFS scan mirror, where i equals 1 or 2.

References

Barnes, R.A., 1994: *SeaWiFS Data: Actual and Simulated.* [World Wide Web page.] From URLs: `http://seawifs.gsfc.nasa.gov/SEAWIFS/IMAGES/spectra1.dat` and `/spectra2.dat` NASA Goddard Space Flight Center, Greenbelt, Maryland.

——, 1996a: "Calculation of an equivalent blackbody temperature for the GSFC sphere." In: Barnes, R.A., E-n. Yeh, and R.E. Eplee, 1996: SeaWiFS Calibration Topics, Part 1. *NASA Tech. Memo. 104566, Vol. 39,* S.B. Hooker and E.R. Firestone, Eds., NASA Goddard Space Flight Center, Greenbelt, Maryland, 5–17.

——, 1996b: "A comparison of the spectral responses of SeaWiFS and the SeaWiFS Transfer Radiometer." In: Barnes, R.A., E-n. Yeh, and R.E. Eplee, 1996: SeaWiFS Calibration Topics, Part 1. *NASA Tech. Memo. 104566, Vol. 39,* S.B. Hooker and E.R. Firestone, Eds., NASA Goddard Space Flight Center, Greenbelt, Maryland, 39–48.

——, 1996c: "SeaWiFS center wavelengths." In: Barnes, R.A., E-n. Yeh, and R.E. Eplee, 1996: SeaWiFS Calibration Topics, Part 1. *NASA Tech. Memo. 104566, Vol. 39,* S.B. Hooker and E.R. Firestone, Eds., NASA Goddard Space Flight Center, Greenbelt, Maryland, 49–53.

——, and A.W. Holmes, 1993: Overview of the SeaWiFS ocean sensor. *Proc. SPIE,* **1939,** 224–232.

——, W.L. Barnes, W.E. Esaias, and C.R. McClain, 1994a: Prelaunch Acceptance Report for the SeaWiFS Radiometer. *NASA Tech. Memo. 104566, Vol. 22,* S.B. Hooker, E.R. Firestone, and J.G. Acker, Eds., NASA Goddard Space Flight Center, Greenbelt, Maryland, 32 pp.

——, A.W. Holmes, W.L. Barnes, W.E. Esaias, C.R. McClain, and T. Svitek, 1994b: SeaWiFS Prelaunch Radiometric Calibration and Spectral Characterization. *NASA Tech. Memo. 104566, Vol. 23,* S.B. Hooker, E.R. Firestone, and J.G. Acker, Eds., NASA Goddard Space Flight Center, Greenbelt, Maryland, 55 pp.

——, ——, and W.E. Esaias, 1995: Stray Light in the SeaWiFS Radiometer. *NASA Tech. Memo. 104566, Vol. 31,* S.B. Hooker, E.R. Firestone, and J.G. Acker, Eds., NASA Goddard Space Flight Center, Greenbelt, Maryland, 76 pp.

——, and E-n. Yeh, 1996: "Effects of source spectral shape in SeaWiFS radiance measurements." In: Barnes, R.A., E-n. Yeh, and R.E. Eplee, 1996: SeaWiFS Calibration Topics, Part 1. *NASA Tech. Memo. 104566, Vol. 39,* S.B. Hooker and E.R. Firestone, Eds., NASA Goddard Space Flight Center, Greenbelt, Maryland, 18–38.

——, and R.E. Eplee, 1997: "The 1993 SeaWiFS calibration using band-averaged spectral radiances." In: Barnes, R.A., R.E. Eplee, E-n. Yeh, and W.E. Esaias, 1997: SeaWiFS Calibration Topics, Part 2. *NASA Tech. Memo. 104566, Vol. 40,* S.B. Hooker and E.R. Firestone, Eds., NASA Goddard Space Flight Center, Greenbelt, Maryland, 39–46.

Biggar, S.F., P.N. Slater, K.J. Thome, A.W. Holmes, and R.A. Barnes, 1994: "Preflight solar-based calibration of SeaWiFS." In: McClain, C.R., R.S. Fraser, J.T. McLean, M. Darzi, J.K. Firestone, F.S. Patt, B.D. Schieber, R.H. Woodward, E-n. Yeh, S. Mattoo, S.F. Biggar, P.N. Slater, K.J. Thome, A.W. Holmes, R.A. Barnes, and K.J. Voss, 1994: Case Studies for SeaWiFS Calibration and Validation, Part 2. *NASA Tech. Memo. 104566, Vol. 19,* S.B. Hooker, E.R. Firestone, and J.G. Acker, Eds., NASA Goddard Space Flight Center, Greenbelt, Maryland, 25–32.

——, K.J. Thome, P.N. Slater, A.W. Holmes, and R.A. Barnes, 1995: "Second SeaWiFS preflight solar radiation-based calibration experiment." In: Mueller, J.L., R.S. Fraser, S.F. Biggar, K.J. Thome, P.N. Slater, A.W. Holmes, R.A. Barnes, C.T. Weir, D.A. Siegel, D.W. Menzies, A.F. Michaels, and G. Podesta, 1995: Case Studies for SeaWiFS Calibration and Validation, Part 3. *NASA Tech. Memo. 104566, Vol. 27,* S.B. Hooker, E.R. Firestone, and J.G. Acker, Eds., NASA Goddard Space Flight Center, Greenbelt, Maryland, 20–24.

Butler, J.J., and B.C. Johnson, 1996: EOS radiometric measurement comparisons at Hughes Santa Barbara Remote Sensing and NASA's Jet Propulsion Laboratory. *The Earth Observer,* **8**(5), 17–19.

Early, E.A., and B.C. Johnson, 1997: "Calibration and characterization of the GSFC sphere." In: Yeh, E-n., R.A. Barnes, M. Darzi, L. Kumar, E.A. Early, B.C. Johnson, J.L. Mueller, and C.C. Trees, 1997: Case Studies for SeaWiFS Calibration and Validation, Part 4. *NASA Tech. Memo. 104566, Vol. 41,* S.B. Hooker, and E.R. Firestone, Eds., NASA Goddard Space Flight Center, Greenbelt Maryland, 3–17.

Eplee, R.E., and R.A. Barnes, 1997: "The SeaWiFS temperature calibration." In: Barnes, R.A., R.E. Eplee, E-n. Yeh, and W.E. Esaias, 1997: SeaWiFS Calibration Topics, Part 2. *NASA Tech. Memo. 104566, Vol. 40,* S.B. Hooker and E.R. Firestone, Eds., NASA Goddard Space Flight Center, Greenbelt, Maryland, 56–62.

Hooker, S.B., W.E. Esaias, G.C. Feldman, W.W. Gregg, and C.R. McClain, 1992: An Overview of SeaWiFS and Ocean Color. *NASA Tech. Memo. 104566, Vol. 1,* S.B. Hooker and E.R. Firestone, Eds., NASA Goddard Space Flight Center, Greenbelt, Maryland, 24 pp., plus color plates.

International Organization for Standardization, 1993: *Guide to the Expression of Uncertainty in Measurement,* International Organization for Standardization, Geneva, Switzerland, 101 pp.

Johnson, B.C., S.S. Bruce, E.A. Early, J.M. Houston, T.R. O'Brian, A. Thompson, S.B. Hooker, and J.L. Mueller, 1996: The Fourth SeaWiFS Intercalibration Round-Robin Experiment (SIRREX-4), May 1995. *NASA Tech. Memo. 104566, Vol. 37,* S.B. Hooker and E.R. Firestone, Eds., NASA Goddard Space Flight Center, Greenbelt, Maryland, 65 pp.

——, F. Sakuma, J.J. Butler, S.F. Biggar, J.W. Cooper, J. Ishida, and K. Suzuki, 1997: Radiometric measurement comparison using the Ocean Color Temperature Scanner (OCTS) visible and near infrared integrating sphere. *J. Res. Natl. Inst. Stand. Technol.,* **102,** 627–646.

——, J.B. Fowler, and C.L. Cromer, 1998: The SeaWiFS Transfer Radiometer (SXR). *NASA Tech. Memo. 1998–206892, Vol. 1,* S.B. Hooker and E.R. Firestone, Eds., NASA Goddard Space Flight Center, Greenbelt, Maryland, 58 pp.

Mueller, J.L., 1993: The First SeaWiFS Intercalibration Round-Robin Experiment, SIRREX-1, July 1992. *NASA Tech. Memo. 104566, Vol. 14,* S.B. Hooker and E.R. Firestone, Eds., NASA Goddard Space Flight Center, Greenbelt, Maryland, 60 pp.

——, and R.W. Austin, 1995: Ocean Optics Protocols for SeaWiFS Validation, Revision 1. *NASA Tech. Memo. 104566, Vol. 25,* S.B. Hooker, E.R. Firestone, and J.G. Acker, Eds., NASA Goddard Space Flight Center, Greenbelt, Maryland, 67 pp.

——, B.C. Johnson, C.L. Cromer, S.B. Hooker, J.T. McLean, and S.F. Biggar, 1996: The Third SeaWiFS Intercalibration Round-Robin Experiment (SIRREX-3), 19–30 September 1994. *NASA Tech. Memo. 104566, Vol. 34,* S.B. Hooker, E.R. Firestone, and J.G. Acker, Eds., NASA Goddard Space Flight Center, Greenbelt, Maryland, 78 pp.

Taylor, B.N., and C.E. Kuyatt, 1994: Guidelines for Evaluating and Expressing the Uncertainty of NIST Measurement Results. *NIST Tech. Note 1297,* US Dept. of Commerce, National Institute of Standards and Technology, Gaithersburg, Maryland, 20 pp.

Tsai, B.K., and B.C. Johnson, 1998: Radiometric Traceability for Fundamental Measurements: Estimation and Evaluation of Combined Standard Uncertainties, *Metrologia,* **35,** 587–593.

Woodward, R.H., R.A. Barnes, C.R. McClain, W.E. Esaias, W.L. Barnes, and A.T. Mecherikunnel, 1993: Modeling of the SeaWiFS Solar and Lunar Observations. *NASA Tech. Memo. 104566, Vol. 10,* S.B. Hooker and E.R. Firestone, Eds., NASA Goddard Space Flight Center, Greenbelt, Maryland, 26 pp.

Yeh, E-n., M. Darzi, and L. Kumar, 1997: "SeaWiFS stray light correction algorithm." In Yeh, E-n., R.A. Barnes, M. Darzi, L. Kumar, E.A. Early, B.C. Johnson, J.L. Mueller, and C.C. Trees, 1997: Case Studies for SeaWiFS Calibration and Validation, Part 4. *NASA Tech. Memo. 104566, Vol. 41,* S.B. Hooker, and E.R. Firestone, Eds., NASA Goddard Space Flight Center, Greenbelt, Maryland, 24–30.

The SeaWiFS Postlaunch Technical Report Series

Vol. 1

Johnson, B.C., J.B. Fowler, and C.L. Cromer, 1998: The SeaWiFS Transfer Radiometer (SXR). *NASA Tech. Memo. 1998–206892, Vol. 1,* S.B. Hooker and E.R. Firestone, Eds., NASA Goddard Space Flight Center, Greenbelt, Maryland, 58 pp.

Vol. 2

Aiken, J., D.G. Cummings, S.W. Gibb, N.W. Rees, R. Woodd-Walker, E.M.S. Woodward, J. Woolfenden, S.B. Hooker, J-F. Berthon, C.D. Dempsey, D.J. Suggett, P. Wood, C. Donlon, N. González-Benítez, I. Huskin, M. Quevedo, R. Barciela-Fernandez, C. de Vargas, and C. McKee, 1998: AMT-5 Cruise Report. *NASA Tech. Memo. 1998–206892, Vol. 2,* S.B. Hooker and E.R. Firestone, Eds., NASA Goddard Space Flight Center, Greenbelt, Maryland, 113 pp.

Vol. 3

Hooker, S.B., G. Zibordi, G. Lazin, and S. McLean, 1999: The SeaBOARR-98 Field Campaign. *NASA Tech. Memo. 1999–206892, Vol. 3,* S.B. Hooker and E.R. Firestone, Eds., NASA Goddard Space Flight Center, Greenbelt, Maryland, 40 pp.

Vol. 4

Johnson, B.C., R.E. Eplee, Jr., R.A. Barnes, E.A. Early, and R.T. Caffrey, 1999: The 1997 Prelaunch Radiometric Calibration of SeaWiFS. *NASA Tech. Memo. 1999–206892, Vol. 4,* S.B. Hooker and E.R. Firestone, Eds., NASA Goddard Space Flight Center, Greenbelt, Maryland, 51 pp.